Vol. 75 • Issue 1 • 2026.

Veterinaria

UNIVERZITET U SARAJEVU • VETERINARSKI FAKULTET •

01
26

ISSN Print: 0372-6827

ISSN Online: 2233-1360

VETERINARIA PUBLISHER:
University of Sarajevo, Veterinary Faculty,
Bosnia and Herzegovina

Web-site: **www.veterinaria.unsa.ba/journal/index.php/vfs**
E-mail: **veterinaria@vfs.unsa.ba**
Fax: +387(33) 61 78 50
Address: Sarajevo, 71000
Zmaja od Bosne 90, Bosnia and Herzegovina

The Journal is indexed by Clarivate Web of Science - BIOSIS Previews, EBSCO, ICI Journal Master List, DOAJ, CAB Abdstract database (CAB International), SEESAmE Publication and Google Scholar.

Design: Arch Design d.o.o., Sarajevo

The Journal „VETERINARIA" is registered in the Records of public media of Ministry of Education, Science and Youth of Sarajevo Canton dated on February 9, 1996, under the number 553.

Content

REVIEW ARTICLE

Estimation of body weight using testicular traits of bucks: A systematic review

Paiyane Faith Molekwa, Ledimo Faith Makgopa, Trudy Lebo Rashijane, Lebogang Emily Mokubedi, Abigail Mmapaseka Phaladi, Madumetja Cyril Mathapo, Thobela Louis Tyasi*

Department of Agricultural Economics and Animal Production, University of Limpopo, Sovenga, South Africa

***Corresponding author**:
Prof. dr. Thobela Louis Tyasi

Address: Private Bag X1106, Sovenga, 0727, Limpopo South Africa
E-mail: louis.tyasi@ul.ac.za
Phone: -
ORCID: 0000-0002-3519-7806

Original Submission:
12 February 2026
Revised Submission:
18 March 2026
Accepted:
24 March 2026

How to cite this article: Molekwa PF, Makgopa LF, Rashijane TL, Mokubedi LE, Phaladi AM, Mathapo MC, Thobela Louis Tyasi TL. 2026. Estimation of body weight using testicular traits of goats: A systematic review. Veterinaria, 75(1), 1-12.

ABSTRACT

Understanding how body weight relates to reproductive traits in goats is important for improving breeding practices and farm productivity. This review looks at existing research on the relationship between body weight and key reproductive traits, such as scrotal circumference, testicular length, and testicular diameter in goats. Databases such as Google Scholar, PubMed, ScienceDirect, and Web of Science were systematically evaluated, and a total of 650 articles were retrieved. After screening, a total of nineteen (n = 19) eligible articles were selected for an in-depth analysis. These studies were published between 1992 and 2024, with 26% (n = 5) originating from India. The systematic review highlights significant variations in methodologies employed, including predictive models and regression analyses. The result indicated that simple linear regression model was mostly used in predicting body weight with 21% (n = 4) of the articles included. The findings showed that the highest coefficient of determination ($R^2 = 0.88$) was recorded on scrotal circumference using simple linear regression model on goats. These findings indicate a strong correlation between body weight and testicular traits, making these models highly reliable for estimating body weight. The findings of this systematic review suggest that scrotal circumference is a reliable indicator of body weight in goats. The findings of this study can be used to assist farmers with limited resources to select bucks for breeding purpose and improving their body weight.

Keywords: Body measurements, bucks, scrotal circumference, testicles, testicular characteristics

INTRODUCTION

Goats, specifically indigenous breeds, play a crucial role in the livelihoods of rural farmers by providing them with meat and milk, thereby contributing to both nutritional needs and income generation (Raji et al., 2008). Their ability to adapt to harsh environments, low input cost and socio-cultural importance improve their value in resource limited settings. Goat manure helps improve soil fertility which supports farming systems and improve rural farmers' livelihoods and maintain food security (Mathapo et al., 2025). Within the livestock industry, goat's body weight is recognized as a fundamental economic trait, particularly in relation to market pricing, breeding and other management practices (Mathapo and Tyasi, 2022). Body weight is often used as an indirect measure of fertility, serving as a critical indicator of overall health and reproductive potential (Mathemba et al., 2025). Testicular characteristics, including

doi.org/10.51607/22331360.2026.75.1.1

testicular diameter, length and scrotal circumference, are utilized as indirect selection criteria for the genetic improvement of fertility in livestock production (Waheed et al., 2011). These traits are measurable attributes that reflect the reproductive capacity of male animals (Lephuting et al., 2024). When assessed alongside body weight, these traits are instrumental in evaluating the breeding suitability of males, which is essential for achieving successful reproduction in livestock operations (Kerketta et al., 2015). Therefore, selecting bucks with high reproductive potential is crucial in farming (Kefelega and Wakalemahu, 2017). However, methods for identifying bucks with superior fertility are limited at a rural level due to insufficient information on measurable male traits related to fertility, fertility testing information and the challenges and costs associated with gathering fertility data on individual males (Gemeda and Workalemadu, 2017). By leveraging the relationship between body weight and testicular traits, farmers can make more informed decisions in selecting breeding stock based on desirable attributes. This approach is likely to enhance reproductive performance and improve the quality of offspring. Thus, the objective of this study was to systematically investigate the associations between body weight and testicular traits in goats. The findings of this research will provide valuable insights that can assist resource-limited farmers in selecting fertile bucks for breeding, ultimately contributing to improved livestock productivity.

MATERIAL AND METHODS

Eligibility criteria

The components of the research question —Population, Exposure and Outcomes (PEO) — were identified in this systematic review. The population was defined as goats, with testicular traits being the exposure, and the outcomes being the estimation of body weight linked with testicular traits. Prior to initiating the study, a search for PEO elements was carried out using Google Scholar, ScienceDirect, PubMed, and Web of Science.

Search strategy

Investigators performed a systematic review of articles using databases such as Google Scholar, PubMed, ScienceDirect, and Web of Science employing various combinations of keywords such as "testicular traits", "estimation of body weight", "body measurement" and "goats". The search was completed on the 20th of November 2025. The key terms were combined in various combinations. The study focused exclusively on research published in English. The PRISMA was used to outline the methods of identification and selection of articles as descripted by Moher et al. (2009).

Inclusion criteria

Articles that appeared in multiple databases were excluded prior to the eligibility screening process. The inclusion criteria were articles that evaluated the relationship between body weight and testicular traits of goats and published in English.

Exclusion criteria

Several exclusion criteria were implemented to eliminate irrelevant studies. Research focusing on species other than goats and duplicate records were excluded from the systematic review. Furthermore, any article that did not investigate the relationship between body weight and testicular traits in goats were also excluded. Additionally, articles examining traits unrelated to testicular traits were excluded as well.

Data extraction

The authors independently selected and extracted articles for the systematic review and reached a general agreement regarding all the materials. The articles that met the criteria had the authors name, year of publication, country of publication, and model type, in accordance with the established inclusion and exclusion criteria.

Ethical considerations

To ensure the quality of the report, all authors ethically considered issues such as data manipulation, misconduct, plagiarism, and informed consent while conducting the systematic review.

RESULTS

Search results

A flowchart illustrating the identification and selection process of articles along with the reason of exclusion is presented in Figure 1. The initial search was conducted using Google Scholar, PubMed, ScienceDirect and Web of Science using the keywords ('Estimation' OR 'Prediction' AND 'Body weight' OR 'Body measurement' AND 'Testicular traits' OR 'Testicular characteristics' AND 'Goats' OR 'Bucks' OR 'Capra

aegagrus hircus'), resulting in 650 studies (n = 650). After removing 266 duplicates (n = 266), 384 studies remained (n = 384). The screening of title and abstract led to 30 (n = 30) articles remaining. After filtering out all the studies that did not meet the criteria, nineteen (n = 19) studies were included in this systematic review.

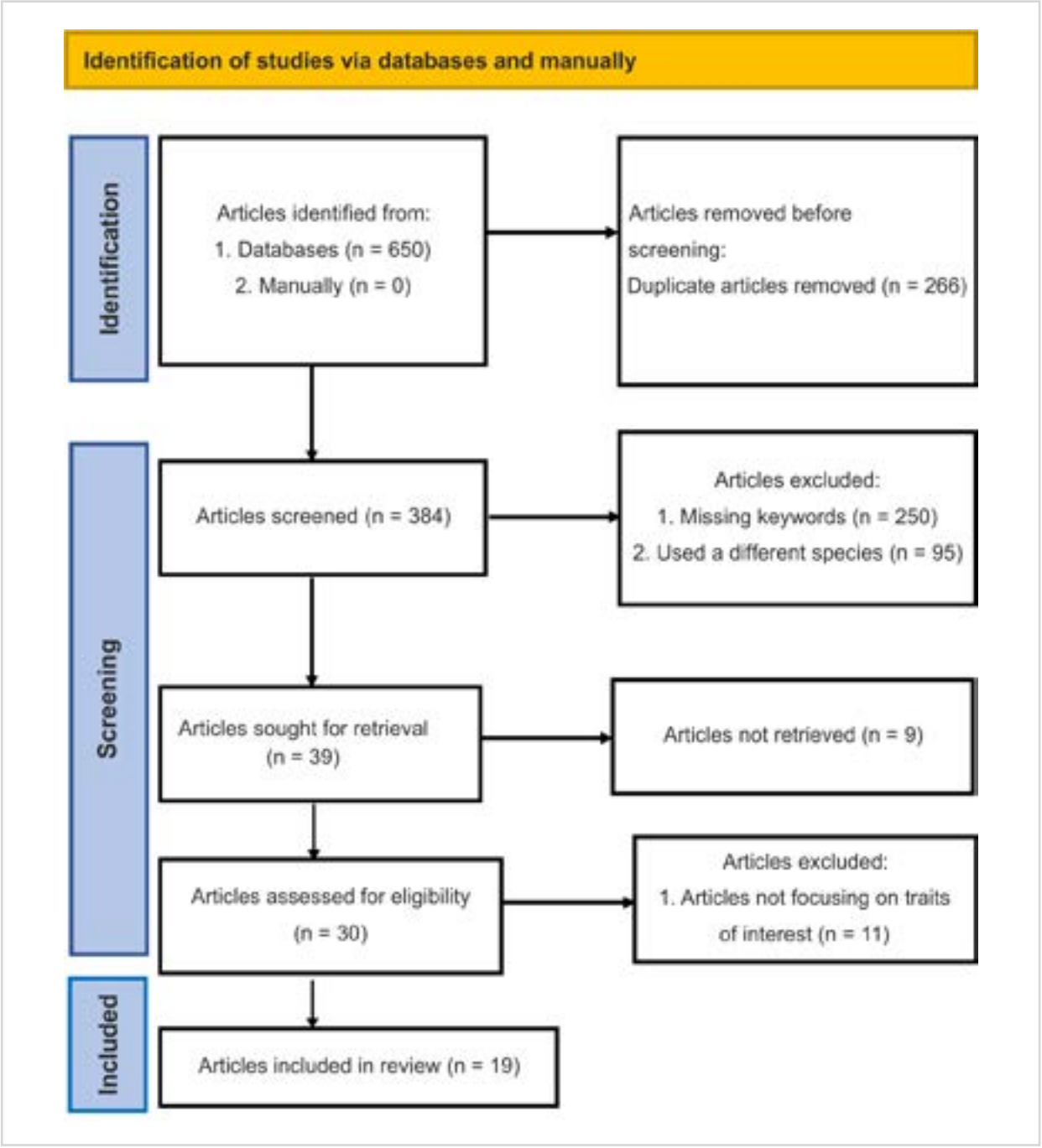

Figure 1 Flow chart of the process of study selection

Characteristics of included literature

Table 1 shows the characterization of 19 articles that are included in the systematic review. The result indicated that nineteen (n = 19) articles out of the nineteen (n = 19) articles used were conducted in Africa (Raji et al., 2008; Mathapo et al., 2024; Mekasha et al ., 2008; Akinyemi et al., 2014; Ouchene-Khelifi and Ouchene, 2021; Lephuting et al., 2025; Ajani et al., 2015; Gemeda and Workalemadu, 2017; Obande et al., 2015). The use of age groups (e.g., categorization into Grade 1, Grade 2, Grade 3 based on months) was prevalent, with six articles (n = 6) using different age groups (Gemeda and Workalemadu, 2017; Kerketta et al., 2015; Akinyemi et al., 2014; Kabiraj et al., 2011; Mekasha et al., 2008; Ouchene-Khelifi and Ouchene, 2021). The results showed that the most goat breeds used in the 19 articles were the Red Sokoto (Obande et al., 2015; Raji et al., 2008; Ajani et al., 2015) and the Black Bengal (Kabiraj et al., 2011; Khan et al., 2022).

Table 1 Characteristics of included studies

Author	Year	Country	Goat breed	Model	Traits studied	Environmental condition	Age (months)
Gemeda and Workalemahu	2017	Ethiopia	Long-eared Somali Woyto-Guju Afar	Predictive Model	SC, TV, TL, TW, BW, EW, BCS, TD	Subtropical	Gr 1 - > 12 Gr 2 - 12 - 24 Gr 3 - < 24
Kerketta *et al*	2015	India	Local goat of Rohilkhad	Multiple linear regression	CG, HW, BL, PG, TC TL, TW, TT, TV	Subtropical	Gr 1 - > 24 Gr 2 - 12 - 24 Gr 3 - 6 - 12
Lephuting *et al*	2024	South Africa	Savanna	Predictive Model	TL, TD, SC	Subtropical	24 - 36
Akinyemi *et al*	2014	Nigeria	West African Dwarf	Predictive Models	SC, TL, TD, TW, CW, Td, BW, TV, CW	Tropical	Gr 1 - 6 - 12 Gr 2 - 18 - 24 Gr 3 - 30 - 36
Mathapo *et al*	2024	South Africa	Nguni	Multivariate Adaptive Regression Splines	TL, TC, TW, TWT, BW, BL, HG, RH, WH, SH	Subtropical	12 – 48
Mathapo and Tyasi	2022	South Africa	Boer	Simple linear regression model	TL, SC, BW, BL, HG, RH, WH, SH	Subtropical	12 – 24
Ouchene-Khelifi and Ouchene	2021	Algeria	Arabia	Predictive models	BSC, BW, TW, EW, TL, TD, SC, E, WH, BL, CC, AC, Sc	Semi-Arid	Gr 1 - > 12 Gr 2 - 12 - 24 Gr 3 - < 24
Raji *et al*	2008	Nigeria	Red Sokoto Borno	Multiple linear regression model	BW, SC, SL, TW	Semi-Arid	12 – 36

Author	Year	Country	Goat breed	Model	Traits studied	Environmental condition	Age (months)
Waheed *et al*	2011	Pakistan	Beetle	Regression Model	SC, TW, SL, GH, RH, WH, BW	Hot desert	24 – 30
Ajani *et al*	2015	Nigeria	Red Sokoto	_	BW, SC, TW, TD, TL, EL, GSM, SV	_	24
Kadam *et al*	2020	India	Beetle Osmanabadi	_	SC, BW, SV, SMC	_	24
Ford *et al*	2009	USA	Boer Kiko	Regression Model	BCS, CG, WH, BL, BW, SC, TC	_	9 – 12
Obande *et al*	2015	Nigeria	Red Sokoto West African Dwarf	Regression Model	BW, SC, A	Tropical	3 – 27
Okere *et al*	2014	USA	Crossed Boer goats	_	CG, WH, BL, BCS, BW, SW, SC, TST	_	± 4
Khan *et al*	2022	India	Sirohi Barbari Black bengal	ANOVA and Duncan's multiple range test	SC, TL, TW, TT, BW, SV, SMC	Subtropical	18 – 39
Alam *et al*	2024	India	Sirohi Jamnapari	ANOVA and Duncan's multiple range test	BW, SC, SMC, SV	_	36 – 48
Mekasha *et al*	2008	Ethiopia	Aris-Bale Central highlands Afar Boram Woito-Guji	_	BW, SC, TW, BCS	_	Gr 1 - < 14 Gr 2 – 14 - 19.5 Gr 3 - 19.6 – 24
Kabiraj *et al*	2011	Bangladesh	Black bengal	ANOVA and Duncan's multiple range test	BW, SC, SV, SPC, TW		Gr 1 - 6 – 12 Gr 2 – 18 – 24 Gr 3 - 30 – 36
Bilaspuri and Singh	1992	India	Malabari	Regression model	BL, BW, CH, PG, TS, BW, TL, TW, TH, TV, SC	_	4 – 11

- = Not indicated, BCS = Body condition score, BW = Body weight, TW = Testicular weight, EW = Epididymal weight, TL = Testicular length, TD = Testicular diameter, E = Epididymis, WH = Withers height, TT = Testicular thickness, BL = Body length, CC = Chest circumference , AC = Abdominal circumference, Sc = Spiral circumference, SC = Scrotal circumference, HG = Heart girth, RH = Rump height, WH = Withers height, SH = Sternum height, CW = Caudal weight, TD = Testicular density, TV = Testicular volume, CW = Corpus weight, TWT = Testicular width, SV = Sperm viability, GSM = Gonadal sperm motility, SV = Sperm volume, SMC = Sperm concentration, TC = Testicular consistency, A = Age, SW = Shoulder width, TST = Total serum testosterone levels

Publications by year

Figure 2 illustrates the distribution of published articles by year. Analysis of the nineteen (n = 19) reviewed articles revealed that only one (n = 1) publication each came from the years 1992 (Bilaspuri and Singh et al., 1992), 2009 (Ford et al., 2009), 2017 (Gemeda and Workalemadu, 2017), 2020 (Kadam et al., 2020), and 2021 (Ouchene-Khelifi and Ouchene, 2021). These years had the lowest publication count, each with one article. Conversely, the highest number of publications (n = 3) came from the years 2024 (Mathapo et al., 2024; Lephuting et al., 2024; Alam et al., 2024) and 2015 (Kerketta et al., 2015; Obande et al., 2015; Ajani et al., 2015), followed by the years 2008 (Raji et al., 2008; Mekasha et al., 2008), 2011 (Waheed et al., 2011; Kabiraj et al., 2011), 2014 (Akinyemi et al., 2014; Okere et al., 2014) and 2022 (Mathapo and Tyasi, 2022; Khan et al., 2022), each with the second-highest number of publications (n = 2).

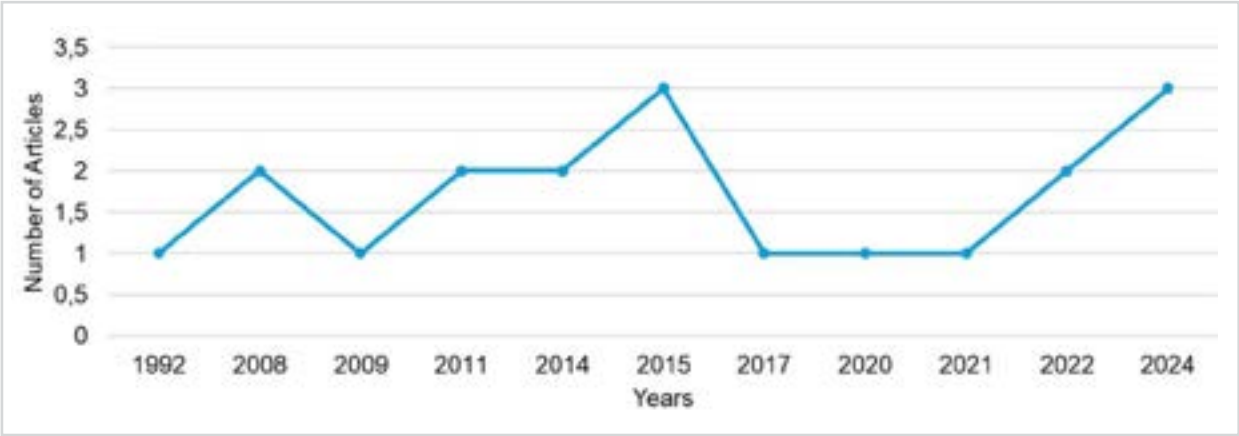

Figure 2 Publications by year

Publications by country

Figure 3 summarizes the distribution of articles published by country. Amongst the 19 reviewed articles, the result showed that the articles were from only 7 countries (Ethiopia, India, Algeria, Pakistan, Nigeria, South Africa, USA, Bangladesh). The results showed that the highest published articles (n = 4) were from India (Kerketta et al., 2015; Kadam et al., 2020; Alam et al., 2024; Khan et al., 2022) and Nigeria (Akinyemi et al., 2014; Raji et al., 2008; Obande et al., 2015; Ajani et al., 2015). South Africa (Mathapo and Tyasi, 2022; Mathapo et al., 2024; Lephuting et al., 2024) followed, providing three notable articles (n = 3). Ethiopia (Gemeda and Workalemadu, 2017; Mekasha et al., 2008) and the USA (Okere et al., 2014; Ford et al., 2009) had the second least number of articles (n = 2). Lastly, Algeria (Ouchene-Khelifi and Ouchene, 2021), and Pakistan (Waheed et al., 2011) each accounted for the least number of articles (n = 1).

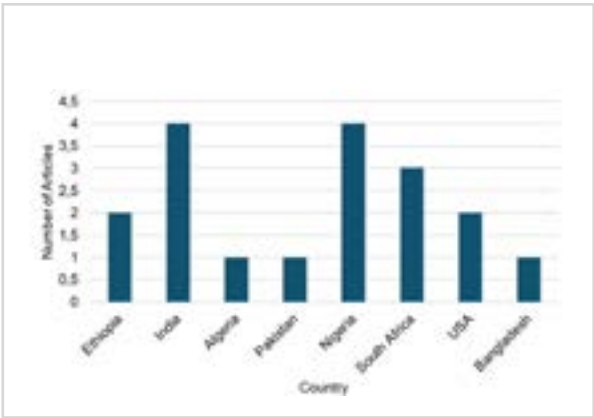

Figure 3 Publications by country

Publications by environmental conditions

Figure 4 summarizes the distribution of articles published based on environmental conditions. The result showed that out of 19 articles used in the review, 31% (6 out of 19 articles) focused on subtropical environments (Kerketta et al., 2015; Gemeda and Workalemadu, 2017; Mathapo and Tyasi, 2022; Mathapo et al., 2004; Lephuting et al., 2024; Khan et al., 2022). Secondly, 10% (2 out of 19) articles explored semi – arid environments (Ouchene and Ouchene, 2020; Raji et al., 2008) and tropical environments (Akinyemi et al., 2014; Obande et al., 2015). Lastly, only one article (5%; 1 out of 19 articles) examined the hot desert environment (Waheed et al., 2011).

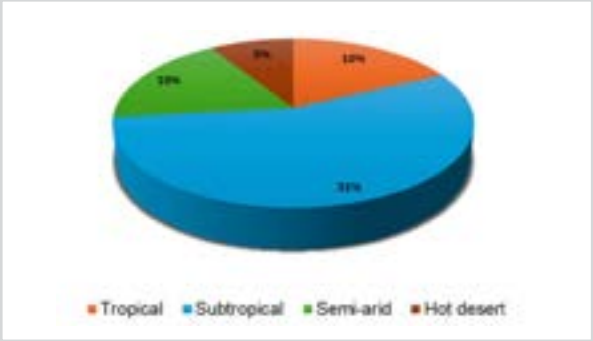

Figure 4 Publications by environmental conditions

Testicular traits used to predict body weight

Figure 5 represents the different testicular traits used to predict body weight. Out of 19 reviewed articles, the highest used trait was scrotal circumference with sixteen articles (n = 16), followed by testicular length (n = 11) and testicular width (n = 10), while the least used predictor was testicular circumference with only two articles (n = 2).

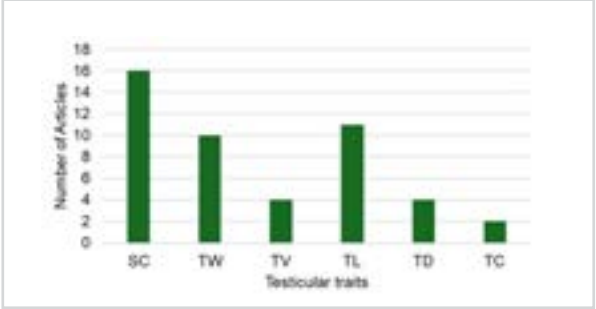

Figure 5 Most common testicular traits used to predict body weight

SC = Scrotal circumference,
TW = Testicular weight,
TV = Testicular volume,
TL = Testicular length,
TD = Testicular diameter,
TC = Testicular circumference

Distribution of articles using simple linear regression model to find testicular traits that best predict body weight

Table 2 indicates the distribution of articles that used simple linear regression model to find testicular traits that can be used to predict body weight. Out of nineteen (n = 19) articles, four (n = 4) articles used simple linear regression model. The findings showed that Akinyemi et al. (2014) demonstrated the highest predictive accuracy, with both testicular length and weight achieving a perfect goodness of fit (R^2 = 1.00). This indicates a strong correlation between the body weight and the testicular traits, making these models highly reliable for estimating body weight through the mentioned traits. For example, the Red Sokoto breed had lower goodness of fit values (R^2 ranging from 0.41 to 0.62), suggesting that the models may not explain the variability in these traits as effectively as observed in other breeds. The findings showed that Waheed et al. (2011) demonstrated a moderate predictive accuracy, with both testicular length and scrotal circumference achieving a goodness of fit (R^2 = 30.0 and 42.5). The scrotal circumference had a p-value ($P<0.05$) which indicated that it is an important factor in predicting body weight.

Table 2 The distribution of articles which used simple linear regression model to find testicular traits

				Goodness of fit		
Author and year	Breed	Traits	Model	R^2	RSME	P value
Raji *et al*., 2008	Red Sokoto	SL	Y = 1.344+0.634SL	0.602	-	P<0.01
		SC	Y = 4.206+0.563SC	0.517	-	P<0.01
		TWT	Y = 16.664+0.462TWT	0.414	-	P<0.01
		SL,SC,TWT	Y = 0.747+0.490SL+0.091SC+0.010TWT	0.625	-	P<0.01
	Borno White	SL	Y = 10.150+0.771SL	0.794	-	P<0.01
		SC	Y = 4.699+0.711SC	0.705	-	P<0.01
		TWT	Y = 14.544+0.676TWT	0.657	-	P<0.01
		SL,SC,TWT	Y = 9.151+0.689SL+0.091SC+0.	0.795	-	P<0.01
Akinyemi *et al*., 2014	West African Dwarf (Group A)	TL	Y = 0.819 + 0.1452SC	0.897	-	-
		TD	Y = -2.945 +3.546BW	0.772	-	-
		TV	Y = -3.134 + 3.447BW	0.698	-	-
		TW	Y = 13.758 – 0.759SC	0.683	-	-
		CAP	Y = -0.390 + 0.216BW	0.364	-	-
	West African Dwarf (Group B)	TL	Y = 7.866 + 0.252BW	0.585	-	-
		TD	Y = 2.877 + 0.060BW	0.388	-	-
		TV	Y = 15.458 +1.561BW	0.538	-	-
		TW	Y = 13.060 + 1.740BW	0.651	-	-
		CAP	Y = 0.700 + 0.169BW	0.700	-	-
		COR	Y = -0.047 + 0.069	0.631	-	-
	West African Dwarf (Group C)	TL	Y = 5.200 + 0.025PG	1.00	-	-
		TW	Y = -58.500 + 1.500HG	1.00	-	-
Lephuting *et al.*, 2024	Savanna	Sc	BW= -90.20 + 5.83 SC	0.81	108.80	-
		TL	BW = -76.62 + 8.1 TL	0.73	155.09	
		TD	BW = -1.417 +3.5 TD	0.18	474.41	
Mathapo and Tyasi, 2022	Boer	SC	Y = 8.55 +1.197SC	17.8	-	-
		TL	Y = 45.54 +0.29TL	0.00	-	-
Waheed *et al.*, 2011	Beetle	SC	Y = 0.322 + 2.654 SC + 0.98 Age	42.5	-	P<0.05
		TL	Y = 1.202 +1.805 TL +0.27 Age	30.4	-	NS

= Not indicated, SL = Scrotal length, SC = Scrotal circumference, TWT = Testicular weight, TL = Testicular length, NS = Not Significant, BCS = Body condition score, HG = Heart Girth, BW = Body weight, PG = Paunch Girth, WH = Wither height, TW = Testicular weight, TD = Testicular diameter, TV = Testicular volume, TDY = Testicular density, CAP = Caput weight, COR = Corpus weight, CAU = Caudal weight.

Correlation coefficient between body weight and testicular traits

Table 4 presents the association between testicular traits and body weight as reported in nineteen articles. Out of these nineteen (n = 19) articles, fifteen articles (n = 15) demonstrated significant positive correlations between body weight and several testicular traits, particularly focusing on scrotal circumference (SC), testicular length (TL), and testicular weight (TW). Notably, Khan et al. (2022) highlighted highly significant correlations, with a correlation coefficient of 0.80** for SC, reflecting a robust relationship between body weight and this trait. The results further indicate variation in the correlation strengths among the studies. Some articles reported very strong relationships, exemplified by Lephuting et al. (2024), who found a correlation coefficient of 0.90** for scrotal circumference (SC). In contrast, other studies, such as those by Ajani et al. (2015) and Kadam et al. (2020), presented moderate to weak correlations, suggesting a less pronounced association between body weight and testicular traits in those contexts. Additionally, research conducted by Ouchene-Khelifi and Ouchene (2021) yielded primarily non-significant or inconclusive results, reflecting a mixed correlation landscape that lacked clear trends.

Table 4 Correlation between body weight and testicular traits

Authors	Testicular traits										
	SC	TL	TD	TV	TWT	TT	Tl	SV	SCN	TW	SL
Mathapo and Tyasi et al., 2022	0.44^{*}	0.01^{*}	-	-	-	-	-	-	-	-	-
Waheed et al., 2011	0.43^{*}	0.30^{ns}	-	-	-	-	-	-	-	-	-
Khan et al., 2022	0.80^{**}	0.67^{**}	-	-	0.83^{**}	0.63^{**}		0.82^{**}	-0.22	-	-
Lephuting et al., 2024	0.90^{**}	0.86^{**}	-	0.42^{*}	-	-	-	-	-	-	-
Okere et al., 2014	0.61^{***}	-	-	-	-	-	0.18^{***}	-	-	-	-
Kabiraj et al., 2011	-	0.78^{*}	-	-	-	-	-	0.92^{**}	0.85^{**}	0.93^{**}	
Gemeda and Workalemahu, 2017	(Afar and LES) 0.54^{**} (Woyto – Guji) 0.66^{**}	0.82^{**} 0.95^{**}	0.78 0.92^{*}	0.60^{**} 0.41^{**}	0.90^{**} 0.82^{**}	-	-	-	-	-	-
Ouchene-Khelifi and Ouchene, 2021	0.85	0.72	0.84		0.75	-	-	-	-	-	-
Raji et al., 2008	0.67^{**}	-	-	-	0.67^{**}	-	-	-	-	-	0.74^{**}
Ajani et al., 2015	0.47^{**}	0.18	0.30^{*}	-	-	-	-	-	-	0.50^{**}	-
Pradip D. Kadam et al., 2020	(Beetle) 0.20s (Osmanabadi) 0.11^{ns}	-	-	-	-	-	-	0.62^{ns} 0.07^{ns}	0.30^{s} 0.14^{ns}	-	-
Ford et al., 2009	(Boer) 0.87^{**} (Kiko) 0.78^{**}	-	-	-	-	-	-	-	-	-	-
Obande et al., 2015	(Red sokoto) 0.92^{***} (WAD) 0.78^{***}	-	-	-	-	-	-	-	-	-	-
Alam et al., 2024	(Sirohi) 0.74^{**} (Jampari) 0.91^{***}	R - 0.64^{**} L - 0.56^{*} R - 0.91^{***} L - 0.92^{***}	R - 0.16 L - 0.23 R - 0.68^{**} L - 0.62^{**}	R - 0.22 L - 0.30 R - 0.98^{***} L - 0.86^{***}	-	-	-	-	-	-	-
Mekasha et al., 2008	0.61^{***}	-	-	-	0.51^{***}	-	-	-	-	-	-
Kabiraj et al., 2011	-	0.78^{**}	-	-	0.93^{**}			0.92^{**}	0.85^{**}	-	-

Authors	Testicular traits										
	SC	TL	TD	TV	TWT	TT	Tl	SV	SCN	TW	SL
Bilaspuri and Singh, 1992	0.87***	0.91***	-	0.84***	-	-	-	-	-	0.98**	-
Mathapo et al., 2024	-	-	-	-	-	-	-	-	-	-	-
Akinyemi et al., 2014	0.45**	0.69***	0.61***	0.66***	0.72***	-	-	-	-	-	-

_ = Not indicated, SL = Scrotal length, SC = Scrotal circumference, TW = Testicular weight, Tl = Testosterone level, NS = Not Significant, TWT = Testicular weight, TD = Testicular diameter, TV = Testicular volume, TT = Testicular thickness, TL = Testicular length, R = Right, L = Left, * = $P < 0.05$, ** = $P < 0.01$, , *** = $P < 0.0001$, SV = Sperm volume, SMC = Sperm concentration, S = Significant

DISCUSSION AND CONCLUSION

In the quest for enhanced goat breeding success, understanding the intricate relationship between body weight and testicular traits emerges as a crucial factor, offering farmers the potential to unlock improved fertility and productivity in their herds (Gemeda and Workalemahu, 2017). The objective of this systematic review was to systematically evaluate and synthesize existing research on the relationship between body weight and testicular characteristics in goats, aiming to identify key patterns and correlations that can inform breeding practices and reproductive management across diverse goat breeds and environments. Understanding this relationship can improve breeding strategies, enabling farmers to select animals with optimal reproductive potential based on easily measurable traits (Waheed et al., 2011). The findings by Mathapo and Tyasi (2022) showed that scrotal circumference had a positive statistically significant correlation with body weight, whereas testicular length had a non-significant correlation with body weight. The findings of Lephuting et al. (2024) demonstrated effective predictive models for scrotal circumference. On the other hand, the model for testicular diameter in the Savanna breed showed a significantly lower coefficient of determination. This indicates a poor fit, suggesting that testicular diameter is not a reliable predictor of body weight in this context. Mathapo and Tyasi (2022) reported coefficient of determination values for scrotal circumference and testicular length, indicating that the models for these traits are not effective predictors. The study highlighted that discrepancies in findings may be influenced by differences in goat breeds, emphasizing the need for breed-specific research (Ahmed and Kawmani, 2019). To the best of our knowledge, this is the first systematic review that focuses on estimating the relationship between body weight and testicular traits in goats. Therefore, there are no other systematic reviews available for comparison on this topic. Our results imply that scrotal circumference could be used to determine the live body weight of goats. The contribution of this study to the body of knowledge is to suggest that there is a relationship between body weight and testicular traits that exist in goats. The limitations of this systematic review include potential breed-specific variations that may affect the generalizability of the results to all goat populations, as well as the influence of nutritional and environmental factors on body weight and testicular measurements, which were not controlled or varied across the included studies. Hence, it is recommended to conduct further studies focusing on specific goat breeds to better understand how breed characteristics influence the relationship between body weight and testicular traits.

In conclusion, scrotal circumference is a practical and reliable alternative selection trait for breeding bucks, with clear implications for enhancing fertility and productivity in goat production systems. The establishment of a regression model using scrotal circumference to estimate body weight is also an important factor in breeding decisions. With the observed variability in outcomes across different studies, future research should consider the effects of breed and environment to refine our understanding of testicular traits in relation to fertility and body composition in male goats.

ACKNOWLEDGEMENTS

The authors express their gratitude to the University of Limpopo for supplying resources that enabled internet access.

CONFLICT OF INTEREST

The author declares that there is no conflict of interest.

CONTRIBUTIONS

All authors contributed equally to all aspects of the research, data analysis, and the preparation and writing of the manuscript.

REFERENCES

Akinyemi MO, Aina AJ, Ewuola EO, Osaiyuwu OH, Ajao EO. 2014. Relationships between body morphometrics and testicular biometrics of West Africa Dwarf bucks in southwestern Nigeria. Int J Agri Biosc, 3(6), 283-7.

Ford DJ, Okere C, Bolden-Tiller O. 2009. Libido test scores, body conformation and testicular traits in boer and Kiko goat bucks, ARPN J Agric Biol Sci, 4(5), 54-61.

Gemeda AE, and Workalemahu K. 2017. Body weight and scrotal-testicular biometry in three indigenous breeds of bucks in arid and semiarid Agroecologies, Ethiopia J Vet Med, 2017(1), 5276106. https://doi.org/10.1155/2017/5276106.

Kadam PD, Raut MR, Sontakke SH, Khadase JR. 2020. A study of age, body weight and scrotal circumference on semen production in buck. Int J Curr Microbiol App Sci, 9, 1284-88.

Kabiraj SK, Hoque SM, Khandoker MAM, Husain SS. 2011. Testicular biometry and its relationship with body weight and semen output of black Bengal bucks in Bangladesh. J Cell Anim Biol, 5(2), 27-32.

Kerketta S, Singh M, Patel BHM, Dutt T, Upadhyay D, Bharti PK, et al. 2015. Relationships between age, body measurements, testicular measurements and total ejaculation of semen in local goat of Rohilkhand region. Small Rumin. Res, 130, 193-6.

Khan A, Thakur MS, Joshi S, Shukla SN, Khare A, Khare V, et al. 2022. Association of body weight with testicular and semen quality parameters in Indian goat breeds. J Anim Sci Technol, 64(1), 45-52.

Lephuting K, Selala LJ, Mokoena K, Tyasi TL. 2024. Phenotypic correlation between body weight and testicular measurement traits of savanna breeding bucks. Adv Anim Vet Sci, 12(7), 1286-9.

Mathapo MC, Tyasi TL, Mugwabana TJ. 2025. Breeding objectives and trait preferences of Nguni goat farmers in Limpopo province, South Africa. Trop. Anim Health Prod, 57(2), 49.

Mathapo MC, Tyasi TL. 2022. Relationship between testicular traits, body measurements, and body weight in Boer goat bucks. Pak J Zool, 54(6), 2957. Doi: https://dx.doi.org/10.17582/journal.pjz/20210508200550.

Obande GE, Dawuda PM, Oyedipe EO, Odeh S. 2015. Correlation between scrotal circumference, age and live body weight in red sokoto and West African dwarf bucks. J Vet Sci, 10, 127-36.

Okere C, Keith L, and Bolden-Tiller O. 2014. The relationship between body conformation, testicular traits and serum testosterone levels in pre-pubertal male boer goat crosses. Am J Exp Agric, 4(12), 1812-19.

Ouchene-Khelifi NA, and Ouchene N. 2021. Relationships between age, body measurements, and testicular measurements in Arabia bucks in Algeria. Trop Anim Health Prod, 53(1), 91.

Raji AO, Igwebuike JU, and Aliyu J. 2008. Testicular biometry and its relationship with body weight of indigenous goats in a semi-arid region of Nigeria. ARPN J Agric Biol Sci, 3(4), 6-9.

Waheed A, Khan MS, and Ahmed AN. 2011. Relationships among testicular traits, body measurements and body weight in Beetal male goats in Pakistan. J Inst Sci Tech, 1(1), 59-62.

Procjena tjelesne mase korištenjem testikularnih osobina kod jaraca: Sistematski pregled

SAŽETAK

Razumijevanje odnosa između tjelesne mase i reproduktivnih osobina kod koza važno je za unapređenje praksi uzgoja i produktivnosti na farmama. Ovaj pregledni članak analizira postojeća istraživanja o povezanosti tjelesne mase i ključnih reproduktivnih osobina, kao što su obim skrotuma, dužina testisa i promjer testisa kod jaraca. Baze podataka poput Google Scholar, PubMed, ScienceDirect i Web of Science sistematski su pregledane, te je ukupno prikupljeno 650 članaka. Nakon selekcije, ukupno devetnaest (n = 19) relevantnih članaka odabrano je za detaljnu analizu. Studije su objavljene između 1992. i 2024. godine, pri čemu 26% (n = 5) potiče iz Indije. Sistematski pregled ističe značajne varijacije u primijenjenim metodologijama, uključujući prediktivne modele i regresione analize. Rezultati su pokazali da je jednostavni linearni regresioni model najčešće korišten za predviđanje tjelesne mase, u 21% (n = 4) uključenih članaka. Najveći koeficijent determinacije ($R^2 = 0,88$) zabilježen je za obim skrotuma korištenjem jednostavne linearne regresije kod jaraca. Ovi rezultati ukazuju na snažnu korelaciju između tjelesne mase i testikularnih osobina, čineći ove modele vrlo pouzdanim za procjenu tjelesne mase. Rezultati ovog sistematskog pregleda sugerišu da je obim skrotuma pouzdan pokazatelj tjelesne mase kod jaraca. Nalazi ove studije mogu pomoći farmerima sa ograničenim resursima u odabiru jaraca za reprodukciju i unapređenje njihove tjelesne mase.

Ključne riječi: Jarci, obim skrotuma, testisi, testikularne osobine, tjelesne mjere

REVIEW ARTICLE

Cardiomyopathies in veterinary medicine: A comprehensive review across canine, feline, and equine species

Jasmin Čaluk*[1], Ermin Šaljić[2], Selma Čaluk[1], Aida Bešić[2], Belkisa Izić[3], Muhamed Katica[2]

[1]Kardiocentar Outpatient Medical Center, Sarajevo, Bosnia-Herzegovina
[2]Department of Clinical Sciences Veterinary Medicine, University of Sarajevo-Veterinary Faculty, Sarajevo, Bosnia-Herzegovina
[3]Department of Nuclear Medicine, University Clinical Center Tuzla, Tuzla, Bosnia-Herzegovina

***Corresponding author:**
Prof. dr. Jasmin Čaluk

Address:
Kranjčevićeva 12, 71000 Sarajevo, Bosnia and Herzegovina
Phone: +38761280803
ORCID: 0000-0002-1932-7690
E-mail: j.caluk@gmail.com

Original Submission: 13 January 2026
Revised Submission: 02 March 2026
Accepted: 11 March 2026

How to cite this article: Čaluk J, Šaljić E, Čaluk S, Bešić A, Izić B, Katica M. 2026. Cardiomyopathies in veterinary medicine: A comprehensive review across canine, feline, and equine species. Veterinaria, 75(1), 13-26.

ABSTRACT

Cardiomyopathies constitute a major cause of morbidity, mortality, and performance limitation across veterinary species. Although the overarching concept of myocardial disease spans veterinary and human medicine, its phenotype, clinical consequences, diagnostic pathways, and therapeutic strategies differ substantially between dogs, cats, and horses. Dilated cardiomyopathy (DCM) and arrhythmogenic cardiomyopathy (ACM/ARVC) dominate in predisposed dog breeds and reflect a combination of heritable, nutritional, and metabolic influences. Feline cardiomyopathy is overwhelmingly defined by hypertrophic cardiomyopathy (HCM), a disease shaped by diastolic dysfunction, left atrial enlargement, and risk of arterial thromboembolism (ATE). Restrictive cardiomyopathy (RCM), though less common, carries a particularly poor prognosis due to its severe impairment of diastolic filling. In horses, clinically significant cardiomyopathies are predominantly acquired, often arising from myocarditis, systemic disease, or maladaptive athletic remodeling associated with high-performance training. Performance decline, exercise-induced arrhythmias, or poor recovery rather than overt heart failure often herald equine myocardial disease. Diagnosis across species is anchored in echocardiography, supported by electrocardiography, Holter monitoring, and cardiac biomarkers such as troponin and NT-proBNP. Therapeutic approaches range from evidence-based interventions—such as pimobendan in preclinical canine DCM and clopidogrel for feline ATE prophylaxis—to largely empirical management of equine myocarditis and arrhythmia. Early identification of high-risk patients, understanding species-specific disease trajectories, and recognizing which interventions meaningfully alter prognosis are central to improving long-term outcomes. This review synthesizes current knowledge regarding the biology, clinical expression, diagnostic evaluation, and evidence-supported treatment of cardiomyopathies in dogs, cats, and horses. Emphasis is placed on practical clinical decision-making, early recognition, and integration of species-specific considerations important for general practitioners, cardiologists, and equine performance clinicians.

Keywords: Cats, dogs, horses, echocardiography, ventricular dysfunction

doi.org/10.51607/22331360.2026.75.1.13

List of Abbreviations

ACM/ARVC –	Arrhythmogenic cardiomyopathy / Arrhythmogenic right ventricular cardiomyopathy
ACTH –	Adrenocorticotropic hormone
ATE –	Arterial thromboembolism
CHF –	Congestive heart failure
DCM –	Dilated cardiomyopathy
DNA –	Deoxyribonucleic acid
ECG –	Electrocardiogram
ELISA –	Enzyme-linked immunosorbent assay
HCM –	Hypertrophic cardiomyopathy
HOCM –	Hypertrophic obstructive cardiomyopathy
LA –	Left atrium
LV –	Left ventricle
LVOTO –	Left ventricular outflow tract obstruction
NT-proBNP –	N-terminal pro–B-type natriuretic peptide
PCR –	Polymerase chain reaction
RNA –	Ribonucleic acid
RCM –	Restrictive cardiomyopathy
VPC –	ventricular premature complex
VT –	Ventricular tachycardia

INTRODUCTION

Cardiomyopathies in veterinary medicine encompass a wide spectrum of primary myocardial disorders that impair systolic function, restrict diastolic filling, alter ventricular geometry, or predispose the heart to arrhythmias and sudden death. Although rooted in universal principles of myocardial pathophysiology, veterinary cardiomyopathies express themselves through species-specific patterns influenced by genetics, body size, athletic physiology, and even environmental and nutritional factors (Sasaki et al., 2017; Fuentes et al., 2020; Grzeczka et al., 2022). Dogs predominantly develop dilated cardiomyopathy (DCM) or arrhythmogenic right ventricular cardiomyopathy (ARVC), diseases that are often heritable and may remain occult for long periods (Payne et al., 2015; Meurs, 2017; Meurs et al., 2014; Zibetti et al., 2025). Cats most frequently develop hypertrophic cardiomyopathy (HCM), which is the leading cause of cardiac morbidity in the species and closely mirrors aspects of human HCM in its diastolic abnormalities and risk of thromboembolism (Kittleson and Côté, 2021; Grzeczka et al., 2024). Horses, in contrast, primarily experience acquired cardiomyopathies associated with myocarditis, systemic inflammatory conditions, toxic injury, or the cumulative effects of intensive athletic training (Mogg, 1999; Avison et al., 2025).

The impact of cardiomyopathy extends beyond structural changes to include debilitating clinical syndromes such as congestive heart failure (CHF), life-threatening arrhythmias, poor performance, collapse, and sudden cardiac death (Summerfield et al., 2012; Cunningham and Dos Santos, 2022). These outcomes have substantial welfare, economic, and performance implications, especially for working animals and equine athletes. Early diagnosis is critical but complicated by the often-silent progression of disease, particularly in cats and in certain dog breeds such as Doberman Pinschers (Matos et al., 2024; Shen et al., 2022).

Advances in veterinary cardiology have transformed diagnostic capabilities. Echocardiography is central to phenotype identification, while Holter monitoring and exercise ECG have become indispensable in recognizing arrhythmogenic conditions in dogs and horses (Grden et al., 2020; Meurs, 2017; Meurs et al., 2014; Zibetti et al., 2025). Cardiac biomarkers, including NT-proBNP and troponin, have facilitated screening and risk stratification in both small animals

and equine patients (Guillaumin, 2024; Nath et al., 2024). Recently, a relatively cost-effective, small, practical, and manageable smartphone-based digital stethoscope (DS) device has also been developed. It allows simultaneous recording of electrocardiographic and phonocardiographic traces directly on a smartphone (Bozzola et al., 2024). This represents a significant advantage over the traditional manual stethoscope, whose clinical utility is diminishing-particularly during the auscultation of cats that frequently purr throughout the respiratory cycle (Ferasin et al., 2022; Katica and Hadžimusić, 2023).

This review synthesizes current understanding of cardiomyopathies in dogs, cats, and horses (Table 1), emphasizing comparative pathophysiology, early recognition, evidence-based treatment, and prognosis. The goal is to provide a clinically oriented, species-specific guide for practitioners managing myocardial disease in their daily work.

Table 1 Overview of cardiomyopathy phenotypes across canine, feline, and equine species

DOGS (key phenotypes)	CATS (key phenotypes)	HORSES (key phenotypes)
Dilated CM (DCM)	Hypertrophic CM (HCM)	Myocarditis-related CM
Arrhythmogenic CM (ARVCM/ACM)	Restrictive CM	Exercise-associated maladaptive remodeling
	Risk of ATE	

Legend: ACM – Arrhythmogenic cardiomyopathy; ARVCM – arrhythmogenic right-ventricular cardiomyopathy; ATE – arterial thromboembolism; CM – cardiomyopathy; DCM – dilated cardiomyopathy; HCM – hypertrophic cardiomyopathy

Canine Cardiomyopathies

Dilated Cardiomyopathy

Overview and Pathogenesis

Dilated cardiomyopathy (DCM) is one of the most clinically important cardiac diseases in dogs, particularly in large and giant breeds such as Doberman Pinschers, Great Danes, Irish Wolfhounds, and Boxers (Peterson et al., 2021; Summerfield et al., 2012; Schober et al., 2022). It is characterized by progressive eccentric remodeling, reduced systolic function, activation of neurohormonal pathways, and eventual CHF or sudden arrhythmic death. Microscopically, DCM reflects myocyte degeneration, mitochondrial dysfunction, apoptosis, and interstitial fibrosis (Monnet et al., 1995; Shen et al., 2022).

Genetic predisposition is strongly supported, with heritable variants identified in several breeds (Meurs, 2017; Meurs et al., 2014; Zibetti et al., 2025). Nutritional factors, including taurine deficiency, carnitine deficiency in certain lines, and diet-associated cardiomyopathy linked to grain-free or legume-heavy diets—have gained increasing recognition (Shen et al., 2022). These nutritionally mediated forms may be reversible if identified early.

Clinical Presentation

The early course of DCM is frequently silent. Many dogs show no outward abnormalities until extensive myocardial degeneration has occurred (Summerfield et al., 2012; Sasaki et al., 2017). Owners may report subtle fatigue, decreased stamina, or occasional coughing. In Doberman Pinschers, ventricular arrhythmias often precede structural dilation, making syncope or episodic weakness the first presenting signs (Meurs, 2017; Cunningham and Dos Santos, 2022).

As disease progresses, dogs may develop left-sided CHF with pulmonary edema or biventricular failure with ascites. Auscultation may reveal a systolic murmur due to functional mitral regurgitation, a gallop rhythm, or arrhythmias. However, many dogs in the preclinical stage have completely normal auscultatory findings (Ware and Bonagura, 2020), highlighting the need for breed-based screening.

Diagnosis

Echocardiography is the gold standard for DCM diagnosis (Fig. 1), demonstrating LV dilation, reduced ejection fraction, fractional shortening, and often left atrial enlargement (Schober et al., 2022). Because normal LV dimensions differ among breeds, breed-specific reference ranges are essential (Fuentes et al., 2020).

Holter monitoring is critical, especially in Doberman Pinschers, to detect ventricular premature complexes (VPCs) and runs of ventricular tachycardia (VT) that may precede echocardiographic changes (Meurs, 2017; Cunningham and Dos Santos, 2022). A burden ≥300 VPCs/day is often considered abnormal in this breed (Meurs et al., 2014).

Cardiac biomarkers add value: NT-proBNP correlates with myocardial stretch, while cardiac troponin indicates active myocardial injury (Guillaumin et al., 2024).

Dietary history and taurine/carnitine profiling are indicated in potential nutritional DCM (Shen et al., 2022).

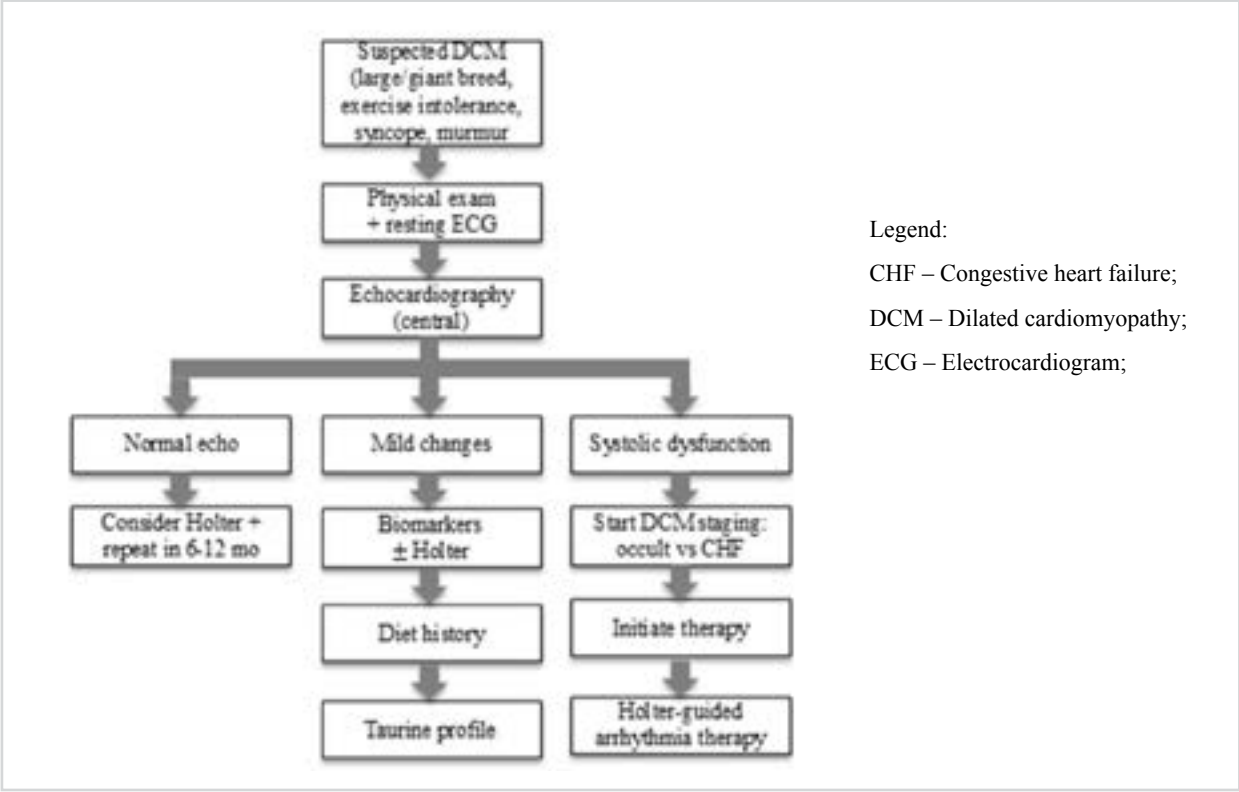

Figure 1 Diagnostic approach to suspected canine dilated cardiomyopathy

Therapy

Evidence-supported therapy for DCM is best established in dogs. The Protect study demonstrated that pimobendan significantly delays the onset of CHF or sudden death in Doberman Pinschers with occult DCM (Summerfield et al., 2012). Pimobendan is now the standard treatment once systolic dysfunction is documented.

In CHF, treatment includes furosemide, pimobendan, ACE inhibitors, and spironolactone (Fuentes et al., 2020). Arrhythmias requiring treatment may be managed with sotalol, mexiletine, or combination therapy (Cunningham and Dos Santos, 2022).

Nutritional DCM may improve with dietary correction and taurine/carnitine supplementation (Shen et al., 2022).

Prognosis

Outcomes vary by breed and disease stage. Doberman Pinschers often have the poorest prognosis due to malignant arrhythmias (Meurs, 2017). Once CHF develops, median survival typically ranges from several months to 1–2 years depending on response to therapy (Summerfield et al., 2012).

Arrhythmogenic Cardiomyopathy (ARVC/ACM)

Overview and Pathophysiology

Arrhythmogenic cardiomyopathy—classically arrhythmogenic right ventricular cardiomyopathy (ARVC)—is most commonly recognized in Boxer dogs but can occur in other breeds, including English Bulldogs and mixed breeds (Meurs, 2017; Cunningham and Dos Santos, 2022). It is defined by fibrofatty infiltration of the myocardium, particularly the right ventricle, creating an arrhythmogenic substrate that predisposes to ventricular premature complexes (VPCs), ventricular tachycardia (VT), syncope, and sudden death (Meurs et al., 2014). Genetic predisposition is strong (Ruiz-Guerrero and Barriales-Villa, 2018). A mutation in the striatin gene has been identified in Boxers, although genotype–phenotype correlations vary, and a negative genetic test cannot exclude disease (Adin et al., 2019; Meurs, 2017; Shen et al., 2022).

Clinical Presentation

ARVC is frequently occult during early stages. Many affected Boxers appear outwardly healthy and maintain normal activity levels despite significant arrhythmia burden (Cunningham and Dos Santos, 2022). The disease often manifests first as episodic syncope, weakness, or collapse. Owners may describe transient "staring spells," occasional disorientation, or short-lived episodes of unsteadiness following exertion (Meurs et al., 2014; Zibetti et al., 2025). Sudden death may be the initial presentation.

On examination, arrhythmias may be intermittently auscultated as irregular pulses or pulse deficits. Because resting ECG may be normal, ARVC often requires more intensive rhythm evaluation.

Diagnosis

Twenty-four-hour Holter monitoring is the cornerstone of ARVC diagnosis (Fig. 2). In Boxers, >100 VPCs/day is considered suspicious, and >300 VPCs/day increases concern for ARVC, while >1,000 VPCs/day or runs of VT strongly support diagnosis (Meurs, 2017; Cunningham and Dos Santos, 2022). Morphology of VPCs may be monomorphic or polymorphic, and complexity often correlates with disease severity.

Echocardiography can be normal early in the course but may later show right ventricular dilation, decreased right ventricular systolic function, or biventricular enlargement (Ware and Bonagura, 2020). In some dogs, ARVC progresses to a DCM-like phenotype with significant systolic dysfunction (Meurs, 2017).

Cardiac troponin may be mildly elevated in some cases, reflecting myocyte injury (Guillaumin, 2024).

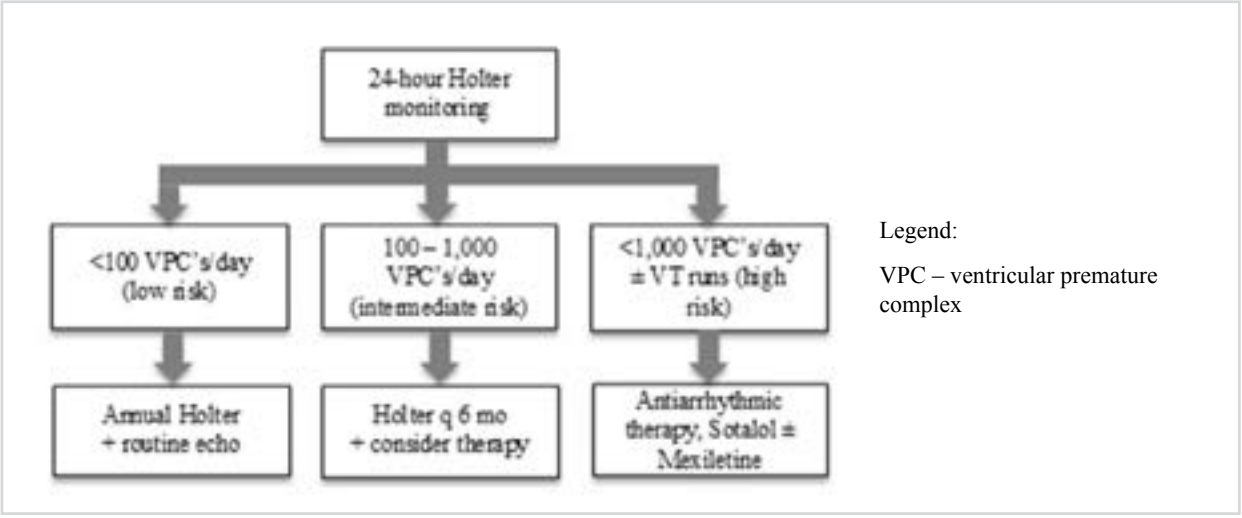

Figure 2 Holter-based ARVC risk stratification in Boxers

Treatment

Treatment focuses on suppression of ventricular arrhythmias and prevention of syncope or sudden death. Sotalol is typically first-line therapy and is effective in reducing VPC burden in many Boxers (Cunningham and Dos Santos, 2022). For severe cases, sotalol is combined with mexiletine. Atenolol is less effective for ARVC unless dynamic outflow obstruction also exists (Shen et al., 2022).

Exercise restriction is strongly recommended due to risk of VT during intense activity.

Dogs with structural progression may also require pimobendan and standard CHF therapy if systolic dysfunction evolves (Fuentes et al., 2020).

Prognosis

Prognosis varies considerably. Dogs with low to moderate arrhythmia burden can live many years with antiarrhythmic therapy (Cunningham and Dos Santos, 2022). Dogs with malignant VT, syncope, or biventricular involvement have significantly shorter survival times (Meurs, 2017).

Feline Cardiomyopathies

Hypertrophic Cardiomyopathy (HCM)

Overview

Hypertrophic cardiomyopathy is the most common cardiac disease of domestic cats, with prevalence estimates ranging from 10% to over 15% depending on population (Fuentes et al., 2020; Grzeczka et al., 2024). It is a primary myocardial disorder characterized by concentric left ventricular hypertrophy, impaired diastolic relaxation, and increased left atrial pressure that predisposes cats to CHF and arterial thromboembolism (ATE) (Guillaumin, 2024).

Genetic mutations in MYBPC3 are well documented in Maine Coon and Ragdoll breeds (Grzeczka et al., 2024), although the majority of domestic cats with HCM remain genetically uncharacterized.

Pathophysiology

Microscopically, HCM exhibits myocyte disarray, interstitial fibrosis, and small-vessel disease leading to ischemia and diastolic impairment (Casu and Prodi, 2014). These abnormalities increase ventricular stiffness, elevate filling pressures, and result in atrial stretch and enlargement (Sasaki et al., 2017). Some cats develop dynamic left ventricular outflow tract obstruction (LVOTO) due to systolic anterior motion (SAM) of the mitral valve—a subset known as HOCM (Fuentes et al., 2020).

Clinical Presentation

HCM is often silent. Many cats remain clinically normal for years, with diagnosis occurring incidentally during routine examination or pre-anesthetic screening (Hogan et al., 2015). When present, early signs include subtle lethargy, decreased jumping, or intermittent tachypnea during stress.

Progressive diastolic failure leads to CHF, manifesting as acute respiratory distress with open-mouth breathing, tachypnea, pulmonary edema, or pleural effusion (Fuentes et al., 2020). A gallop sound is a valuable and specific auscultation finding. Dynamic obstruction may produce a systolic murmur, although murmurs are not specific for HCM.

Aortic thromboembolism presents suddenly with hind limb pain, paralysis, hypothermia, and absent femoral pulses (Guillaumin, 2024).

Table 2 Echocardiographic differentiation of HCM, HOCM, and RCM in cats

HCM	HOCM	RCM
Thick LV walls	LV wall thickening	Normal/mild thickening
Small LV cavity	SAM of mitral valve	Severe LA enlargement
LA enlargement	LVOTO gradient ↑	Restrictive filling
Diastolic dysfunction	± Systolic murmur	Diastolic failure

Legend: ACM – CM – cardiomyopathy; HCM – hypertrophic cardiomyopathy; HOCM – hypertrophic obstructive cardiomyopathy; LA – left atrium; LV – left ventricle; LVOTO – left ventricle outflow tract occlusion; RCM – restrictive cardiomyopathy; SAM – systolic anterior motion

Diagnosis

Echocardiography is required to diagnose HCM (Table 2). Key findings include increased LV wall thickness (>5.5 mm in most cats), preserved or hyperdynamic systolic function, and left atrial enlargement (Fuentes et al., 2020). Doppler-echo evaluation identifies diastolic dysfunction or dynamic LVOTO.

Thoracic radiographs help confirm CHF but cannot differentiate cardiomyopathy forms.

NT-proBNP is valuable for distinguishing cardiac from respiratory causes of dyspnea (Guillaumin, 2024). Troponin elevation may indicate active myocardial injury and correlates with severity.

Treatment

Asymptomatic HCM

There is no proven disease-modifying therapy for asymptomatic cats without significant left atrial enlargement (Fuentes et al., 2020). Atenolol may be used in obstructive forms but has not demonstrated long-term benefit in non-obstructive disease.

Symptomatic HCM and CHF

Cats in CHF require:

- Oxygen
- Furosemide
- Thoracocentesis for pleural effusion

ACE inhibitors may be added, although evidence for their benefit remains mixed (Fuentes et al., 2020).

Atenolol or diltiazem can be used in HOCM to reduce LVOTO and improve filling (Casu and Prodi, 2014).

ATE Prevention

Clopidogrel is the preferred antithrombotic agent (Fig. 3), supported by the FAT CAT trial demonstrating superiority to aspirin (Hogan et al., 2015). Candidates include cats with:

- Severe LA enlargement
- Spontaneous echo contrast
- Previous ATE
- Markedly elevated NT-proBNP (Guillaumin, 2024)

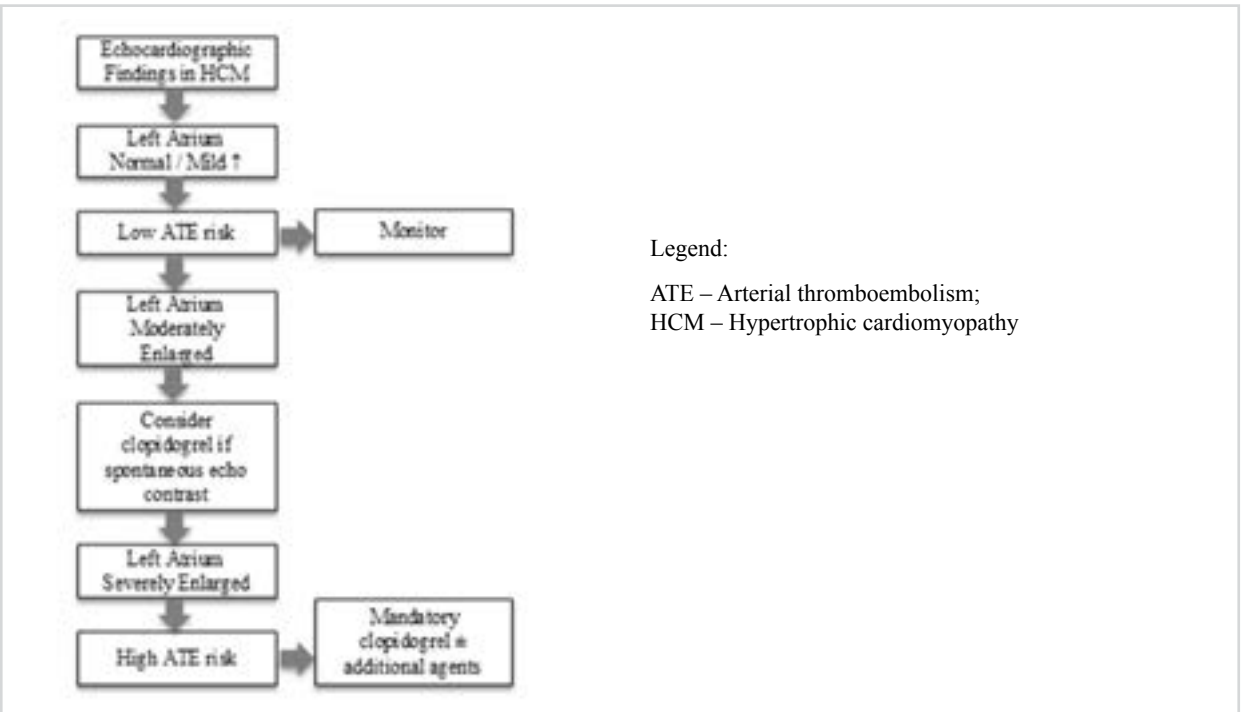

Figure 3 Risk stratification algorithm for arterial thromboembolism in cats

Prognosis

Prognosis is variable. Cats with mild HCM may live many years without progression (Fuentes et al., 2020). Severe left atrial enlargement or ATE confers a poor prognosis. Median survival after first CHF episode ranges from 6 months to 2 years, depending on management and severity (Hogan et al., 2015).

Restrictive Cardiomyopathy (RCM)

Overview and Pathophysiology

Restrictive cardiomyopathy is the second most important feline cardiomyopathy and is characterized by severe diastolic dysfunction with nondilated but stiff ventricles (Casu and Prodi, 2014). Endomyocardial fibrosis is a hallmark feature. Because the ventricle cannot fill properly, left atrial enlargement is typically marked.

Clinical Presentation

RCM frequently presents with CHF, significant left atrial enlargement, and high risk of ATE (Fuentes et al., 2020). Clinical signs mirror advanced HCM, including tachypnea, dyspnea, anorexia, or acute hind limb paresis.

Diagnosis

Echocardiography shows large atria, normal or minimally thickened ventricular walls, and restrictive transmitral flow patterns (Casu and Prodi, 2014). Radiographs reveal pulmonary edema or pleural effusion in CHF.

Treatment and Prognosis

Therapy parallels HCM with CHF: diuretics, cautious vasodilators, and antithrombotic therapy (Hogan et al., 2015). Ventricular compliance cannot be corrected, making prognosis guarded to poor. Median survival is typically shorter than HCM, often measured in months (Fuentes et al., 2020).

Equine Cardiomyopathies

Overview

Unlike dogs and cats, horses rarely develop primary inherited cardiomyopathies. Instead, most clinically important myocardial diseases in horses are acquired, arising from myocarditis, systemic disease, inflammation, toxins, or maladaptive remodeling secondary to intense athletic training (Mogg, 1999; Nath et al., 2024).

Cardiac disease in horses often first appears as decreased performance, poor recovery after exertion, abnormal sweating, or exercise-induced arrhythmias rather than overt signs of CHF (Avison et al., 2025).

Equine Cardiomyopathies (Continued)

Etiology and Pathogenesis

Myocarditis

Myocarditis is the most frequent cause of clinically relevant cardiomyopathy in horses and may arise from viral, bacterial, parasitic, immune-mediated, fungi or toxic etiologies (Mogg, 1999; Nath et al., 2024., Šaljić et al., 2020). Viral causes historically included equine influenza and equine herpesvirus, whereas bacterial sources include *Streptococcus spp., Clostridium spp.*, and endotoxemia associated with colitis or septicemia (Mogg, 1999). Parasitic burdens, including *Strongylus vulgaris* migration, may also contribute.

Inflammation results in myocyte necrosis, interstitial edema, and conduction abnormalities that predispose the horse to arrhythmias and exercise intolerance (Nath et al., 2024). Chronic myocarditis leads to myocardial fibrosis and long-term systolic dysfunction.

Systemic or Metabolic Injury

Systemic inflammatory disease, colic, endotoxemia, heat stroke, or severe electrolyte disturbances can cause myocardial injury through oxidative stress, calcium dysregulation, or microvascular dysfunction (Mogg, 1999). Horses with neurologic disease may develop catecholamine-associated myocardial injury similar to stress-induced cardiomyopathy in humans (Vitale et al., 2025).

Exercise-Associated Maladaptive Remodeling

Elite equine athletes undergo marked physiologic cardiac remodeling characterized by increased chamber size, wall thickness, stroke volume, and vagal tone (Avison et al., 2025). In some individuals, the transition from physiologic to maladaptive remodeling occurs when chronic high-intensity training produces fibrosis, conduction abnormalities, or arrhythmogenic substrate (Nath et al., 2024). The challenge for clinicians is distinguishing adaptive remodeling from early cardiomyopathy (Fig. 4).

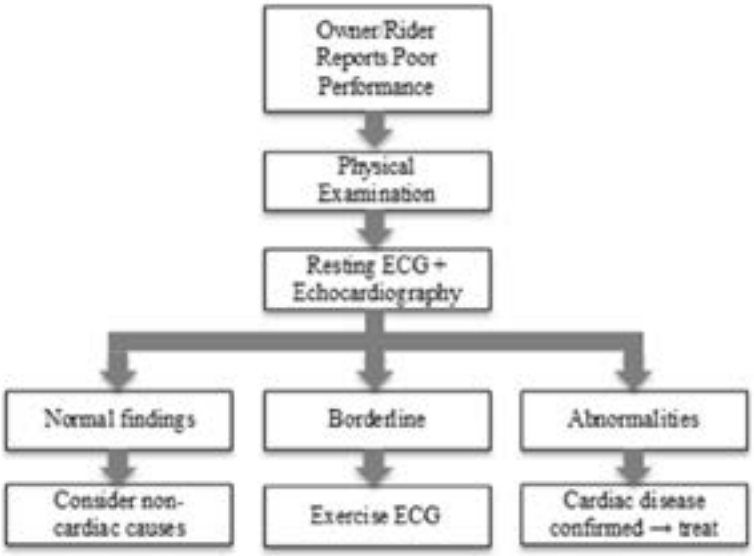

Figure 4 Algorithm 400 for Evaluating Performance Decline in Horses

Clinical Presentation

Clinical manifestations vary but often begin with:

- Performance decline (Avison et al., 2025)
- Exercise intolerance or early fatigue
- Excessive sweating or delayed recovery
- Exercise-induced arrhythmias (Nath et al., 2024)
- Coughing or respiratory effort (advanced CHF)
- Collapse or sudden death (severe arrhythmogenic disease)
- General weakness
- Tachycardia
- Uneven and irregular pulse
- Dyspnea
- Arterial hypotension

Because respiratory disease, orthopedic pain, or poor conditioning can mimic these findings, cardiac disease must be considered within a broad differential.

Diagnosis

History and Physical Examination

A detailed training history is essential. Duration of conditioning, competition level, frequency of high-intensity exercise, and recent systemic illness guide suspicion (Avison et al., 2025). Auscultation may reveal murmurs (often physiologic) or arrhythmias. Second-degree AV block at rest is common in healthy horses; persistence during exercise suggests underlying pathology (Nath et al., 2024).

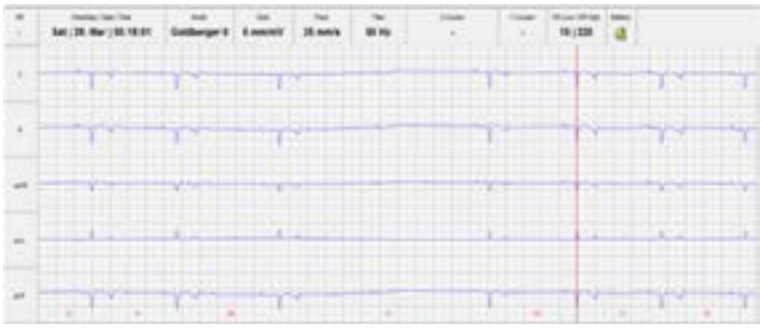

Figure 5 Second-degree AV block in a sport horse at rest

Electrocardiography

Resting ECG may identify premature atrial or ventricular complexes, but has limited sensitivity. **Exercise ECG** or continuous telemetry during exertion is critical for detecting arrhythmias that only manifest under load (Nath et al., 2024). Sustained or complex VT is highly concerning.

Echocardiography

Echocardiography evaluates chamber size, systolic function, wall motion, and pericardial effusion. Horses with maladaptive remodeling may demonstrate regional akinesia, hypokinesia, or reduced LV fractional shortening (Mogg, 1999; Nath et al., 2024). Significant atrial enlargement or valvular regurgitation (especially tricuspid) also raises concern.

Biomarkers

Cardiac troponin (Fig. 5) is an important indicator of myocardial injury (Nath et al., 2024). Mild increases may follow strenuous exercise, but persistent or marked elevations require further evaluation. NT-pro BNP is less well validated in horses but may assist in identifying myocardial stress.

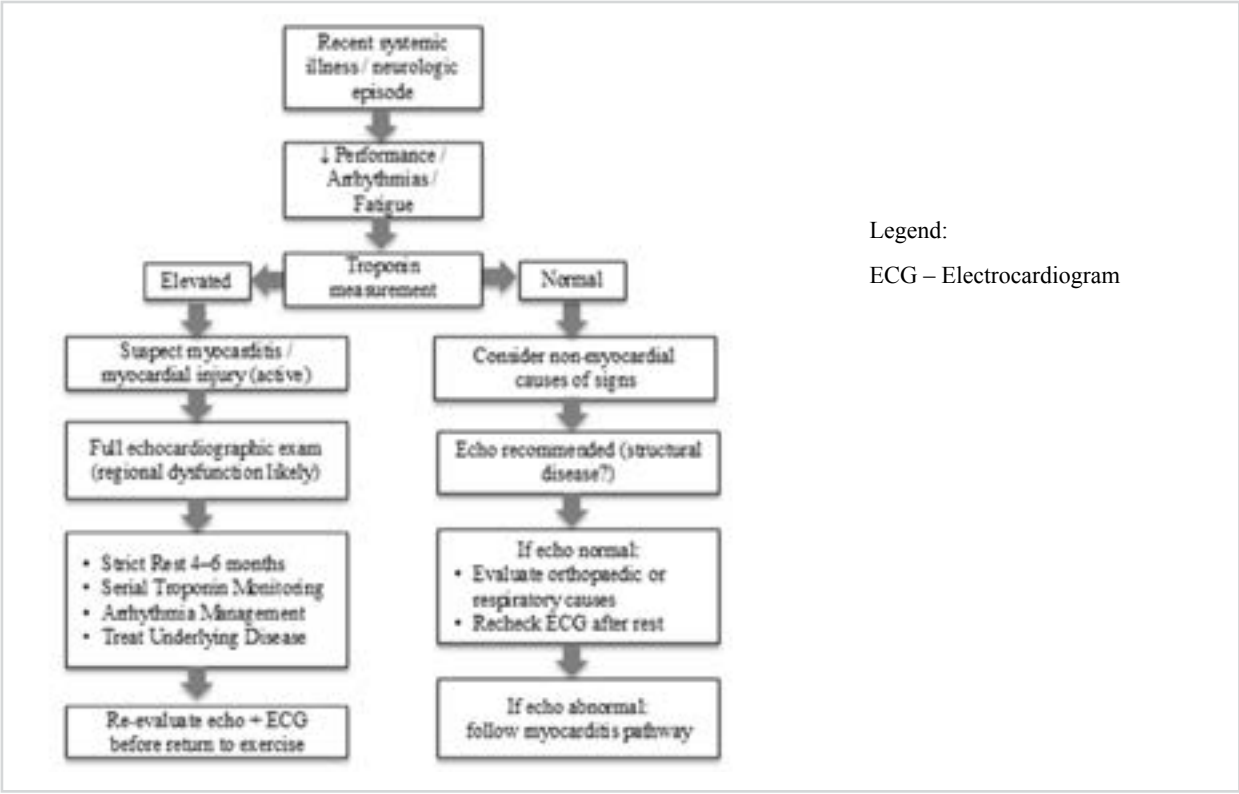

Figure 5 Diagnostic and management pathway for myocarditis-associated cardiomyopathy in horses

Additional Diagnostics

Endomyocardial biopsy is rarely feasible in equine practice due to procedural risks. Bloodwork may reveal inflammation, CK elevation, or electrolyte abnormalities.

Approach and Technique

Endomyocardial biopsy in horses is most commonly performed on the right ventricle.

The horse is kept standing and sedated

Vascular access is obtained via the jugular vein

A biopsy forceps (bioptome) is advanced into the heart under:

- echocardiographic guidance and/or
- fluoroscopic control (Decloedt et al., 2016).

Risks and Complications

Endomyocardial biopsy in horses is associated with several potential risks, including:

- Cardiac arrhythmias during the procedure
- Myocardial or ventricular wall perforation
- Hemopericardium
- Thromboembolism
- Infection (Decloedt et al., 2016).

Therapeutic Considerations

General Management Principles

Treatment of equine cardiomyopathy is often empirical and directed toward:

- **Resolving underlying disease**
- **Supporting myocardial recovery**
- **Controlling arrhythmias**
- **Preventing collapse during exercise**

Myocarditis Management

Strict rest is essential and often lasts 4–6 months (Mogg, 1999). Anti-inflammatory treatments, such as corticosteroids or NSAIDs, must be used judiciously due to variable evidence and risk of adverse effects. Specific therapy is indicated when an infectious cause is identified (Vitale et al., 2025).

Serial troponin measurements help track myocardial recovery.

Arrhythmia Management

Atrial fibrillation (AF) and ventricular arrhythmias can accompany cardiomyopathy.

- **AF** may be treated with quinidine or electrical cardioversion depending on duration and athletic expectations (Mogg, 1999).
- **Ventricular arrhythmias** require rest, correction of electrolyte disturbances, and in severe cases, antiarrhythmic therapy such as sotalol (Vitale et al., 2025).
- Exercise restriction is mandatory when ventricular arrhythmias are present.

Congestive Heart Failure

CHF is less common in horses but treated using furosemide, judicious vasodilators, and supportive care (Mogg, 1999). Long-term prognosis is guarded.

Comparative and Integrative Considerations Across Species

Distinguishing Primary vs Secondary Cardiomyopathy

Although cardiomyopathies in dogs, cats, and horses diverge in etiology, expression, and prognosis (Fig. 6), several unifying diagnostic and therapeutic principles apply across species. Understanding these integrative themes can improve clinical reasoning and the veterinarian's ability to recognize disease early.

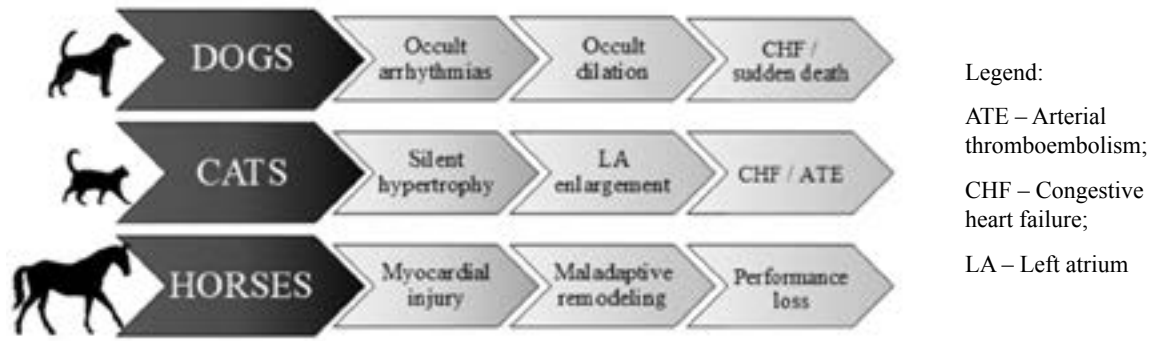

Figure 6 Comparative timeline of cardiomyopathy progression in dogs, cats, and horses

A recurring challenge is differentiating primary cardiomyopathy from secondary myocardial changes caused by systemic disease, pressure overload, endocrine disorders, or nutritional imbalance.

- **Cats:** Systemic hypertension, hyperthyroidism, followed by myocarditis, tumor infiltration (lymphoma), and pseudohypertrophy cause concentric hypertrophy that mimics HCM (Fuentes et al., 2020).
- **Dogs:** Taurine deficiency, carnitine imbalance, or diet-associated DCM can resemble idiopathic DCM but may be reversible (Shen et al., 2022).
- **Horses:** Systemic inflammatory disease or endotoxemia frequently precedes myocardial injury (Nath et al., 2024).

Correct classification determines prognosis and treatment approach.

Common Diagnostic Strategies

Echocardiography

Echocardiography is central across species. In dogs, LV dilation and reduced systolic function support DCM, whereas in cats, LV concentric hypertrophy with normal systolic function supports HCM (Fuentes et al., 2020). In horses, echo helps differentiate physiologic remodeling from cardiomyopathy-associated dysfunction (Nath et al., 2024).

ECG and Holter Monitoring

Holter monitoring is particularly valuable in:

- **Dobermans** for detecting occult DCM (Summerfield et al., 2012)
- **Boxers** for diagnosing ARVC (Meurs, 2017; Cunningham and Dos Santos, 2022)

In horses, exercise ECG is vital for arrhythmia detection (Avison et al., 2025).

Biomarkers

NT-proBNP supports differentiation between cardiac and non-cardiac dyspnea in cats and early detection of DCM in dogs (Guillaumin, 2024). Troponin is useful in detecting myocarditis across species (Nath et al., 2024; Vitale et al., 2025).

Therapeutic Principles Across Species

When Treatment Meaningfully Improves Outcomes

- **Dogs (DCM):** Pimobendan delays CHF and sudden death in occult DCM (Summerfield et al., 2012).
- **Cats (ATE):** Clopidogrel prevents ATE recurrence (Hogan et al., 2015).
- **Horses (Myocarditis):** Rest is the most critical intervention (Mogg, 1999).

When Treatment Has Limited Impact

- Advanced feline RCM often carries a poor prognosis despite optimal therapy (Casu and Prodi, 2014).
- Severe equine cardiomyopathy associated with extensive fibrosis responds poorly to medication (Nath et al., 2024).

Understanding these therapeutic boundaries is essential for compassionate, realistic client counseling.

ACKNOWLEDGEMENTS

The authors thank staff at University of Sarajevo - Veterinary Faculty, as well as colleagues and staff at Kardiocentar Outpatient Medical Center and the University Clinical Center Tuzla for their contributions and insights. No external funding was received for this work.

REFERENCES

Adin D, Defrancesco TC, Keene B, Tou S, Meurs K, Atkins C, et al. 2019. Echocardiographic phenotype of canine dilated cardiomyopathy differs based on diet type. J Vet Cardiol 21,1–9. https://doi.org/10.1016/j.jvc.2018.11.002

Avison A, Physick-Sheard PW, Pyle WG. 2025. Performance horses as a model for exercise-associated cardiac arrhythmias and sudden cardiac death. J Mol Cell Cardiol Plus, 12,100452. doi: 10.1016/j.jmccpl.2025.100452.

Bozzola C, Ortolina A, Guffanti I, Alberti E, Bronzo V, Zucca E. 2024. Evaluation of a digital stethoscope for electrocardiographic recording in donkeys: Preliminary results. J Equine Vet Sci, 135, 105048. doi.org/10.1016/j.jevs.2024.105048.

Bregoli M, Dediasi K, Pasolli C. 2006. Antibiotic resistant E.

coli in free-ranging alpine wild ruminants. In: VII Conference of the European Section of the Wildlife Diseases Association. pp. 78.

Casu G, Prodi A. 2014. Early myocardial responses in feline ischemic heart disease. J Feline Med Surg, 16, 201-8.

Cunningham SM, Dos Santos L. 2022. Arrhythmogenic right ventricular cardiomyopathy in dogs. J Vet Cardiol, 40, 156-69. Doi: 10.1016/j.jvc.2021.07.001. PMID: 34503916.

de Sousa FG, Pinto T, Marques AJ. 2025. Clinical, diagnostic, and therapeutic advances in feline hypertrophic cardiomyopathy. Vet Sci, 12(3), 289. doi: 10.3390/vetsci12030289.

Decloedt A, De Clercq D, Ven S, van der Vekens N, Chiers K, van Loon G. 2016. Right atrial and right ventricular ultrasound-guided biopsy technique in standing horses. Equine Vet J, 48(3), 346-51. doi: 10.1111/evj.12433.

Ferasin L, Ferasin H, Cala A, Creelman N. 2022. Prevalence and Clinical Significance of Heart Murmurs Detected on Cardiac Auscultation in 856 Cats. Vet Sci, 9(10), 564.

Fuentes VL, Abbott J, Chetboul V, Côté E, Fox PR, Häggström J, et al. 2020. ACVIM consensus statement on diagnosis and management of cardiomyopathies in cats. J Vet Intern Med, 34(3), 1062-77. Doi:10.1111/jvim.15747

Grden D, Gotić I, Šmit M, Crnogaj N, Brkljača Bottegaro K, Šimonji D, et al. 2020. Veterinarska stanica, 51(1), 33-45. Doi.org/10.46419/vs.51.1.4

Grzeczka A, Graczyk S, Pasławski R, Pasławska U. 2024. Genetic Basis of Hypertrophic Cardiomyopathy in Cats. Curr Issues Mol Biol. 46(8), 8752-66. Doi: 10.3390/cimb46080517

Guillaumin J. 2024. Feline Aortic Thromboembolism: Recent advances and future prospects. J Feline Med Surg, 26(6), 1098612X241257878. Doi: 10.1177/1098612X241257878.

Hogan DF, Fox PR, Jacob K, Keene B, Laste NJ, Rosenthal S, et al. 2015. Secondary prevention of cardiogenic arterial thromboembolism in the cat: The double-blind, randomized, positive-controlled feline arterial thromboembolism; clopidogrel vs. aspirin trial (FAT CAT). J Vet Cardiol. 1,306-17. Doi: 10.1016/j.jvc.2015.10.004.

https://doi.org/10.21542/gcsp.2018.28

Katica M, Hadžimusić N. 2023. Pathophysiological aspects of electrocardiogram and urinalysis. Univerzitetska knjiga; Sarajavo: Dobra knjiga. (In Bosnian).

King AS. 1993. Apparatus urogenitalis. In: Baumel JJ, King AS, Breazile JE, et al. (Eds), Handbook of Avian Anatomy: Nomina Anatomica Avium (2nd ed., pp. 329-390). Cambridge, USA: Nuttall Ornithological Club.

Kittleson MD, Côté E. 2021.The Feline Cardiomyopathies: 1. General concepts. J Feline Med Surg, 23(11), 1009-1027. doi: 10.1177/1098612X211021819.

Matos JN, Silva J, Regada S, Rizzo S, Beato MS, Basso C. 2024. Hypertrophic cardiomyopathy in a dog: a systematic diagnostic approach. J Vet Cardiol, 51, 1e8 doi.org/10.1016/j.jvc.2023.10.002

Meurs KM, Stern JA, Reina-Doreste Y, Spier AW, Koplitz SL, Baumwart RD. 2014. Natural History of Arrhythmogenic Right Ventricular Cardiomyopathy in the Boxer Dog: A Prospective Study, J Vet Int Med, 28(4), 1214-20, https://doi.org/10.1111/jvim.12385

Meurs KM. 2017. Arrhythmogenic Right Ventricular Cardiomyopathy in the Boxer Dog: An Update. Vet Clin North Am Small Anim Pract. 2017 Sep;47(5):1103-1111. Doi: 10.1016/j.cvsm.2017.04.007.

Mogg TD. 1999. Equine cardiac disease. Clinical pharmacology and therapeutics. Vet Clin North Am Equine Pract, 15(3), 523-34. Doi: 10.1016/s0749-0739(17)30130-x

Monnet E, Orton EC, Salman M, Boon J. 1995. Idiopathic dilated cardiomyopathy in dogs: survival and prognostic indicators. J Vet Intern Med, 9(1), 12-7. Doi: 10.1111/j.1939-1676.1995.tb03266.x

Nath LC, Saljic A, Buhl R, Elliott A, La Gerche A, Ye C, et al. 2024. Histological evaluation of cardiac remodelling in equine athletes. Sci Rep,14(1), 16709. doi: 10.1038/s41598-024-67621-6.

Papazoglou LG, Basdani E. 2015. Exploratory laparotomy in the dog and cat. https://www.cliniciansbrief.com/ (accessed 15 February 2026).

Payne JR, Borgeat K, Connolly DJ. 2015. Dilated cardiomyopathy in Dobermans: diagnostic considerations. J Vet Cardiol, 17, S283-S296.

Peterson EN, Hansson K, Lundgren J. 2021. Early predictors of heart failure in Doberman Pinschers with occult DCM. Acta Vet Scand, 63, 49. Doi: 10.1186/s13028-021-00591-7

Reef VB, Marr CM, Bowen MI. 2020. Equine Cardiology. 2nd ed. Hoboken, USA: Wiley-Blackwell.

Ruiz-Guerrero L, Barriales-Villa R. 2018. Storage diseases with hypertrophic phenotype. Glob Cardiol Sci Pract, 12(3), 28. Doi: 10.21542/gcsp.2018.28.

Šaljić E, Ćutuk A, Tandir F, Hrković-Porobija A. 2020. Bolesti kardiovaskularnog Sistema konja. UNSA-Veterinarski fakultet, Sarajevo; Dobra knjiga, 196 p. (In Bosnian).

Sasaki K, Mutoh T, Shirota K, Kawashima R. 2017. Cardiomyopathies in Animals (17th Chapter). In: Cardiomyopathies - Types and Treatments. Kirali K. (Ed.), IntechOpen, Doi: 10.5772/65060 (Available on: https://www.intechopen.com/chapters/52188), (Accessed: 20 January 2026)

Schober KE, Fox PR, Abbott J, Côté E, Luis Fuentes V, Novo Matos JN, et al. 2022. Retrospective evaluation of hypertrophic cardiomyopathy in 68 dogs. J Vet Intern Med, 36, 865-76.

Shen L, Estrada AH, Meurs KM, Sleeper M, Vulpe C, Martyniuk CJ, et al. 2022. A review of the underlying genetics and emerging therapies for canine cardiomyopathies. J Vet

Cardiol, 40, 2-14. Doi: 10.1016/j.jvc.2021.05.003.

Summerfield NJ, Boswood A, O'Grady MR, Gordon SG, Dukes-McEwan J, Oyama MA, et al. 2012. Efficacy of pimobendan in the prevention of congestive heart failure or sudden death in Doberman Pinschers with preclinical dilated cardiomyopathy (the PROTECT Study). J Vet Intern Med, 26 (6), 1337-49. Doi: 10.1111/j.1939-1676.2012.01026.x.

Vitale V, Velloso Álvarez A, de la Cuesta-Torrado M, Neira-Egea P, Vandecandelaere M, Tee E, et al. 2025. Can Acute Neurological Disease Cause Cardiomyopathy in Horses? Animals, 15(10), 1447. https://doi.org/10.3390/ani15101447

Ware WA, Bonagura JD. 2020. Cardiac performance in small animals with cardiomyopathy. Vet Clin North Am Small Anim Pract, 50, 917-37.

Zibetti FL, Waller SB, Santana GM, Guiot ÊG, Ramos HH, Magnabosco MW, et al. 2025. Arrhythmogenic Right Ventricular Cardiomyopathy in English Bulldog with Brachycephalic Obstructive Airway Syndrome (BOAS). Acta Sci Veterinariae, 53. Doi.org/10.22456/1679-9216.142097

Kardiomiopatije u veterinarskoj medicini: Detaljan pregled kod pasa, mačaka i konja

SAŽETAK

Kardiomiopatije predstavljaju glavni uzrok morbiditeta, mortaliteta i ograničenja performansi kod različitih životinjskih vrsta. Iako opći koncept bolesti miokarda obuhvata i veterinarsku i humanu medicinu, njen fenotip, kliničke posljedice, dijagnostički put i terapijske strategije značajno se razlikuju između pasa, mačaka i konja. Kod pasa, dilatativna kardiomiopatija (DCM) i aritmogenetska kardiomiopatija (ACM/ARVC) dominiraju u predisponiranim rasama i odražavaju kombinaciju nasljednih, nutritivnih i metaboličkih faktora. Kardiomiopatije kod mačaka su uglavnom definisane hipertrofičnom kardiomiopatijom (HCM), bolesti oblikovane dijastolnom disfunkcijom, proširenjem lijeve pretkomore i rizikom od arterijske tromboembolije (ATE). Restriktivna kardiomiopatija (RCM), iako rjeđa, ima posebno lošu prognozu zbog ozbiljnog oštećenja dijastolnog punjenja. Kod konja, klinički značajne kardiomiopatije su pretežno stečene, te često nastaju kao posljedica miokarditisa, sistemske bolesti ili maladaptivnog atletskog remodeliranja povezanim sa intenzivnim treninzima. Pad performansi, aritmije izazvane vježbom ili loš oporavak, a ne očigledno zatajenje srca, često nagovještavaju srčanu bolest kod konja. Dijagnoza kod svih vrsta oslanja se na ehokardiografiju, uz podršku elektrokardiografije, Holter monitoringa i srčanih biomarkera kao što su troponin i NT-proBNP. Terapijski pristupi kreću se od intervencija zasnovanih na dokazima – poput pimobendana kod pretkliničke DCM kod pasa i klopidogrela za profilaksu ATE kod mačaka – do uglavnom empirijskog tretmana miokarditisa i aritmija kod konja. Rano prepoznavanje pacijenata visokog rizika, razumijevanje bolesti specifičnih za svaku vrstu i prepoznavanje intervencija koje značajno mijenjaju prognozu ključni su za poboljšanje dugoročnih ishoda. Ovaj pregledni rad objedinjuje trenutno znanje o biologiji, kliničkom ispoljavanju, dijagnostičkoj evaluaciji i terapiji kardiomiopatija kod pasa, mačaka i konja. Poseban naglasak stavljen je na praktično kliničko odlučivanje, ranu detekciju i integraciju specifičnih faktora za svaku vrstu, što je važno za veterinare opće prakse, kardiologe i kliničare u oblasti performansi konja.

Ključne riječi: Mačke, psi, konji, ehokardiografija, ventrikularna disfunkcija

RESEARCH ARTICLE

Nebulized phenylboronic acid significantly improves body weight in newly hatched male chicks of light laying hen lines

Hrvoje Mazija[1,2*], Siniša Ivanković[1,3], Damir Đermić[1,3], Ernest Goldschmidt[1,5], Mirta Balenović[6], Zlatko Janječić[1,4]

[1]Croatian Institute for Experimental and Translational Oncology CIETO, 10040 Zagreb, Koledinečka 3, Croatia
[2]Faculty of Veterinary Medicine, University of Zagreb, 10000 Zagreb, Heinzelova 55, Croatia
[3]Ruđer Bošković Institute, 10000 Zagreb, Bijenička 54, Croatia
[4]Faculty of Agriculture, University of Zagreb, 10000 Zagreb, Svetošimunska 25, Croatia
[5]Goldschmidt Ltd., 10000 Zagreb, Otona Kučere 66, Croatia
[6]Poultry Center, Croatian Veterinary Institute, 10000 Zagreb, Heinzelova 55, Croatia

[*]**Corresponding author:**
prof. emer. dr. sc. Hrvoje Mazija
Address: Heinzelova 55 10 000 Zagreb/ Croatia
ORCID: 0000-0002-7547-1742
E-mail: mazija@vef.hr

Original Submission: 07 April 2025
Revised Submission: 21 October 2025
Accepted: 10 March 2026

How to cite this article: Mazija H, Ivanković S, Đermić D, Goldschmidt E, Balenović M, Janječić Z. 2026. Phenylboronic acid administered by the nebulization to newly hatched male chickens of light laying hens significantly improve their body weight. Veterinaria, 75(1), 27-38.

ABSTRACT

The aim of the study was to present a unique method to prevent the culling of male chicks of light laying hens by making them available for commercial use. A method for administering phenylboronic acid to chicks by nebulization is described. A group of 30 male chicks was exposed to FBA aerosol in a SONOVAC® device for 120 seconds and compared with two control groups of 30 chicks each (male and female) nebulized with saline solution. All chicks were fed identical diets: starter (20.37% protein) until 21 days of age, followed by finisher (17.72% protein) until 77 days of age. Housed on the floor, the chicks remained in optimal health. At 77 days of age, the mean body weight of the PBA group was 1681.07 g, compared to 1629.45 g in the control groups, with feed conversion ratios of 2.24 and 2.26 kg/kg, respectively. From day 42 onwards, the PBA group consistently achieved higher body weights than the control group, and exhibited lower feed conversion ratios.

These preliminary studies indicate significant potential for the economic utilization of male chicks of light laying hen lines. It is necessary to determine the optimal fattening duration, feed composition during the growing period, and assess the organoleptic and chemical properties of edible tissues to provide relevant practical indicators. The described procedure could significantly contribute to animal welfare, to which the member states of the European Union are committed. At the same time, it is a less expensive and more accessible method compared to those previously described in this context.

Keywords: Economic utilization, phenylboronic acid, male layer chicks, nebulization

doi.org/10.51607/22331360.2026.75.1.27

INTRODUCTION

According to EPRS (European Parliamentary Research Service), approximately 330 million newly hatched male chicks of light-line hybrids are culled annually in EU countries immediately after sexing. They are considered a by-product of future egg-laying hens, due to their slow growth and low body mass at the possible age of utilization (Rutt and Hornbek, 2024). Estimates for the world are significantly higher, and 7 billion male chicks are culled annually. The strict distinction between fattening hybrids and future egg-laying hens for consumption was described in 1959 (Wood-Gush, 1959; Buzala and Janicki, 2016). According to the EU regulation (Council Regulation 1099/2009) on the protection of animals, the maceration and gassing procedure is allowed for killing no later than 72 hours after laying (Rutt and Hornbek, 2024). We deliberately describe the methods used to cull male chicks in order to emphasize the need to preserve their lives, while also offering a procedure by which these chicks can be used economically. Suffocation of chicks is performed by enclosing them in plastic bags, whereas electrocution is killing by electric shock. On the other hand, maceration can be carried out by crushing between rollers or shredding with rotating knives. The most inhumane and most traumatic method for the staff is cervical dislocation. The EFSA (European Food Safety Authority) sees the maceration process as contrary to animal welfare due to a number of mechanical defects that can cause fear and suffering. For this reason, nine EU member states demanded a ban on the culling of male chicks in 2022.

Instead of culling male chicks, various methods of determining their sex before hatching (*in ovo* sexing) have been proposed. The difficulty in determining the sex of newly hatched chicks lies in the fact that only some light hybrid chicks - brown females and yellow males - can be distinguished by the color of their down. Therefore, determining the sex of chicks before hatching (*in ovo*), allows the removal of male embryos so that only female chicks hatch. *In ovo* identification and removal of male embryos is certainly a more humane approach to breeding future laying hens that prevents unnecessary suffering and pain of hatched male chicks. A general overview of current *in ovo* sex discrimination procedures in chickens, ducks, geese and quails was prepared by Jia et al. (2023). Invasive methods are based on determining molecular properties (chromosome content in the cell nucleus, detection of sex hormones in the allantoic fluid, evidence of RNA by PCR, genetic analysis of blastoderm cells). Non-invasive methods determine the acoustic properties of the embryo, its morphological characteristics, the shape of the eggshell, the arrangement of blood vessels in the chorioallantoic membrane, and they also use spectral analysis (Preusse et al., 2023), magnetic resonance, volatile component analysis, and others.

Very significant progress has been made in separating male and female chicken embryos in recent times. Preusse et al. (2023) described highly sensitive *in ovo* sexing of chickens by sequentially exposing fertile eggs to fluorescence light. After 93-106 hours of incubation, the eggs are sequentially exposed to fluorescence light at 532 nm and 785 nm. The sex-related differences in the fluorescence intensities are based on the embryonic hemoglobin synthesis. With the accuracy of 96% for sex determination, the hatching rate was not reduced. Similarly, Chen et al. (2025) described an early sexing method during the chicken embryonic development. Based on Loop-mediated isothermal amplification (LAMP), it targets the male chicken Z chromosome gene DMRT1. The LAMP amplicon is producing a fluorescent product detectable by a portable light apparatus. Fertilized eggs, after approximately 4 days of incubation, are exposed to LAMP, and the chromosome for male embryos is visually detected. A different approach is provided by Taylor-Smith (2023) who describes exposing fertilized eggs to specific sound vibrations during the first six days of incubation. The sound waves induce genomic changes, causing male chicks to develop ovaries and hatch as females. The same procedure has no effect on female chicks.

It is clear that all of the described tests are difficult to perform in production practice and are likely to be expensive. *In ovo* sex determination is justified when compared to all procedures that are carried out after hatching, as none of these methods allow the economic exploitation of hatched male chicks. After determining the sex of the embryos, the male chicks are removed from the incubator and can be used as a quality source of protein in livestock feed, pet food or in laboratory research (Dahm, 2022).

Another aspect of sex determination and male embryo removal is welfare, specifically regarding the feeling of pain at the moment the embyros are destroyed, often by culling. Therefore, it is imporant to know the exact moment at which the procedure should be performed. This research is significant for animal welfare,

particularly in the context of *in ovo* sex determination, where male embryos are identified and culled during incubation. The goal is to perform this procedure before the embryos are capable of consciously perceiving pain.

The comprehensive review by Mace and Knight (2025) on the development of pain perception in chick embryos indicates that the onset of such perception may be earlier than the commonly cited 13 days of incubation, although the review itself suggests that pain perception may commence around embryonic day 18 - three days before hatching - and possibly earlier.

The relevant literature is scarce and only recently describes any chemicals or agents that, when applied to the respiratory system of newly hatched male broiler chicks by nebulization, significantly increase their body weight until the period of economic exploitation. An exceptionally beneficial effect was achieved by the application of the pentadecapeptide BPC 157 (Mazija et al., 2024). A nebulization treatment of newly hatched male broiler chicks for 30 or 60 seconds significantly stimulated faster body weight gain compared to the control group. In 35 days, chicks exposed to the BPC 157 aerosol for 60 seconds achieved 2,297 grams with the lowest feed consumption (1.64 kg/kg), and the highest, 3,032 grams, at the age of 42 days but with a slightly higher feed consumption (1.73 kg/kg). At the same time, control chicks reached a weight of 2,230 g in 35 and 2,979 g in 42 days, respectively.

Phenylboronic or benzene boric or 6H5B(OH)2 acid (Anzai, 2016) is a white powder often used in organic synthesis. It is stable and easy to handle. Chagelishvili et al. (2023) used chelated forms of boron bound to methionine and glutamine. When applied to broiler chicks in feed and at different ratios of 50, 100 and 150 mg per kilogram, during 35 days of fattening, they showed a beneficial effect on daily and final body weight gain and feed conversion.

The success of this research prompted us to apply the same procedure but to male chicks of light hybrid hens. Namely, phenylboronic acid (FBA), an agent that we assumed, based on relevant data (Miller et al., 2001), could stimulate their faster growth to an extent that is economically justified. At the same time, it is an alternative to all the procedures described so far that prevent the culling of male chicks or, importantly , reduce the costs of incubating eggs of light hybrid hen lines before removing the males after sexing. The present study addresses this approach.

MATERIAL AND METHODS

Animals and applied methods

Male chicks of light Lohmann Brown hybrids were used in the experiment. A total of three groups, each consisting of 30 birds, were formed: two male groups (M) and one female group (F). Immediately after hatching, all chicks were vaccinated subcutaneously against infectious bursal disease virus (IBDV), and transported to the experimental facility at the Faculty of Agriculture, University of Zagreb, within 24 hours.

The male control group received physiological saline solution (SS) via nebulization, while the experimental male group (PBA) was treated with an aqueous solution of phenylboronic acid using the same method. The female group was administered SS following the same procedure. Birds were monitored daily throughout the experiment. No health issues were observed, except for a single mortality in the male SS control group on day seven, attributed to a non-specific mechanical cause.

At the end of the trial, all birds were individually weighed. Blood samples were collected by severing the jugular vein following cervical dislocation to determine specific serum IBDV antibody titers.

Ethics Committee Approval

This study was approved by the Ethics Committee of the Faculty of Agriculture, University of Zagreb, Croatia (No. 251-7-29-0111-22-2).

Animal welfare

The chicks were housed in the experimental unit of the Department of Nutrition, Faculty of Agriculture, which is exclusively designated for poultry research and is the only licensed facility in Croatia (JIBG HR 60185418). Birds were reared on litter flooring with hanging feeders and drinkers positioned along the walls. Room temperature was initially maintained using electric heaters according to the age of the birds until reaching the optimal 22°C. Ventilation was provided by natural gravitational airflow.

Ultrasonic nebulizer and administering FBA

The SONOVAC® device, which generates 95% of the aqueous suspension of vaccines with a diameter of 3-5 microns, was used. Nebulization, as a method of administering various vaccines or agents, has been extensively described as very effective, with a faster onset and achievement of longer-lasting specific

immunity (Ervaćinović, 2010; Mazija et al., 2010). In our study, a solution of 1 g FBA in 200 ml of water was used. This solution was placed in one of the heads of the SONOVAC® device, and the transport box with the chicks in two compartments (15 in each) was placed in the spray chamber. There they were exposed to the FBA suspension aerosol for the aforementioned 120 seconds. The same procedure was repeated with the control group and the group of females sprayed with distilled water.

Feeding of animals

Only two feed mixtures were used for standard fattening of chicks, the starter until the age of 21 days, followed by the finisher until the end of the experiment when the chicks were 77 days old. The chemical composition of these feeds is presented in Table 1.

Table 1 Chemical composition of feed used in chick feeding

A nutrient	Unit of measurement	Starter	Finisher	Mineral	Unit of measurement	Starter	Finisher
Proteins	%	20.37	17.72	Ca	%	0.98	0.54
Crude fiber	%	4.49	40.29	P	%	0.73	0.45
Ash	%	5.45	3.84	Na	%	0.196	0.158
Total fat	%	5.26	4..3	Cu	mg/kg	13.00	26.00
Water	%	11.15	12.91	Mn	mg/kg	110.00	130.00
Starch	%	42.33	46.33	Zn	mg/kg	144.00	14600
Sugar	%	3.96	299	Fe	mg/kg	362.00	244.00
				Mg	%	0.20	0.16
Metabolic energy	MJ/kg	12.54	12.35	K	%	0.1	0.683

Serological analyses

The serum anti-IBD antibody titers were determined as prescribed by the manufacturer in a commercial enzyme-linked immunosorbent assay (ELISA) kit (Idexx Laboratories Inc, Westbrook, ME, USA). Serum dilutions were prepared in a ratio of 1:500 (1 µL of serum in 500 µL of dilution). The optical density (OD) at a wavelength of 650 nanometers (nm) was measured using a microplate reader EL 800 Universal Microplate Reader (Bio-Tek Instruments, Inc, USA) and processed with the computer program "xChek Assay Management System" (Version 3.3., Idexx Laboratories, Inc, Westbrook, ME, USA). Antibody titers were determined by converting the sample/positive ratio according to a formula provided by the manufacturer, with a positive ELISA titer cut-off determined as 396.

Statistical analysis

Data exhibited a hierarchical longitudinal structure with repeated measurements nested within birds and birds nested within subgroups (pens). Subgroups were considered experimental units for treatment allocation. Body weight data were analyzed using linear mixed-effects models with subgroup and bird identity as random effects and treatment group, time, and their interaction as fixed effects. A first-order autoregressive covariance structure was applied to account for correlation among repeated measurements within birds over time.

Daily weight gain was analyzed using analogous mixed models. Feed conversion ratio (FCR) and production efficiency indices were derived variables based on weight gain and feed intake and were therefore evaluated descriptively and, where appropriate, analyzed at the subgroup level. ELISA antibody titers were log-transformed prior to analysis to account for right-skewed distributions and compared among groups. Estimated marginal means were compared using Tukey-adjusted post hoc tests where applicable. Statistical significance was set at $p < 0.05$.

RESULTS

We have already mentioned that the health of the chicks during the experiment was optimal, so in the SS M control group, at the age of seven day,s one chick (0.3%) died, while no deaths were recorded in the PBA or female groups. The procedure for applying FBA or SS did not negatively affect the behavior of the chicks.

The success of feeding the chicks over 11 weeks is shown in Tables 2 and 3. From the achieved results, the EPEF (European Production Efficiency Factor) was calculated according to the equation (Huff et al., 2013):

EPEF = Average daily gain (grams) x % survival/ Feed conversion (kg/kg) x 10

Table 2 Dynamics of body weight gain of male and female chicks in the control and experimental groups (grams)

Age - days	SS M*	PBA M**	SS F*
1	38.80	38.00	36.63
7	97.76	95.90	78.68
14	137.66	143.03	118.54
21	258.86	263.07	208.86
28	391.93	406.77	301.93
35	525.31	508.80	406.21
42	663.72	694.97	522.93
49	817.97	875.03	658.93
56	1010.83	1075.33	798.04
63	1190.48	1251.57	922.82
70	1431.03	1452.14	1076.07
77	1629.45	1681.07	1105.40

* SS - physiological saline solution

** PBA - phenylboronic acid

Mixed-effects analysis confirmed a significant effect of time on body weight ($p < 0.001$), reflecting normal growth patterns. Body weights differed descriptively among groups over time, with final mean values of 1629.45 g in SS M, 1681.07 g in PBA M, and 1105.40 g in SS F chicks. Estimated marginal means demonstrated numerically higher body weights in the BA M group from day 42 onward, consistent with descriptive trends. From the first day of life, female chicks were 1.37 g lighter than male chicks, and this difference persisted until the end of the experiment at the age of 77 days. Only at the age of 35 days were male chicks given SS 16.5 g heavier than those given FBA.

From the results shown (Table 1), body mass values were extracted for the periods 1–21 days, when chicks consumed the initial feed mixture, and 22–42 days, when fattening chicks typically consumed the finishing meal. Separately, values were provided for the period 22–77 days, when they consumed only the finishing mixture, and finally for the overall conversion using both meals over 1–77 days (Table 3). This was done to establish guidelines for the use of feeds with different compositions during extended chick fattening. The following tables present the daily body weight gain of chicks (Table 3) and the feed conversion during the experiment (Table 4).

Table 3 Daily body weight gain of chicks during rearing (g)

		Daily gain	
Experimental group (% survival)	SS M (99.79 %)	PBA M (100 %)	SS F (100 %)
Age - days			
1-21 (21)	11.58	11.85	9.06
22-42 (20)	22.18	21.60	15.70
22-77 (55)	25.63	26.47	16.30
1-77 (77)	21.21	21.91	14.24

Table 4 Feed conversion (kg/kg) during the weekly period of chick rearing

Experimental group	SS M	PBA M	SS F
Age - days			
7	3.16	2.96	2.90
14	1.83	1.66	2.06
21	1,89	1.99	1.67
28	2.07	2.00	2.42
35	2.85	2.79	2.90
42	2.65	2.06	2.60
49	2.74	2.30	2.79
56	3.32	3.13	3.29
63	3.83	3.56	3.80
70	3.69	3.56	3.96
77	4.12	3.55	4.52

Except at 21 days of age, chicks in the PBA group had lower feed conversion compared to both control groups (SS M and SS F).

Table 5 Feed conversion in chicks (kg/kg) of different groups during selected growing periods

	Feed conversion (k/kg)		
Experimental group	SS M (9.79%)***	PBA M (100%)***	SS F (100%)***
Age - days			
1-21 (21)*	1.71	1.64	1.96
22-42 (20)**	2.52	2.28	2.64
22-77 (55)**	3.16	2.87	3.25
1-77 (77)**	2.44	2.26	2.61

(*initial, ** final, *** % survival)

Chicks in the PBA group consumed the least amount of feed for weight gain during the described periods compared to other groups. Because FCR and EPEF are derived from primary production variables, these metrics were interpreted descriptively at the subgroup level. Across all periods, the PBA M group consistently exhibited lower FCR and higher EPEF values compared with control groups, indicating improved production efficiency.

The following table (Table 6) shows the EPEF of the chick groups during different fattening periods, in order to determine the justification for the duration of breeding male chicks of light hybrid lines.

Table 6 EPEF of the chicken group in the experiment during the experiment period

Experimental group	SS M	PBA M	SS F
Age - days			
1-21	67.52	72.04	46.09
22-42	88.02	94.74	59.47
22-77	81.11	92.23	50.15
1-77	86.67	96.96	54.40

In all described periods, the group of chicks exposed to FBA achieved the highest EPEF values.

Serological test result

The blood serum of chicks from all three experimental groups contained specific antibodies for infectious bursal disease virus (IBD), but in different titers. Table 7 shows the average values of ELISA titers at the age of 77 days when the chickswere sacrificed.

Table 7 Values of ELISA titers of specific antibodies for IBD virus in blood serum of chicks from experimental and control groups at the age of 77 days

M-SS	M-PBA	F-SS
1469	1060	2266
4240	943	2144
1187	2266	1998
3494	3152	1481
1363	3190	876
1351	2376	336
455	2253	2328
943	3582	4967
1563	1327	2825
2876		3126

* all sera contained specific antibodies

** one serum from each of these groups did not contain antibodies to the IBD virus

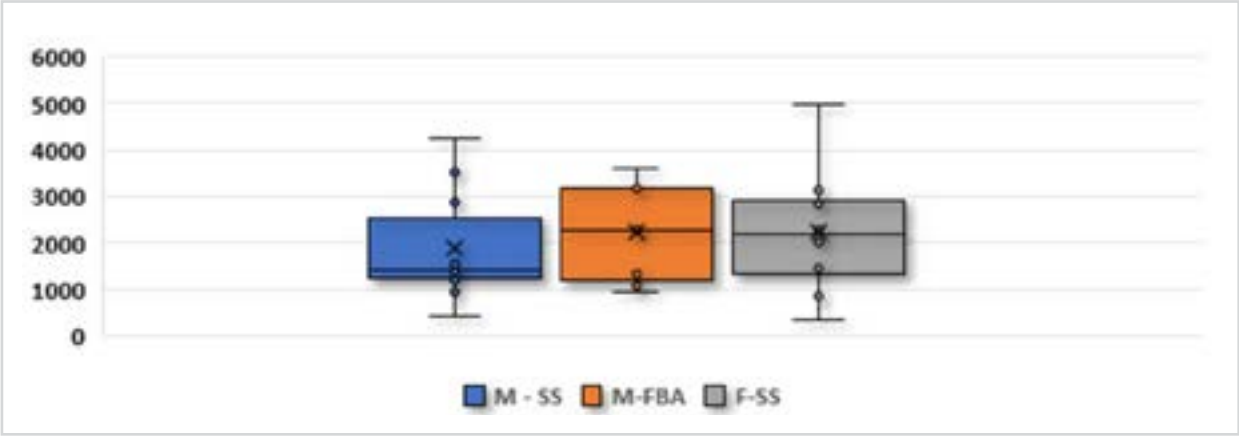

Figure 1 Comparison of ELISA titers of IBD virus in blood serum in chicks at the age of 77 days

ELISA titers were right-skewed and therefore analyzed following logarithmic transformation. Analysis of log-transformed titers showed no statistically significant differences among groups ($p = 0.691$). Descriptively, mean antibody titers were lowest in SS M chicks, whereas the M-PBA and SS F groups showed similar values. The lowest mean titer was observed in male chicks treated with SS M. The M-PBA and SS F groups had similar mean titers, both higher than SS M. Variability remained considerable in all groups, and these descriptive differences were not statistically significant.

DISCUSSION AND CONCLUSION

Sexing of light-line hybrid chicks, which are future layers, while still *in ovo* during incubation, represents an economic loss regardless of the method. It comes down to numerous factors, including the costs of raising parent flocks of layers to sexual maturity, incubating eggs, and the possible application of the procedure for sexing embryos either *in ovo* or, which is the most expensive and inhumane, culling already hatched male chicks.

The use and feeding of male chicks of light hybrids is possible, but with varying success, as evidenced by a number of studies. All of them report a slow increase in body weight of chicks and the achievement of slaughter weight (1096.00 g) at an age of mainly 9-10 weeks (Popova et al., 2022, Damme and Ristic, 2003).

This research represents an original and different approach to accelerating the growth and weight gain of male light hybrid chicks. It differs in the fact that the substance used for this purpose is phenylboronic acid (FBA), which has no harmful effects on the health of poultry or other animals. In fact, its antitumor effect is mentioned (Li et al., 2022; Bradke et al., 2008). Furthermore, there is a new approach in the application of FBA by nebulization (Mazija, 1997), with the most significant aspect being its single administration to newly hatched chicks while still in the hatchery. This approach enables the use of the procedure in practically all production settings, including large-scale farms, small hatcheries, distribution to small poultry farmers in rural areas, free-range breeding and similar contexts. Nebulization, the application of very fine particles of a mainly aqueous suspension of vaccines or other preparations, has been described by Mazija and Štimac (1999), and Ervaćinović et al. (2010). Recently, Čukelj et al. (2024) compared two methods of vaccinating newly hatched broiler chicks against Infectious Bursal Disease. The Winterfield 2512 vaccine, in complex with specific protective immunoglobulins, was administered either intramuscularly as recommended by the manufacturer or by nebulization. The time required for vaccination was significantly reduced compared to parenteral vaccination, replacing five workers for the same number of chicks. Compared to male chicks in the control group, those treated with FBA at the age of 21 days, by which time they were all eating the initial feed, achieved a greater body weight gain of 4.21 grams compared to the SS M group and 55.21 grams compared to the SS F (Table 2). At the age of 42 days, the usual duration of broiler fattening, the difference between the groups increased: the PBA group reached a weight of 694.97 g, which is 31.25 g more than the SS M chicks and 72.04 g more than the SS F. The final weight achieved by PBA chicks in the 11th week of life is 1681.07 g, 51.62 more than the SS M and even 575.40 g than the SS F chicks. These results are comparable to those described by Popova et al. (2022) who also fed male Lohmann Brown hybrid chicks continuously with a mixture containing 20.00% protein, achieving body weights of 427.71 g in the fifth week and 1115.93 g in the ninth week. In a subsequent study (Popova et al., 2023), similar results were obtained , with body weights of 329.00 g in the fifth week and 1096.00 g in the ninth week, representing lower performance compared to the results observed in the present study. Compared to the SS M and SS F groups, the chicks achieved the greatest body weight gain (Table 2), reaching 263.07 grams, which is 4.21 grams more than the SS M group and 55.21 grams more than the SS F group.

At 42 days of age, the usual age for the utilization of broiler chicks, the PBA M group achieved an average weight of 694.97 g, which is 31.25 g more than the chicks of the SS M group and 72.04 g more than the female chicks (SS F). The final body weight of the PBA M chicks achieved at the 11th week was 1681.07 g, 51.62 g more than the SS M chicks and even 575.40 g more than the female chicks (SS F). The described success is significantly more favorable than that described by Lumbo et al. (2024). At 45 days of age, chicks fed either free range or "organic" feed (OF) had identical body weights of 0.52 kg. At 59 days, their weights were 0.72 kg and 0.75 kg, at 87 days 1.13 kg and 1.01 kg, and at the end of fattening on day 101, 1.30 kg and 1.21 kg, respectively. The feed conversion of free-range chicks at the age of 45 to 87 days was 4.25 kg and 5.64 kg in OF chickens. From day 45 to day 101 of life, total weight gain was 4.83 kg and 5.73 kg, respectively. These results are significantly less favorable than those described using FBA. Of particular note is the lower feed consumption required to achieve weight gain in PBA chicks (Tables 4 and 5) throughout the entire trial period. This results in higher EPEF of chicks in the PBA group (Table 6) during all 77 days of the experiment.

The level of specific ELISA antibodies for IBD (Table 7) partly supports the data reported by Leitner et al. (2002). The titer at the end of the experiment was the lowest in

SS M chicks, whereas M-FBA and SS F chicks showed similar mean values. Although numerically higher titers were observed in M-PBA and SS F groups compared with SS M group, these differences were not statistically significant. Furthermore, the highest body mass was observed in PBA M chicks (1681.07 g) compared to 1629.45 g (SS M) and female chicks (1105.4 g). This is consistent with the finding that female chicks achieve higher serum antibody titers at an earlier age (Van der Most et al., 2011). In the present study, this pattern should be interpreted cautiously, since the serological differences among groups were descriptive rather than statistically significant. The relevant literature does not mention the immunomodulatory effect of FBA, making this the first study to describe it.

In conclusion, it should be emphasized that these are preliminary studies which indicate that the application of phenylboronic acid via nebulization to newly hatched male chicks of light hybrid hens promotes greater body weight gain, thus increasing their economic suitability for meat production. While the observed effect on the immune response is suggestive, it was not statistically confirmed in the present dataset. Moreover, FBA enhanced feed efficiency. In addition, the described procedure reduces the cost of producing laying hens for egg consumption and, most importantly, allows for the prevention of culling male chicks by enabling their removal from production before hatching. Thus, the procedure provides significant for animal welfare while also supporting increased food production, which could help alleviate hunger in less developed countries.

Future research should more closely and accurately determine the organoleptic and other properties of meat and edible offal of male chicks to which FBA was applied, which we only anecdotally believe are more favorable compared to meat from fattening chickens. It is also necessary to determine the most favorable content and dynamics of changes in the composition of feed mixtures, and finally determine the optimal dose of FBA.

The process we are applying aims to transform the current unacceptable practice, from an animal welfare perspective, of culling male chicks under EU guidelines, into an ethical and commercially viable substrate. Its particular significance is underscored by the findings of Danish scientists from the University of Copenhagen (21 March 2024, Researcher: “Seven billion newly hatched chicks are killed every year – but a ban is not the solution”), who explain in detail why banning the culling of male shallow hybrids is not an acceptable solution. This is mainly because many male chicks are exported to countries where they are raised in entirely unethical conditions until they reach a body mass suitable for meat consumption. The solution would be to produce only female chicks, which can be achieved by removing male embryos at various stages of incubation. Finally, the damage caused by incubating eggs and killing newly hatched or *in ovo*-identified male chicks is estimated at US$1 per egg, which is a sufficiently convincing reason to continue the study we presented. Although mixed-effects analysis did not demonstrate statistically significant differences between the PBA M and SS M groups at the predefined significance level, consistent numerical advantages in body weight gain, feed efficiency, and EPEF were observed in PBA-treated chicks. Given the relatively small subgroup sample size, these findings should be interpreted as biologically relevant trends warranting confirmation in larger-scale studies.

ACKNOWLEDGEMENT

The authors express their gratitude to the staff of the Department of Nutrition, Faculty of Agriculture, Zagreb, for their generous help in maintaining optimal conditions for the chicks in the experiment. Special thanks to the technician at the Poultry Centre, Veterinary Institute, Zagreb, who performed the blood testing.

CONFLICT OF INTEREST

The authors declared that there is no conflict of interest.

CONTRIBUTION

Conception: HM, SI; Supervision: SI, DĐ; Fundings: EG, ZJ; Materials: SI, DĐ; Data Collection and/or Processing: MB, ZJ; Analysis and Interpretation of the Data: MB, ZJ; Literature Review: EG; Writing: HM; Critical Review: HM

REFERENCES

Anzai JI. 2016. Recent progress in electrochemical biosensors based on phenylboronic acid and derivatives. Mater Sci Eng C Mater Biol Appl, 1(67), 737-46. doi: 10.1016/j.msec.2016.05.079.

Arciniega-Martínez IM., Romero-Aguilar KS, Farfán-García ED, García-Machorro J, Reséndiz-Albor AA, Sorino-Ursua MA et al. 2022. Diversity of effects induced by boron-containing compounds on immune response cells and on antibodies in basal state. J. Trace Elem Med Biol 69, 126901, doi: 10.1016/j.jtemb.2021.126901

Baldinger L, Bussemas R. 2021. Dual purpose production of eggs and meat - Part 1: cockerels of crosses between layer and meat breeds achieve moderate growth rates while showing unimpaired animal welfare. Org Agr, 11, 489–98.

Bradke TM, Hall C, Carper SW, Plopper GE. 2008. Phenylboronic acid selectively inhibits human prostate and breast cancer cell migration and decreases viability. Short Communication. Cell Adhes and Migr 2, 3, 153-60.

Brümmer N, Christoph-Schulz I, Karolina Rovers A. 2018. Consumers' Perspective on Dual-purpose Chickens as Alternative to the Killing of Day-old Chicks. Int J Food System Dynamics, 9(5), 390-8. doi: http://dx.doi.org/10.18461/ijfsd.v9i5.951390

Buzala M, Janicki B. 2016. Review: effects of different growth rates in broiler breeder and layer hens on some productive traits. Poult Sci, 95, 2151-9.

Chagelishvili GA, Chkuaeli A, Chagelishvili AA, Beshkenadze IA, Klarjeisvili NA, Gogaladz MA, et al. 2023. Synthesis of boron chelates and their usage in broiler feeding. World J Adv Res Rev, 19(01), 19-27. doi: 10.30574/wjarr.2023.19.1.1277

Chen Q, Su C, Li S, Zhang Z, Yang Y, Yang Y et al. 2025. A sensitive and rapid visual method of chicken sexing based on LAMP-CRISPR/Cas12a system. Brit Poultry Sci. 2025 Aug;66(4):531-538. doi: 10.1080/00071668.2025.2454963..

Čukelj P, Balenović M, Janječić Z, Bedeković D, Amšel Zelnika T, Zdolec G, et al. 2024. Comparison of the effect of vaccines against infectious bursal disease administered parenterally or by nebulization to newly hatched chicks (in Croatian, English summary). Proc. XV Symp. Poultry Days 2024 with international participation (Balenović M. Ed.). Croatian Veterinary Institute, Zagreb, pp 128-36.

Dahm J. 2022. Commission to propose EU-wide phaseout of male chick killing. [cited 2025 Oct 20]. Available from: https://www.euractiv.com/news/commission-to-propose-eu-wide-phaseout-of-male-chick-killing/

Damme K, Ristic M, 2003. Fattening performance, meat yield and economic aspects of meat and layer type hybrids. World Poultry Sci J, 59, 51-3.

Englmaierová M, Skrivan M, Taubner T, Skrivanová V. 2020. Performance and Meat Quality of Dual-Purpose Cockerels of Dominant Genotype Reared on Pasture. Animals (Basel) 10(3), 387. https://doi.org/10.3390/ani10030387

Ervaćinović Ž. 2010. Immunogenicity of vaccine viruses administered to newly hatched chicks by nebulization at different times. Dissertation. University of Zagreb, Faculty of Veterinary Medicine. Zagreb, (in Croatian).

Hernandez-Patlan D, Solis-Ceuz B, Adhikari B, K. Pontin KP, Latorre JD, Baxter MFA et al. 2019. Evaluation of the antimicrobial and intestinal integrity properties of boric acid in broiler chickens infected with Salmonella enteritidis: Proof of concept. Res Vet Sci 123, 7-13.

Huff GR, Huff WE, Jalukar S, Oppy J, Rath N, Packialakshmi B. 2013. The effects of yeast feed supplementation on turkey performance and pathogen colonization in a transport stress/Escherichia coli challenge. Poultry Sci, 92(3), 655-62.

Icken W, Schmutz M. 2013. Lohmann dual–Layer and Broiler at the very same time. Poult. News, Lohmann Tierzucht 2, 8-10.

Jansen HA, Dolberg F. 2003. A conceptual framework for using poultry as a tool in poverty alleviation. [cited 2025 October 10]. Available from: https://assets.publishing.service.gov.uk/media/57a08cdce5274a31e00014d0/AskovJensen.

Jia N, Li B, Zhu J, Wang H, Zhao Y, Zhao W. 2023. A Review of Key Techniques for in Ovo Sexing of Chicken Eggs. Agriculture, 13, 677. doi.org/10.3390/ agriculture13030677.

Kollmansperger S, Anders M, Werner J, Saller AM, Weiss L, Süß SC et al. 2023. Nociception in Chicken Embryos, Part II: Embryonal Development of Electroencephalic Neuronal Activity *In Ovo* as a Prerequisite for Nociception Animals, 13(18), 2839; https://doi.org/10.3390/ani13182839

Leitner G, Dan Heller E, Friedman A. 1989. Sex-related differences in immune response and survival rate of broiler chickens. Vet Immunol Immunopathol, 21(3-4):249-60. doi: 10.1016/0165-2427(89)90035-4.

Lichovníková M, Jandásek J, Jůzl M, Dračková E. 2009. The meat quality of layer males from free range in comparison with fast growing chickens. Czech J. Anim Sci 54, (11), 490-97.

Li S, Hou XH, Ma Y, Wang Z. 2022. Phenylboronic-acid-based Functional Chemical Materials for Fluorescence Imaging and Tumor Therapy. *ACS Omega* 7 (3), 2520-32, doi: 10.1021/acsomega.1c06558

Lumbo NB, Salces AJ, Oliveros MCR, Nuez III JAI, Albaladejo BHM, Dominguez JMD. 2024. Growth and Carcass Performance of Male White Leghorn Fed with Organic and Commercial Free-Range Diets raised under Extensive Rearing System. Mindanao J Sci Tech, 22 (1), 164-80.

Mace L, Knight A 2025. Development of the capacity to suffer in embryos and chicks: a systematic review of relevant studies. Front. Vet. Sci., 23 Sec. Anim Behav Welfare 12 – 2025. https://doi.org/10.3389/fvets.2025.1698528.

Mazija H, Cajavec S, Ergotić N, Ciglar-Grozdanić I, Gottstein Z, Ragland WL. 2010. Immunogenicity and Safety of Queensland V4 and Ulster 2C Strains of Newcastle Disease Virus Given to Maternally Immune, Newly Hatched Chickens by Nebulization. Avian Dis, 54, 99-103.

Mazija H, Janječić Z, Bedeković D, Kiš G, Filipič B, Balenović M et al. 2024. The effect of gastric pentadecapeptide BPC 157 on fattening performance of male broiler chickens. Proc. XV Symp. Poultry Days 2024 with international participation (Balenović, M. Ed.). (Croatian, English summary) Croatian Veterinary Institute Zagreb. pp 95-100.

Mazija H, Šerman V. 2007. Welfare towards animals and humans; to what extent are they in conflict? (Croatian), Krmiva, 49, 6, 347-56.

Mazija H, Štimac T. 1999. Ultrasonic sprayer for vaccines against Marek's disease and other poultry diseases. Croatian Patent Gazette, 4 (1999) 877.

Miller D, Wheals BB, Beresfor DN, Sumpter JP. 2001. Estrogenic Activity of Phenolic Additives Determined by an In Vitro Yeast Bioassay. Environ Health Perspect, 109, 133-8.

Mueller S, Kreuzer M, Siegrist M, Mannale K, Messikommer RE, Gangnat ID. 2018. Carcass and meat quality of dualpurpose chickens (Lohmann Dual, Belgian Malines, Schweizerhuhn) in comparison to broiler and layer chicken types. Poultry Sci 97, 3325-36.

Muth PC, Ghaziani S, Klaiber I, Zárate AV. 2018. Are carcass randmeat quality of male dual-purpose chickens competitive compared to slow-growing broilers reared under a welfare-enhanced organic system? Org Agr, 8, 57–68.

Philipp J. 2022. Utilization of male layer chickens (Bovans White and Isa Brown) for meat production under free-ranged system. Vet Anim Sci, 48(2), 1-7.

Popova T, Petkov E, Ignatova M, Vlahova-Vangelova D, Balev D, Dragoev S, et al. 2022. Male Layer-Type Chickens – an Alternative Source for High Quality Poultry Meat: a Review on the Carcass Composition, Sensory Characteristics and Nutritional Profile. Brazilian J Poultry Sci, 24 (03). 1-9. doi.org/10.1590/1806-9061-2021-1615.

Popova T, Petkov E, Ignatova M, Dragoev S, Vlahova-Vangelova D, et al. 2023. Growth performance, carcass composition and tenderness of meat in male layer-type chickens slaughtered at different age. CR Acad Bul Sci 76, 156-64.

Preusse G, Porstmann V, Bartels T, Schnabel C, Galli R, Koch E, et al 2023. Highly sensitive and quick *in ovo* sexing of domestic chicken eggs by two wavelength fluorescence spectroscopy. Analy Bioanal Chem 415, 603-13.

Rutt R, Hornbek M 2024. UCPH Research: Seven billion newly hatched chicks are killed every year but a ban is not solution. UCPH Faculty of science, Anim prod , 21 March 2024.

Torre A, Muth PCJ, Capote C, Rodríguez M, Fresno A, Valle Zárate. A 2019. Suitability of dual-purpose cockerels of 3 different genetic origins for fattening under free-range conditions. Poult Sci, 98(12), 6564-71.

Van der Most PJ, de Jong B, Parmentier HK, Verhulst D. 2011. Trade-off between growth and immune function: a meta-analysis of election experiments. Funct Ecol, 25, 74–80.

Wood-Gush D. 1959. A history of the domestic chicken from antiquity to the 19th century. Poultry Sci, 38, 321-6.

Fenilborna kiselina primijenjena nebulizacijom tek izleženim muškim pilićima lakih kokošaka nosilja značajno poboljšava njihovu tjelesnu težinu

SAŽETAK

Opisan je jedinstveni pristup za sprječavanje ubijanja muških pilića od hibrida nesilica. Aerosol otopine fenilborne kiseline (PFBA) se daje nebulizacijom jednodnevnim muškim pilićima. Pilići su izloženi PFBA u grupe od po 30 ptica u trajanju od 120 sekundi u SONOVAC® uređaju i upoređene sa kontrolnim grupama po jedne muške i ženske grupe, koje su primale destilovanu vodu istom metodom. Svi pilići su hranjeni starterom do 21. dana, a zatim finalnom smjesom do 77. dana starosti. Pilići su bili smješteni na podu u oboru dizajniranom za eksperimentalne svrhe. Prosječna tjelesna masa PFBA pilića u dobi od 77 dana iznosila je 1681,07 g, a kontrola 1629,45 g, sa omjerom konverzije hrane od 2,24 kg/kg, prema 2,26 kg/kg. Od 42. dana života, PFBA pilići su konstantno postizali veću tjelesnu masu sa nižim omjerom konverzije hrane u odnosu na SS piliće. Ove studije jasno pokazuju da je moguće ekonomski iskoristiti muške kokoši lakog hibrida tretirajući ih kao hibride sporog rasta. Međutim, da bi se to postiglo, potrebno je optimizirati sastav hrane tokom cijelog perioda rasta i odrediti karakteristike svih jestivih tkiva pilića kao pokazatelje proizvodne prakse. Metoda također doprinosi dobrobiti životinja, na što su se obavezale zemlje članice EU. Daleko je jeftiniji i stoga pristupačniji od svih drugih metoda opisanih u ovom kontekstu.

Ključne riječi: Fenilborna kiselina, laki hibridi, nebulizacija, muški pilići, tjelesna težina

RESEARCH ARTICLE

Molecular characterisation of *Cysticercus tenuicollis* (*Taenia hydatigena* cysts) in goats in Ibadan, Nigeria

Akinkunmi O. Idowu [1], Olamilekan G. Banwo[2*], Olalekan T. Jeremiah[3], Olusegun A. Fagbohun[4], Michael I. Takeet[1]

[1]Department of Veterinary Parasitology and Entomology, College of Veterinary Medicine, Federal University of Agriculture, Abeokuta
[2]Department of Veterinary Medicine, University of Ibadan; Consortium for Advanced Research Training in Africa (CARTA) Doctoral Fellow, Nigeria
[3]Department of Veterinary Medicine, University of Ibadan, Nigeria
[4]Department of Veterinary Microbiology, University of Ibadan, Nigeria

***Corresponding Author**:
Dr. Olamilekan Gabriel Banwo

Address: Department of Veterinary Medicine, Faculty of Veterinary Medicine, University of Ibadan, Oyo State, Nigeria
Phone: +2348038293440
ORICID: 0000-0002-0686-1544
E-mail: olamilekanbanwo@gmail.com

Original Submission:
09 February 2026
Revised Submission:
24 March 2026
Accepted: 27 March 2026

How to cite this article: Idowu AO, Banwo OG, Jeremiah OT, Fagbohun OA, Takeet MI. 2026. Molecular characterisation of Cysticercus tenuicollis (*Taenia hydatigena cysts*) in goats in Ibadan, Nigeria. Veterinaria, 75(1), 39-50.

ABSTRACT

Cysticercus tenuicollis, the larval stage of *Taenia hydatigena*, is a common cause of cysticercosis associated with economic losses in small ruminants. Despite its wide distribution, molecular data on Nigerian *T. hydatigena*, particularly from *C. tenuicollis*, remain limited. This study aimed to molecularly characterize *T. hydatigena* from *C. tenuicollis* isolates recovered from goats slaughtered in southwestern Nigeria using mitochondrial gene markers. *C. tenuicollis* cysts were collected from slaughtered goats and subjected to conventional polymerase chain reaction (PCR) amplification of partial mitochondrial cytochrome c oxidase subunit 1 (COX1) and 12S ribosomal RNA (12S rRNA) genes. All samples yielded successful amplification for both genes. Sequence analysis of five representative subsets confirmed all isolates as *T. hydatigena*, showing high nucleotide similarity with reference sequences from GenBank (98.2–99.1% for COX1 and 97.3–98.9% for 12S rRNA). Nucleotide diversity was low across isolates for both markers, indicating limited intraspecific variation. Phylogenetic analysis using the Neighbor-Joining method revealed that Nigerian isolates clustered within the global *T. hydatigena* clade and were closely related to isolates from Europe, Asia, and North Africa. No distinct regional lineage was observed. Minor differences in tree topology between COX1- and 12S rRNA-based phylogenies were consistent with marker-specific evolutionary characteristics. Overall, this study confirms the identity and phylogenetic placement of *T. hydatigena* infecting goats in southwestern Nigeria, revealing close genetic similarity to global isolates. The mitochondrial sequences support dog–livestock transmission, provide a reference for future taeniid epidemiological studies, and establish baseline genetic data to inform evidence-based control strategies.

Keywords: *Cysticercus tenuicollis*, *Taenia hydatigena*, Molecular characterisation, Phylogenetics

INTRODUCTION

Small ruminants constitute vital components of agricultural production systems in Nigeria, playing critical roles in rural livelihoods and national food security (Banwo et al., 2025). However, their productivity is substantially constrained by parasitic infections, among which visceral cysticercosis, caused by *C. tenuicollis*, poses major but historically neglected constraints to profitable small ruminant production in developing countries, threatening the economic viability and public health safety of the caprine value chain (Lawan et al., 2024; Magala et al., 2024).

C. tenuicollis remains poorly characterized at the molecular level in West Africa, despite its substantial burden in Sub-Saharan Africa (Idowu et al., 2024). Abattoir-based surveys in Nigeria have shown sustained transmission in goats, with a prevalence of 38.2% reported in slaughtered Red Sokoto goats at Ibadan, and cysts distributed across visceral organs. This enzootic circulation in a major livestock hub underscores the regional importance of understanding the parasite's genetic structure and population dynamics (Idowu et al., 2024).

Notably, Ohiolei et al. (2019) provided the first molecular description and phylogenetic analysis of *T. hydatigena* from Nigerian sheep and goats using three mitochondrial genes, establishing foundational sequence data for this species in West Africa. At the broader regional level, Lawan et al. (2024) conducted a systematic review of *C. tenuicollis* epidemiology across tropical small ruminant populations, highlighting persistent knowledge gaps in molecular characterisation within Sub-Saharan Africa. The present study builds directly on these foundations by generating additional mitochondrial sequence data from goats slaughtered in southwestern Nigeria, thereby contributing to a more comprehensive molecular picture of *T. hydatigena* circulating in West Africa.

C. tenuicollis, the metacestode (larval) stage of *Taenia hydatigena*, represents a cyclophyllidean tapeworm of considerable veterinary and economic significance affecting small ruminants globally. The adult cestode inhabits the small intestine of definitive hosts, including domestic dogs, cats, and wild canids such as wolves and foxes (Jenkins et al., 2014). Infected carnivores release gravid proglottids into the environment through their faeces; oncospheres (eggs) are subsequently liberated from these proglottids, which are later ingested by intermediate hosts, predominantly herbivorous livestock, including sheep, goats, cattle, and swine, during grazing activities (Lawan et al., 2024). While adult parasites cause minimal pathology in definitive hosts, larval stages impose substantial economic burdens through condemnation of infected viscera at slaughter facilities and reduced productivity in affected animals (Lawan et al., 2025).

C. tenuicollis imposes considerable economic burdens on small ruminant husbandry systems in endemic regions, beyond direct production losses arising from organ condemnation, impaired weight gain, and mortality (Lawan et al., 2024). Traditional parasitological diagnosis relies on morphological examination of metacestodes recovered during postmortem inspection (Magala et al., 2024). However, morphological identification presents challenges when dealing with damaged specimens, immature stages, or closely related taeniid species. Furthermore, the metacestode antigens of *C. tenuicollis* are known to cross-react with those of other larval taeniid cestodes in serological assays, thereby reducing diagnostic specificity when distinguishing among metacestode infections (Hossain et al., 2025). That said, recent molecular studies have demonstrated significant genetic diversity within *T. hydatigena* populations globally, providing insights into parasite evolution, host-parasite relationships, and population structure (Abbas et al., 2021; Dey et al., 2022; Mehmood et al., 2024).

Targeted molecular characterisation using mitochondrial markers, including fragments of the COX1 and 12S rRNA genes, as in this study, has emerged as a powerful tool for confirming species identity, assessing genetic relatedness among isolates, and generating baseline sequence data relevant to understanding transmission patterns (Ohiolei et al., 2019; Rostami et al., 2015).

Mitochondrial genes offer several advantages, including maternal inheritance without recombination, relatively rapid evolutionary rates facilitating population-level differentiation, and high copy number per cell enabling amplification from limited tissue samples (Ohiolei et al., 2019). The cytochrome c oxidase subunit 1 (COX1) gene, widely adopted as the standard DNA barcode for animal species, permits discrimination among closely related species while maintaining conservation among conspecifics (Hebert et al., 2003), while the 12S ribosomal RNA gene serves as an excellent marker for taxonomic classification and phylogenetic inference (Smit et al., 2007).

This study aimed to conduct molecular identification and characterisation of *C. tenuicollis* isolates using COX1 and 12S rRNA gene sequences, and to perform phylogenetic analysis to determine relationships between Nigerian isolates and global *T. hydatigena* populations. This research provides foundational molecular data on *C. tenuicollis* in Nigeria and contributes to a broader understanding of genetic diversity within this important veterinary parasite.

MATERIALS AND METHODS

Study Area and Ethical Considerations

This study was conducted at the Akinyele Central Abattoir in Ibadan, Oyo State, southwestern Nigeria. Ibadan, the capital city of Oyo State, serves as a major livestock trading hub with significant daily throughput of small ruminants originating from smallholder farms around Ibadan and Iseyin; the Guinea savannah, Sahel, and sub-arid climatic zones of northern Nigeria; and border countries such as Niger, Chad, and Mali (Jeremiah and Banwo, 2019). All procedures performed in this study were abattoir-based and did not involve experimentation on live animals. Sample collection was conducted during routine post-mortem meat inspection in strict accordance with the standard operating procedures of the Akinyele Central Abattoir. Permission to collect samples and utilize abattoir data was formally obtained from the Oyo State Veterinary Department and the abattoir management.

Study Design and Parasite Identification

A total of 500 Red Sokoto goats slaughtered at the Akinyele Central Abattoir were examined post-mortem for *C. tenuicollis* using a cross-sectional survey design over three months (Idowu et al., 2024). Of these, 191 animals (38.2%) were confirmed positive, with cysts distributed predominantly across the peritoneum and liver. From the positive animals, twelve cyst samples representing different anatomical locations and animal demographics were randomly selected for molecular analysis. Preliminary identification of *C. tenuicollis* was based on characteristic morphological features, including the presence of a single, long-necked scolex and translucent cyst fluid. The scolex was extracted and examined microscopically for characteristic features of taeniid cestodes.

DNA Extraction

Following visual identification during post-mortem inspection, cysticerci were immediately transferred to sterile universal sample bottles containing 70% ethanol for short-term preservation. DNA extraction was performed within 7 days of collection. Individual protoscoleces were aseptically dissected from cysts and sectioned into small fragments using sterile razor blades. The tissue fragments were homogenized with an equal volume of sterile distilled water using a sterile pestle and mortar. Genomic DNA extraction was performed using the Quick-DNA™ Universal Kit (Zymo Research, Cat. No. D4068, supplied by Inqaba Biotec West Africa Ltd) following the manufacturer's protocol. Extracted DNA was quantified and stored at -20°C until PCR amplification.

PCR Amplification

Two mitochondrial gene targets were amplified: the cytochrome c oxidase subunit 1 (COX1) and the 12S ribosomal RNA (12S rRNA) genes, using primers and conditions previously described by Rostami et al. (2015).

COX1 amplification: A 400 bp fragment was amplified using forward primer JB3 (5'-TTTTTTGGGCATCCTGAGGTTTAT-3') and reverse primer JB4.5 (5'-TAAAGAAAGAACATAATGAAAATG-3').

PCR reactions were performed in 50 µL volumes containing 25 µL OneTaq® Quick-Load® 2X Master Mix (New England Biolabs, Cat. No. M0486, USA), 1 µL each primer (10 µM), 18 µL nuclease-free water, and 5 µL DNA template. Thermal cycling conditions consisted of initial denaturation at 94°C for 2 minutes, followed by 35 cycles of 95°C for 20 seconds, 50°C for 60 seconds, and 72°C for 90 seconds, with final extension at 72°C for 7 minutes.

12S rRNA amplification: A 500 bp fragment was amplified using forward primer 12SRF (5'-AGGGGATAGGACACAGTGCCAGC-3') and reverse primer 12SRR (5'- CGGTGTGTACATGAGCTAAAC-3').

PCR conditions were identical to COX1 amplification except for an annealing temperature of 55°C. All reactions included a no-template negative control to monitor for contamination. Amplification reactions were conducted in a thermal cycler (Edvocycler™; Edvotek®, USA).

Gel Electrophoresis and Visualisation

Amplification products (10 µL) were separated by electrophoresis on 2% (w/v) agarose gels (Sigma, Cat. No. A9539, USA) prepared in 1X TAE buffer (Sigma-Aldrich, Cat. No. T9650, USA), and stained with ethidium bromide (5 µg/mL) (Sigma-Aldrich, Cat. No. E7637, USA). A 100 bp DNA ladder (New England Biolabs, USA) was included for fragment size determination. Electrophoresis was conducted at 85 V for 60 minutes. DNA bands were visualized and photographed using the Molecular Imager® Gel Doc™ XR+ System with Image Lab™ Software (Bio-Rad Laboratories).

DNA Sequencing and Sequence Analysis

PCR products showing clear, single bands of expected sizes were selected for bidirectional Sanger sequencing. Due to resource limitations, a representative subset of samples was prioritised for sequencing: five samples for COX1 and five samples for 12S rRNA, selected on the basis of band clarity and representation of different anatomical collection sites. Raw chromatograms were manually inspected for quality using BioEdit version 7.0 (Hall, 1999). One COX1 sequence was excluded from downstream analysis and GenBank submission due to poor chromatogram quality characterised by ambiguous base calls exceeding acceptable thresholds; the remaining four COX1 sequences (PX715891–PX715894) and five 12S rRNA sequences (PX710001–PX710005) met quality criteria and were deposited in GenBank.

Phylogenetic and Bioinformatic Analysis

Nucleotide sequences were compared against the GenBank database using the Basic Local Alignment Search Tool (BLAST, https://blast.ncbi.nlm.nih.gov/) to confirm species identity and identify closely related sequences. The top-matching sequences representing *T. hydatigena* isolates from diverse geographic locations and hosts were retrieved for comparative analysis. Multiple sequence alignments were performed using ClustalW implemented in MEGA version 11.0 (Tamura et al., 2021).

Phylogenetic trees were constructed using the Neighbor-Joining method with the Kimura 2-parameter distance model. Bootstrap analysis was performed with 1,000 replicates to assess the robustness of phylogenetic groupings. Related *Taenia* species, including *T. solium*, *T. saginata*, *T. asiatica*, *T. multiceps*, and *T. pisiformis*, as well as other cestodes (*Echinococcus multilocularis*, *Hymenolepis diminuta*), were included as outgroups. Genetic distances and nucleotide diversity (π) were calculated using MEGA 11.0.

Sequence Data Submission

All sequences generated in this study were deposited in GenBank under accession numbers: PX715891-PX715894 for COX1 and PX710001- PX710005 for 12S rRNA.

RESULTS

PCR Amplification

All twelve C. tenuicollis samples subjected to molecular analysis yielded successful amplification for both target genes, representing a 100% PCR success rate. Of the twelve PCR-positive samples, a representative subset of five samples per gene was subjected to Sanger sequencing due to resource limitations. Following chromatogram quality inspection, four COX1 sequences met quality thresholds and were retained for analysis; all five 12S rRNA sequences passed quality inspection. The sequences used for phylogenetic analysis are therefore derived from partially overlapping subsets of the twelve amplification-positive samples. COX1 amplification produced clear, single bands of approximately 400 bp, while 12S rRNA amplification generated fragments of approximately 500 bp, consistent with expected product sizes (Figures 1 and 2). No amplification was observed in negative controls, confirming the absence of contamination.

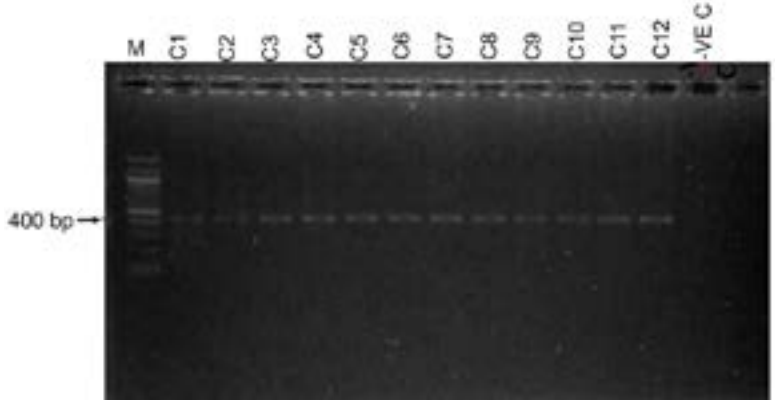

Figure 1 The agarose gel image of the PCR amplicon for the COX1 gene (M- Marker, C1-C12- samples, -VeC- Negative control)

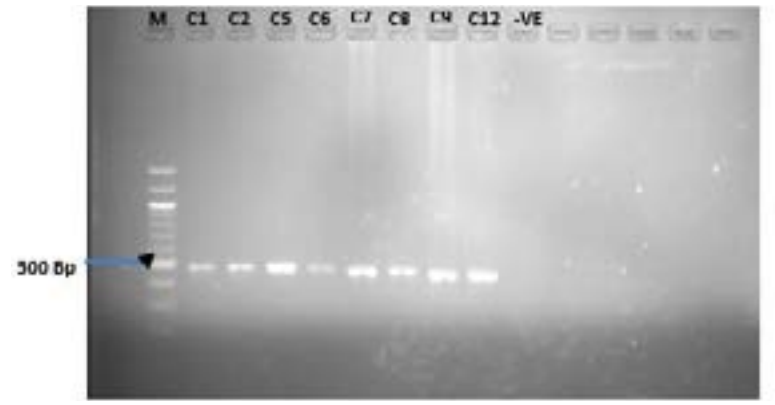

Figure 2 The agarose gel image of the PCR amplicon for the 12s rRNA gene (M-Marker, C1-C12- samples, -VE C- Negative control)

Sequence Identity and Genetic Diversity

BLAST analysis of the COX1 sequences confirmed that all Nigerian isolates corresponded to *T. hydatigena*, showing high nucleotide identity (98.2–99.1%; mean 98.7%) with reference COX1 sequences from GenBank. Similarly, that of 12S rRNA sequences demonstrated 97.3–98.9% identity (mean 98.1%) with established *T. hydatigena* 12S rRNA sequences from various hosts and geographical regions.

Nucleotide diversity analysis revealed low intraspecific variation among Nigerian isolates (π = 0.0024 for COX1; π = 0.0041 for 12S rRNA). The slightly higher diversity observed in the 12S rRNA gene compared with COX1 is consistent with differences in evolutionary constraints between ribosomal and protein-coding mitochondrial regions.

Phylogenetic Relationships

COX1 phylogeny: The Neighbor-Joining phylogenetic tree constructed from COX1 sequences demonstrated that Nigerian *C. tenuicollis* isolates formed a well-supported monophyletic clade (bootstrap value: 87%) that clustered closely with sequences from Mongolia (AB792724.1), Palestine (KM032303.1), Finland (EU544552.1), Great Britain, and Germany (KX962494.1). This clustering pattern suggests genetic affinity between West African isolates and those from Eurasia, despite geographic separation (Figure 3). The Nigerian clade was grouped within the broader *T. hydatigena* cluster, distinct from other *Taenia* species, including *T. solium, T. saginata*, and *T. multiceps*, which formed separate clades with high bootstrap support (>95%).

12S rRNA phylogeny: Phylogenetic analysis of 12S rRNA sequences revealed that Nigerian isolates formed a distinct clade that grouped most closely with sequences from Egypt (KU671391.1), China (GQ228819.1, HQ204206.1), and Iran (JQ717238.1, JQ710608.1) (Table 1). Additional clustering with isolates from Italy (FJ608746.1) and Japan (AB027135.1, AB033410.1)

was observed with moderate bootstrap support (72-84%) (Figure 4). The tree topology differed from that generated using COX1 sequences, reflecting distinct evolutionary constraints acting on ribosomal RNA genes compared to protein-coding genes. Nevertheless, Nigerian isolates consistently grouped within the *T. hydatigena* complex, clearly separated from *T. pisiformis* and *T. multiceps* (bootstrap support >90%).

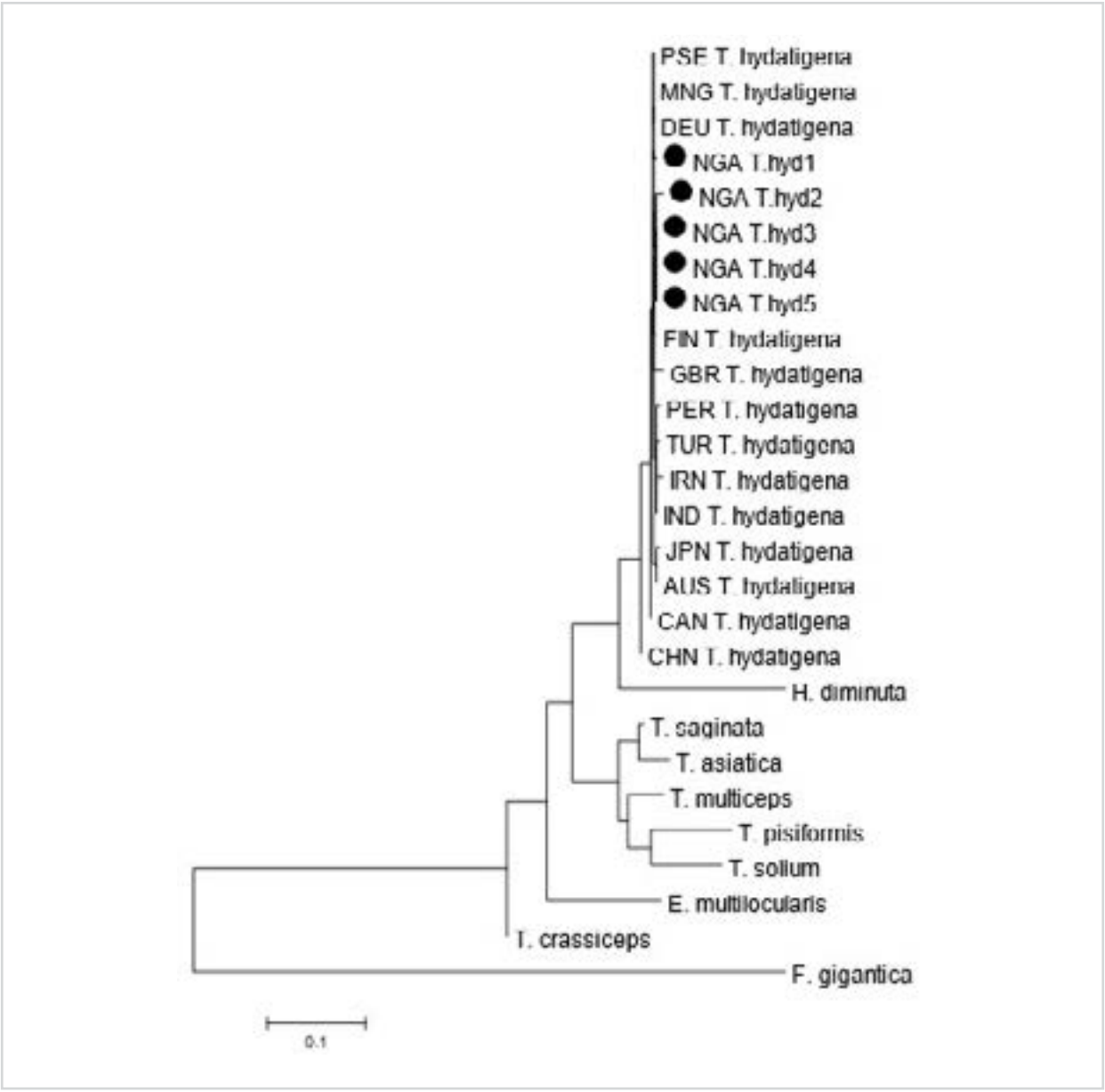

Figure 3 Phylogenetic Tree for COX1 gene using Neighbor-Joining phylogenetic tree based on partial mitochondrial COX1 gene sequences of *T. hydatigena*. Nigerian isolates from goats are shown in bold. Bootstrap values (1,000 replicates) are indicated at branch nodes. Reference sequences were retrieved from GenBank. Scale bar (0.1) represents nucleotide substitutions per site

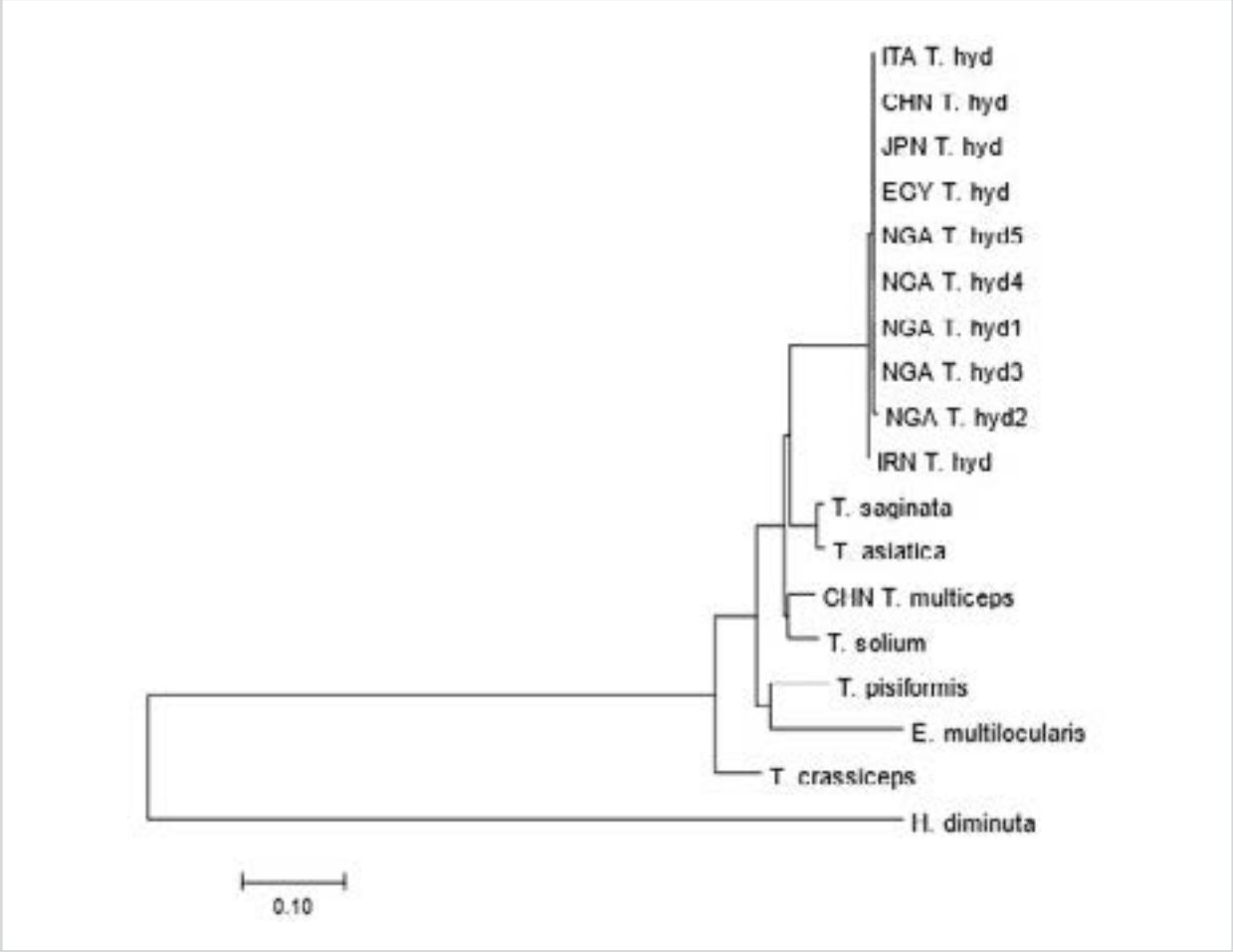

Figure 4 Phylogenetic Tree for 12S rRNA gene using Neighbor-Joining phylogenetic tree based on partial mitochondrial 12S rRNA gene sequences of *T. hydatigena*. Nigerian isolates from goats are shown in bold. Bootstrap values (1,000 replicates) are indicated at branch nodes. Reference sequences were retrieved from GenBank. Scale bar (0.1) represents nucleotide substitutions per site

Table 1 GenBank accession numbers of *T. hydatigena* and related cestode sequences used for phylogenetic comparison

Accession Number	Species	Host	Goat breed	Country Code	Gene
AB792724.1	*T. hydatigena*	Dog	Mongolia	MNG	COX1
KM032303.1	*T. hydatigena*	Sheep	Palestine	PSE	COX1
EU544552.1	*T. hydatigena*	Reindeer	Finland	FIN	COX1
KX962494.1	*T. hydatigena*	Wolf	Germany	DEU	COX1
KU671391.1	*T. hydatigena*	Sheep	Egypt	EGY	12S rRNA
GQ228819.1	*T. hydatigena*	Sheep	China	CHN	12S rRNA
HQ204206.1	*T. hydatigena*	Dog	China	CHN	12S rRNA
JQ717238.1	*T. hydatigena*	Sheep	Iran	IRN	12S rRNA
JQ710608.1	*T. hydatigena*	Sheep	Iran	IRN	12S rRNA
FJ608746.1	*T. hydatigena*	Wild boar	Italy	ITA	12S rRNA

Accession Number	Species	Host	Goat breed	Country Code	Gene
AB027135.1	*T. hydatigena*	Sheep	Japan	JPN	12S rRNA
AB033410.1	*T. hydatigena*	Sheep	Japan	JPN	12S rRNA
AM503316.1	*T. hydatigena*	Dog	Australia	AUS	COX1
KX377742.1	*T. multiceps*	Dog	China	CHN	COX1
GC569096.1	*T. pisiformis*	Rabbit	China	CHN	COX1
NC_004022.1	*T. solium*	Pig	Japan	JPN	Complete mt
NC_009938.1	*T. saginata*	Cattle	Korea	KOR	Complete mt
NC_004826.2	*T. asiatica*	Human	Korea	KOR	Complete mt
NC_000928.2	*Echinococcus multilocularis*	Sheep	Japan	JPN	Complete mt
NC_002767.1	*Hymenolepis diminuta*	Rat	USA	USA	Complete mt
NC_002547.1	*T. crassiceps*	Mice	Australia	AUS	Complete mt

DISCUSSION AND CONCLUSION

This study provides molecular characterisation of *C. tenuicollis* isolates recovered from slaughtered Red Sokoto goats in southwestern Nigeria, generating new regional mitochondrial sequence data for *T. hydatigena* based on COX1 and 12S rRNA gene markers. Modern molecular techniques offer comprehensive insights into parasite biology, population genetics, and phylogeographic structure of helminth parasites (Gasser, 2006).

The successful amplification and sequencing of both COX1 (100% success rate) and 12S rRNA gene fragments from all tested samples validates the utility of these mitochondrial markers for molecular identification and characterisation of taeniid cestodes. The amplicon sizes obtained (approximately 400 bp for COX1 and 500 bp for 12S rRNA) align precisely with those reported by Rostami et al. (2015) in their characterisation of *T. hydatigena* from Iranian sheep, confirming the universality and reliability of these primer sets across diverse geographic populations.

The COX1 gene, widely adopted as the standard DNA barcode for animal species, proved particularly valuable for confirming species identity. Its utility stems from an evolutionary rate that permits discrimination among closely related species while maintaining adequate conservation to reliably group conspecific individuals (Hebert et al., 2003). The high sequence identity (98.2-99.1%, mean 98.7%) observed between Nigerian isolates and reference *T. hydatigena* sequences unequivocally confirms taxonomic identification of these parasites, eliminating uncertainty that might arise from morphological examination alone. These values are comparable to those reported by Rostami et al. (2015), who reported COX1 identities of 97.8–99.4% among Iranian sheep isolates, and to Ohiolei et al. (2019), who reported similarly high sequence conservation among Nigerian sheep and goat isolates using mitochondrial markers, collectively reinforcing the reliability of COX1 as a barcode marker for *T. hydatigena* across diverse geographic populations.

The 12S rRNA gene, being universally present across all domains of life and demonstrating appropriate sequence variation for phylogenetic inference, complemented COX1 analysis by providing additional resolution for examining genetic relationships and estimating divergence among isolates (Smit et al., 2007). The slightly higher variability in 12S rRNA ($\pi = 0.0041$) compared to COX1 ($\pi = 0.0024$) reflects different selective pressures, with ribosomal genes experiencing structural and functional constraints related to ribosome assembly rather than amino acid sequence optimisation.

The 12S rRNA-based topology observed in this study, with Nigerian isolates clustering most closely with sequences from Egypt, China, and Iran, is broadly consistent with findings by Dey et al. (2022), who reported similar phylogenetic affinities between Bangladeshi *T. hydatigena* isolates and Asian reference sequences using 12S rRNA markers, reinforcing the utility of this gene for detecting region-specific clustering patterns within the broader *T. hydatigena* complex.

The relatively low degree of genetic variation observed in both COX1 and 12S rRNA genes among Nigerian isolates and international reference sequences suggests considerable genetic stability within *T. hydatigena* populations globally. Nucleotide diversity values (π = 0.0024 for COX1; π = 0.0041 for 12S rRNA) indicate that *T. hydatigena* exhibits limited intraspecific genetic diversity, consistent with recent findings by Mehmood et al. (2024) and Qurishi et al. (2022), who reported similar patterns in Pakistani and Chinese populations, respectively. Specifically, Mehmood et al. (2024) reported COX1 nucleotide diversity values of π = 0.00260 among Pakistani isolates, while Qurishi et al. (2022) reported similarly low diversity among Chinese and Mongolian *T. hydatigena* populations. The close agreement between our π values and those from geographically distant studies confirms the global conservation of this parasite's mitochondrial genome.

The convergence of low nucleotide diversity values across geographically distant populations — Pakistan, China, Mongolia, and now Nigeria — strongly supports the hypothesis that *T. hydatigena* maintains high global gene flow, most plausibly mediated by the international livestock trade and the widespread distribution of canid definitive hosts across Eurasia and Africa. This has important implications for control, suggesting that locally derived interventions may need to account for the potential introduction of parasite genotypes through imported livestock.

This limited genetic variation likely reflects several biological characteristics of the parasite. First, the generalist nature of *T. hydatigena* regarding both definitive (multiple canid species) and intermediate (sheep, goats, cattle, pigs, wild ungulates) hosts provides numerous opportunities for parasite transmission and maintenance, potentially buffering against genetic drift. Second, the cosmopolitan distribution of both canids and livestock has facilitated global parasite dispersal through historical and contemporary trade networks, maintaining gene flow among geographically separated populations. Third, the relatively short prepatent period following ingestion of cysticercus-infected viscera by definitive hosts facilitates rapid population establishment and ongoing transmission (Abbas et al., 2021).

The phylogenetic analyses yielded complementary yet distinct topologies for the two markers examined, highlighting important aspects of *T. hydatigena* evolution and biogeography. Nigerian isolates clustered with geographically diverse sequences from Europe, Asia, the Middle East, and other regions, rather than forming a distinct West African clade.

The clustering of Nigerian samples with European (Finland, Germany, Great Britain), Middle Eastern (Palestine), and Mongolian isolates based on COX1 sequences suggests complex patterns of parasite dispersal consistent with the broad geographic distribution of canid definitive hosts and historically interconnected livestock trade networks. Similar Eurasian-African clustering patterns have been noted by Abbas et al. (2021), who reported that Egyptian *T. hydatigena* isolates grouped within cosmopolitan Eurasian clades rather than forming regionally distinct lineages, and by Mehmood et al. (2024), who attributed the lack of geographic structuring in Pakistani isolates to ongoing gene flow facilitated by international livestock movement and the wide distribution of canid hosts. The absence of a distinct West African lineage in our COX1 tree is therefore consistent with multiple independent studies that describe a defining characteristic of *T. hydatigena*: a globally panmictic population structure maintained by the cosmopolitan ecology of its hosts (Ohiolei et al., 2019; Mehmood et al., 2024).

For the 12S rRNA marker, the closest relationships were observed with isolates from Egypt, China, and Iran. The clustering with Egyptian isolates is particularly significant, as geographic proximity and historical connections between West Africa and North Africa through the Sahel zone suggest ongoing or historical parasite gene flow across the Sahara. Recent molecular studies by Abbas et al. (2021) demonstrated similar genetic relationships between North African and other global isolates.

Furthermore, the clustering of Nigerian isolates within a broadly distributed Eurasian clade is consistent with the findings of Ohiolei et al. (2019), who similarly reported that *T. hydatigena* isolates from Nigerian sheep and goats grouped within a cosmopolitan clade without forming a distinct West African lineage, suggesting that regional genetic differentiation has not occurred despite geographic separation.

The differing tree topologies generated by COX1 and 12S rRNA analyses highlight the importance of employing multiple molecular markers when investigating parasite phylogenetics. Different evolutionary rates and mutation patterns may contribute to these differences. Despite these topological differences, concordance in

species-level identification (all samples confirmed as *T. hydatigena* with >97% identity) validates both markers while emphasizing the value of multi-locus approaches.

The lack of strong geographic structuring in phylogenetic trees suggests either recent parasite dispersal on evolutionary timescales or ongoing gene flow mediated by livestock movement. Modern globalisation of livestock trade likely maintains connectivity among geographically distant *T. hydatigena* populations, preventing strong phylogeographic differentiation (Mehmood et al., 2024).

It should be noted that a relatively small number of samples (n = 12) were analysed in this study, which represents a notable limitation. While this sample size was sufficient to confirm species identity and establish preliminary phylogenetic placement, broader conclusions regarding population genetic structure and geographic differentiation within Nigeria should be interpreted cautiously. Future studies with larger, geographically diverse sample collections are warranted to validate these findings and characterise the full extent of genetic diversity within Nigerian *T. hydatigena* populations.

While *T. hydatigena* is primarily a veterinary pathogen with negligible zoonotic potential, its impact on livestock productivity through hepatic damage during larval migration, carcass condemnation, and reduced growth rates merits significant attention. The molecular confirmation of *C. tenuicollis* in Red Sokoto goats underscores the urgent need for integrated control strategies targeting both definitive and intermediate hosts.

This study provides mitochondrial genetic evidence confirming the identity of *T. hydatigena* (*C. tenuicollis*) infecting goats slaughtered in southwestern Nigeria, using partial sequences of the COX1 and 12S rRNA genes. The combined application of these two mitochondrial genes enabled species confirmation and robust phylogenetic placement of Nigerian isolates within the global *T. hydatigena* complex.

The high sequence similarity observed between Nigerian isolates and reference sequences from Europe, Asia, and North Africa, together with low intraspecific nucleotide diversity, indicates limited genetic differentiation across geographically distant populations. These findings are consistent with the broad host range and widespread distribution of *T. hydatigena*, suggesting that parasite populations circulating in Nigerian goats form part of a largely conserved and interconnected global population rather than a distinct regional lineage.

From a veterinary and production perspective, the molecular confirmation of *C. tenuicollis* in slaughtered goats highlights the continued circulation of *T. hydatigena* within the dog-livestock transmission cycle in Nigeria. This supports the need for sustained control measures focusing on proper disposal of infected offal, management of owned and stray dogs, and improved awareness among livestock handlers and abattoir workers to reduce environmental contamination and economic losses associated with organ condemnation.

Importantly, the mitochondrial sequence data generated in this study establish a regional genetic reference that can support future molecular epidemiological investigations, comparative studies across West Africa, and long-term surveillance of *T. hydatigena* populations. Such data are essential for monitoring changes in parasite population structure, evaluating the impact of control interventions, and informing evidence-based strategies aimed at reducing the burden of cysticercosis in small ruminant production systems in Nigeria.

ACKNOWLEDGMENTS

The authors appreciate the Staff of the Akinyele Central Abattoir, Ministry of Agriculture and Rural Development, Oyo State, Nigeria, for facilitating the sample collection, and the Department of Veterinary Medicine Laboratory, University of Ibadan, for technical support. O.G. Banwo is supported by the Consortium for Advanced Research Training in Africa (CARTA) programme.

CONFLICT OF INTEREST

The authors declared that there is no conflict of interest.

CONTRIBUTIONS

Conception: AOI, OTJ, OAF; Writing– review and editing: All authors; Data collection and processing: AOI, OGB, OAF; Analysis and interpretation: OGB, OAF, MIT; Materials and supervision: OTJ, OAF.

REFERENCES

Abbas I, El-Alfy ES, Janecek-Erfurth E, Strube C. 2021. Molecular characterization of *Cysticercus tenuicollis* isolates from sheep in the Nile Delta, Egypt and a review on *Taenia hydatigena* infections worldwide. Parasitology, 148(8), 913-33. https://doi.org/10.1017/S0031182021000536

Banwo OG, Oluwadare FA, Olakojo TA, Hamman MM, Lateef AM, Agbajelola VI. 2025. A systematic review and meta-analysis of studies on the prevalence of gastrointestinal parasites among ruminants in Nigeria. Folia Vet, 69(3), 1-15. https://doi.org/10.2478/fv-2025-0021

Dey AR, Anisuzzaman, Hasan M, Hoque MR, Siddiqui TR, Alam MZ. 2022. Morphometry and genetic diversity pattern of *Cysticercus tenuicollis*, an important food-borne taeniid metacestode in goats in Bangladesh. Infect Genet Evol, 105, 105364. https://doi.org/10.1016/j.meegid.2022.105364

Gasser RB. 2006. Molecular tools — advances, opportunities and prospects. Vet Parasitol, 136(2), 69–89. https://doi.org/10.1016/j.vetpar.2005.12.002

Hall TA. 1999. BioEdit: a user-friendly biological sequence alignment editor and analysis program for Windows 95/98/NT. Nucleic Acids Symp Ser, 41, 95-8.

Hebert PDN, Ratnasingham S. 2003. Barcoding animal life: cytochrome c oxidase subunit 1 divergences among closely related species. Proc R Soc B Biol Sci, 270(Suppl 1), S96–S99. https://doi.org/10.1098/rsbl.2003.0025

Hossain MS, Shabir S, Ngwili N, Thomas LF, Falcone FH. 2025. Serological diagnosis of cysticercosis in humans and pigs: status, limitations, and prospects. Front Vet Sci, 12, 1558555. https://doi.org/10.3389/fvets.2025.1558555

Idowu AO, Banwo OG, Jeremiah OT. 2024. Prevalence and distribution of *Cysticercus tenuicollis* (*Taenia hydatigena*) cysts from slaughtered goats at Akinyele, Ibadan, Nigeria. J Appl Vet Sci, 9(3), 35-40. https://doi.org/10.21608/javs.2024.282432.1330

Jenkins DJ, Uwin NAR, Williams TM, Mitchell KL, Lievaart JJ, Armua-Fernandez MT. 2014. Red foxes (*Vulpes vulpes*) and wild dogs (dingoes (*Canis lupus dingo*) and dingo/domestic dog hybrids), as sylvatic hosts for Australian *Taenia hydatigena* and *Taenia ovis*. Int J Parasitol Parasites Wildl, 3, 75-80. https://doi.org/10.1016/j.ijppaw.2014.03.001

Jeremiah OT, Banwo OG. 2019. Haematologic profile and prevalence survey of haemonchosis in various breeds of slaughtered cattle in Ibadan, Nigeria. Niger J Anim Prod, 46(3), 151-62. https://doi.org/10.51791/njap.v46i3.954

Lawan PY, Niba AT, Awah-Ndukum J. 2024. Epidemiology of *Cysticercus tenuicollis* in sheep and goats in the tropics: a systematic review. Vet Med Int, 2024, 7881494. https://doi.org/10.1155/vmi/7881494

Lawan PY, Niba AT, Awah-Ndukum J. 2025. Prevalence, intensity and associated factors of *Cysticercus tenuicollis* in small ruminants in the Northwest Region of Cameroon. Vet Med Sci, 11(3), e70307. https://doi.org/10.1002/vms3.70307

Magala J, Mudde B, Mawadri PA, Guma W, Baguma SD, Okot PO, et al. 2024. *Cysticercus tenuicollis* in visceral organs of goats and sheep in Uganda: a case study in Lira Municipal Abattoir. Open J Anim Sci, 14, 249-59. https://doi.org/10.4236/ojas.2024.144018

Mehmood N, Muqaddas H, Ashraf A, Aslam M, Khan M, Fatima M, et al. 2024. Leading report regarding the molecular epidemiology of *Taenia hydatigena* from Pakistan and global overview of the genetic diversity and population structure of the parasite. Comp Immunol Microbiol Infect Dis, 114, 102248. https://doi.org/10.1016/j.cimid.2024.102248

Ohiolei JA, Luka J, Zhu Q, Yan B, Li L, Magaji AA, et al. 2019. First molecular description, phylogeny and genetic variation of *Taenia hydatigena* from Nigerian sheep and goats based on three mitochondrial genes. Parasit Vectors, 12, 520. https://doi.org/10.1186/s13071-019-3780-5

Qurishi SA, Yan HB, Li L, Ohiolei JA, Alvi MA, Zhang LS, et al. 2022. Comparison of mitochondrial genetic variation of *Taenia hydatigena* cysticerci from China and Mongolia. Parasitol Res, 121(12), 3455-66. https://doi.org/10.1007/s00436-022-07669-3

Rostami S, Salavati R, Beech RN, Babaei Z, Sharbatkhori M, Baneshi MR, et al. 2015. Molecular and morphological characterization of the tapeworm *Taenia hydatigena* (Pallas, 1766) in sheep from Iran. J Helminthol, 89(2), 150-7. https://doi.org/10.1017/S0022149X13000667

Smit S, Widmann J, Knight R. 2007. Evolutionary rates vary among rRNA structural elements. Nucleic Acids Res, 35(10), 3339-54. https://doi.org/10.1093/nar/gkm101

Tamura K, Stecher G, Kumar S. 2021. MEGA11: Molecular Evolutionary Genetics Analysis Version 11. Mol Biol Evol, 38(7), 3022-7. https://doi.org/10.1093/molbev/msab120

Molekularna karakterizacija *Cysticercus tenuicollis* (ciste *Taenia hydatigena*) kod koza u Ibadanu, Nigerija

SAŽETAK

Cysticercus tenuicollis, larvalni stadij *Taenia hydatigena*, čest je uzrok cisticerkoze povezane sa ekonomskim gubicima kod malih preživara. Uprkos širokoj rasprostranjenosti, molekularni podaci o *T. hydatigena* iz Nigerije, posebno iz *C. tenuicollis*, i dalje su ograničeni. Cilj ove studije bio je molekularno karakterisati *T. hydatigena* na osnovu izolata *C. tenuicollis* prikupljenih od koza zaklanih u jugozapadnoj Nigeriji koristeći markere mitohondrijalne DNK. Ciste *C. tenuicollis* su prikupljene od zaklanih koza i podvrgnute konvencionalnoj lančanoj reakciji polimeraze (PCR) za parcijalne gene mitohondrijalnog citohrom c oksidaze podjedinice 1 (COX1) i 12S ribosomalne RNK (12S rRNA). Svi uzorci su dali uspješnu amplifikaciju za oba gena. Analiza sekvenci pet reprezentativnih poduzoraka potvrdila je sve izolate kao *T. hydatigena*, pokazujući visoku sličnost nukleotida sa referentnim sekvencama iz GenBank-a (98,2–99,1% za COX1 i 97,3–98,9% za 12S rRNA). Nukleotidna raznolikost među izolatima bila je niska za oba markera, što ukazuje na ograničenu varijabilnost unutar vrste. Filogenetska analiza primjenom metode Neighbor-Joining pokazala je da se nigerijski izolati grupišu unutar globalne filogenetske grupe *T. hydatigena* i da su blisko povezani sa izolatima iz Evrope, Azije i Sjeverne Afrike. Nije uočena specifična regionalna linija. Male razlike u topologiji stabla između filogenija zasnovanih na COX1 i 12S rRNA bile su u skladu sa evolutivnim karakteristikama specifičnim za markere. Općenito, ova studija potvrđuje identitet i filogenetsko pozicioniranje *T. hydatigena* koja inficira koze u jugozapadnoj Nigeriji, otkrivajući blisku genetsku sličnost sa globalnim izolatima. Mitohondrijalne sekvence podržavaju prenos između pasa i stoke, pružaju referencu za buduće epidemiološke studije taeniida i uspostavljaju osnovne genetske podatke koji mogu informisati strategije kontrole zasnovane na dokazima.

Ključne riječi: *Cysticercus tenuicollis*, *Taenia hydatigena*, molekularna karakterizacija, filogenetika

RESEARCH ARTICLE

Craniometrical characteristics of the Uda and Yankasa breeds of sheep (*Ovis aries*)

Baba Gana Gambo, Muhammad Khalid, Ali Musa Wulgo*, Yagana Bukar Majama, Ibrahim Alhaji Girgiri, Waziri Alhaji Kachamai, Ahmed Yahaya

Department of Veterinary Anatomy, Faculty of Veterinary Medicine, University of Maiduguri, Nigeria

***Corresponding author:**
Dr. Ali Musa Wulgo
Address: Department of Veterinary Anatomy, Faculty of Veterinary Medicine, University of Maiduguri, Nigeria
Phone: +2348143450680
ORCID: 0000-0003-0090-8046
E-mail: amwulgo@unimaid.edu.ng

Original Submission:
29 December 2025
Revised Submission:
20 February 2026
Accepted: 10 March 2026

How to cite this article: Gambo BG, Khalid M, Wulgo AM, Majama YB, Girgiri IA, Kachamai WA, Yahaya A. 2026. Craniometrical characteristics of the Uda and Yankasa breeds of sheep (*Ovis aries*). Veterinaria, 75(1), 51-62.

ABSTRACT

This study aimed to examine and compare the osteometric characteristics of the skulls of Uda and Yankasa sheep breeds. A total of 10 skulls of indigenous sheep breeds, comprising five Uda and five Yankasa rams aged between 12 and 18 months, were used for this study. The samples were obtained from Bauchi Metropolis, Bauchi State, Nigeria and transported to the Gross Anatomy laboratory, Department of Veterinary Anatomy, University of Maiduguri, Borno State, for bone processing. The bones were processed using hot water maceration and soft tissue removal techniques. About 39 cranial and mandibular measurements were identified. Comparative analysis of dorsal, caudal, ventral, lateral, and mandibular parameters revealed no statistically significant differences ($p > 0.05$) between Uda and Yankasa breeds across most measurements. Osteometric findings revealed that viscerocranial length-related parameters such as INL, VCrL, NL, IOL, MDL, and IISL were slightly higher in Yankasa than in Uda. However, neurocranial length-related parameters such as NCrL, ChL and HPL were slightly higher in Uda than in Yankasa. Yankasa also exhibited wider skull profiles, as reflected in IZW, HPW, ChW, IMDAW, NW and NCWLB, although the differences were not statistically significant. This study provides valuable osteometric data on Uda and Yankasa sheep breeds for taxonomic classification, evolutionary studies, and veterinary clinical applications such as regional anesthesia and surgical procedures involving the head.

Keywords: Craniometrics, osteometry, sheep, Uda, Yankasa

INTRODUCTION

There are generally four recognized indigenous sheep breeds in Nigeria (Popoola and Oseni, 2018), among which Uda and Yankasa account for approximately 70% of the estimated 39 million sheep population (Ramalan, 2022). These two breeds exhibit distinct physical features, particularly in their coat color, tail configuration, and growth characteristics (Madikadike and Tyasi, 2024).

The skull serves as a protective framework for the brain and sense organs while supporting the masticatory system. Its shape and dimensions therefore reflect both evolutionary divergence and adaptive responses to diet, climate, and management conditions (Dyce et al., 2010). Studies in craniomorphology and craniometry have proven useful in identifying taxonomic relationships and adaptive modifications resulting from natural selection (Popoola and Oseni,

doi.org/10.51607/22331360.2026.75.1.51

2018). Several researchers have used craniometric parameters to distinguish between different sheep breeds (Atabo et al., 2022; de la Barra et al., 2020). Using multivariate statistical methods, Popoola and Oseni (2018) successfully characterized the Balami, Uda, and Yankasa breeds indigenous to Nigeria. In some breeds of sheep such as Uda and Yankasa, these measurements are invaluable for distinguishing breeds, supporting taxonomic classification, and informing breeding, production, and conservation programs (Hailu, 2022). Although several studies have explored skull development in sheep (Olopade and Onwuka, 2005; Reda et al., 2016; Shehu et al., 2019), there is still limited information on the morphometric and craniometric characteristics of Uda and Yankasa rams native to Nigeria.

Numerous studies have investigated developmental changes in the sheep skull, including those of Olopade and Onwuka (2005), Avdić et al. (2013), Muhamed et al. (2016), Shehu et al. (2019), Dalga and Aslan (2021), Dalga et al. (2022), and Duro et al. (2025). However, there is a paucity of information on morphometric and craniometric variations of the skull, particularly in Uda and Yankasa rams from Nigeria. Therefore, this study aims to examine and compare the skull morphometry and craniometry of Uda and Yankasa rams to generate anatomical data that may facilitate breed identification, classification, and veterinary clinical applications.

MATERIAL AND METHODS

Sample collection

A total of 10 skulls of indigenous sheep breeds, comprising five Uda and five Yankasa rams aged between 12 and 18 months, were employed in this investigation. The samples were obtained from Bauchi Metropolis, Bauchi State, Nigeria, during the *Eid-el-Kabir* festival in June 2025 and transported to the Gross Anatomy laboratory, Department of Veterinary Anatomy, University of Maiduguri, Borno State, Nigeria, for bone processing.

Specimen preparation

Following the procedures described by Salami et al. (2011) and Gambo et al. (2016), all soft tissues adhering to the skulls, including fascia, muscles, ligaments and tendons, were carefully removed using scissors and a scalpel. The skulls were subsequently placed in two separate maceration pots filled with water to allow clear identification and differentiation. The samples were heated to boiling, after which the water was replaced. Polycarboxylate detergents were added to enhance the removal of fat, bone marrow, and any residual soft tissue. The macerated skulls were then immersed in 30% hydrogen peroxide for two days, thoroughly rinsed with water, and air-dried under sunlight. After preparation, the morphology and structural attributes of the cleaned skull bones were examined, and their metric dimensions were measured in centimeters (cm). Photographic documentation of the bones from different anatomical orientations was obtained using a Canon EOS 1300D digital camera.

Landmarks for craniometric measurements

According to the method adopted by Gambo et al. (2016), the following 39 landmarks of the skull (Figure 1-6) were considered.

i. Incisive-Nuchal Length (INL): Distance from the rostral tip of the incisive bone to the external occipital protuberance (nuchal crest).
ii. Viscerocranial Length (VCrL): Measured from the rostral tip of the incisive bone to the naso-frontal suture along the midline.
iii. Neurocranial Length (NCrL): From the frontonasal suture to the lambdoid suture.
iv. Neurocranial Width at Lacrimal Bone (NWLB): Maximum transverse width at the level of the lacrimal bones, just in front of the orbits.
v. Neurocranial Width at Horn Base (NWHB): Maximum distance between the bases of both horn cores on the frontal bone.
vi. Nasal Length at Midline (NLM): From the tip of the nasal bones along the midline to the frontonasal suture.
vii. Nasal Width (NW): Greatest transverse width across the nasal bones.
viii. Inter-Supraorbital Foramen Length (ISOFL): Between the left and right supraorbital foramina, above the orbit (frontal bone).
ix. Distance between the Horn Neck (DHN): Distance between the inner borders of the horn cores where they begin to project from the skull (horn necks).
x. Foramen Magnum Height (FMH): Vertical distance from the dorsal to ventral margin of the foramen magnum.
xi. Foramen Magnum Width (FMW): Horizontal distance from the rostral to caudal margin of the foramen magnum.

xii. Maximum Intercondylar Width (MICW): Widest distance between the occipital condyles (lateral edges).

xiii. Maximum Inter-Paracondylar Width (MIPCW): Maximum distance between the lateral ends of the paracondylar processes.

xiv. Paracondylar Process Length (PCPL): From the base to the tip of the paracondylar process.

xv. Inter-Cornual Protuberance to Foramen Magnum (ICPFM): From the center of the intercornual protuberance to the dorsal margin of the foramen magnum.

xvi. Incisivo-Occipital Length (IOL): Distance from the rostral tip of the incisive bone to the base of the occipital condyle.

xvii. Choana Length (ChL): Measured from the caudal margin of hard palate to basisphenoid bone.

xviii. Choana Width (ChW): Measured transversely between the widest lateral borders of the right and left choanae.

xix. Hard Palate Length (HPL): Measured along the midline from the caudal margin of the hard palate to the rostral tip of the incisive bone.

xx. Palatine Width (HPW): Measured across the widest part of the palatine process, from one lateral edge to the other.

xxi. Inter-incisive Suture Length (IISL): From the rostral tip of the incisive bone to the caudal end of the inter-incisive suture at the maxillary border.

xxii. Incisive Width (IcW): Measured transversely across the most lateral points of the incisive bones.

xxiii. Inter-Zygomatic Width (IZW): Measured from the outermost lateral edge of the right zygomatic arch to the outermost lateral edge of the left zygomatic arch.

xxiv. Orbital Height (ObH): Measured vertically from the dorsal orbital rim to the ventral orbital rim.

xxv. Orbital Width (ObW): Horizontal distance across the widest part of the orbit.

xxvi. Facial Tuberosity to Infraorbital Foramen (FTIOF): From the most prominent point of the facial tuberosity to the mid-caudal margin of the infraorbital foramen.

xxvii. Infraorbital Foramen to Root of Alveolar Tooth (IFRAT): Vertical distance from the infraorbital foramen to the root of the alveolar tooth ventral to it.

xxviii. Mandibular Length (MDL): From the rostral tip of the mandible to the caudal border of the mandibular angle.

xxix. Maximum Height of Mandible (MHMD): Vertical distance from the mandible base to the tip of the coronoid process.

xxx. Base of Mandible to Condyloid Fossa (BMCF): From the ventral border of the mandible to the condyloid fossa.

xxxi. Maximum Height to Condyloid Fossa (MHCF): From the lowest point of the mandible base to the top of the condyloid fossa.

xxxii. Diastemal Length (DL): Distance from the alveolar root of the last incisor to the first premolar.

xxxiii. Lateral Alveolar Root to Mental Foramen (LARMF): From the alveolar root of the lateral incisor to the caudal edge of mental foramen.

xxxiv. Mandibular Symphyseal Length (MSL): From the rostral-most point of the mandibular symphysis to the caudal end of the symphyseal fusion.

xxxv. Base of Mandible to Mandibular Foramen (BMMF): From the lowest point of the base of the mandible to the center of the mandibular foramen (medial side).

xxxvi. Mandibular Foramen to Caudal Border of Mandible (MFCBM): Distance from the mandibular foramen to the posterior edge of the mandible.

xxxvii. Mandibular Body Height (MDBH): From the alveolar margin to the widest part of the base of the mandible.

xxxviii. Intermandibular Angle Width (IMDAW): Between the inner caudal angles of the left and right mandibular halves. This is the transverse width across the mandible at its widest part.

xxxix. Mandibular Foramen to Coronoid Process (MDFCP): From the mandibular foramen to the tip of the coronoid process.

Statistical analysis

The morphometric data generated in this study were analyzed using descriptive statistics and presented as mean ± standard deviation (SD), along with column chart visualizations. Differences between mean values were evaluated using the independent samples t-test. All statistical analyses were performed using the Statistical Package for the Social Sciences (SPSS), version 20.0.

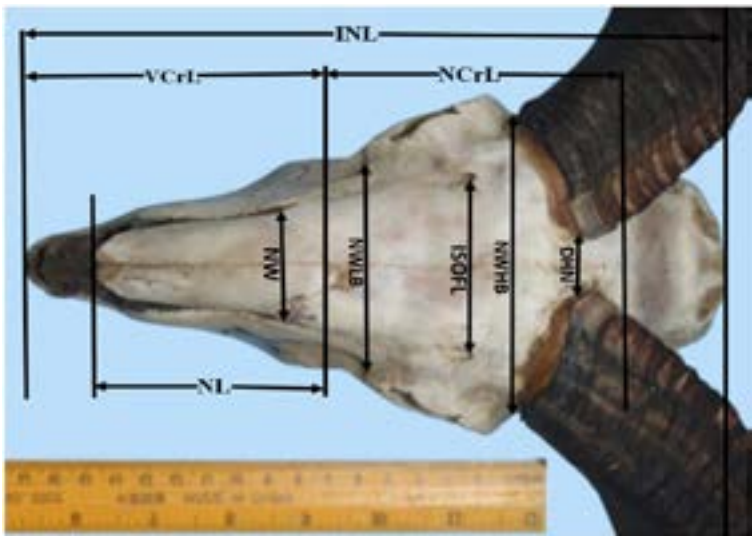

Figure 1 Skull measurements (Dorsal view) showing Incisive-Nuchal Length (INL), Viscerocranial Length (VCrL), Neurocranial Length (NCrL), Neurocranial Width at Lacrimal Bone (NWLB), Neurocranial Width at Horn Base (NWHB), Nasal Length (NL), Nasal Width (NW), Inter-Supra Orbital Foramen Length (ISOFL), Distance between the Horn Neck (DHN)

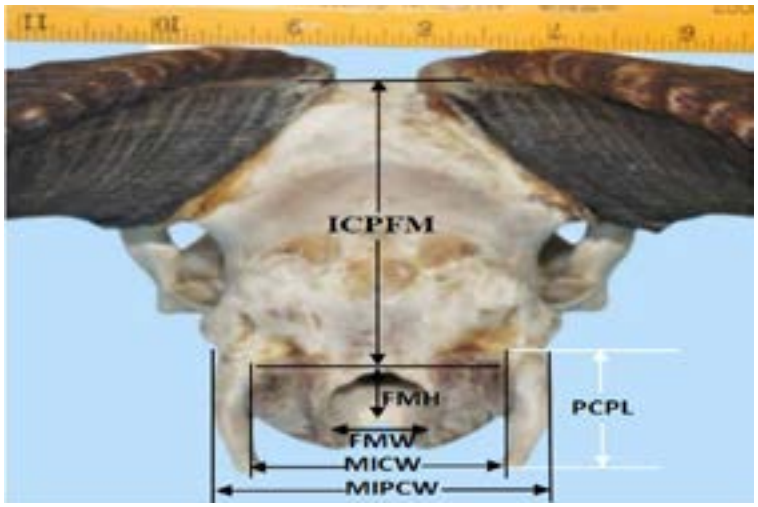

Figure 2 Skull measurements without the mandible (Caudal view) showing Foramen Magnum Height (FMH), Foramen Magnum Width (FMW), Maximum Intercondylar Width (MICW), Maximum Inter-Paracondylar Width (MIPCW), Paracondylar Process Length (PCPL), Inter-Cornual Protuberance to Foramen Magnum (ICPFM)

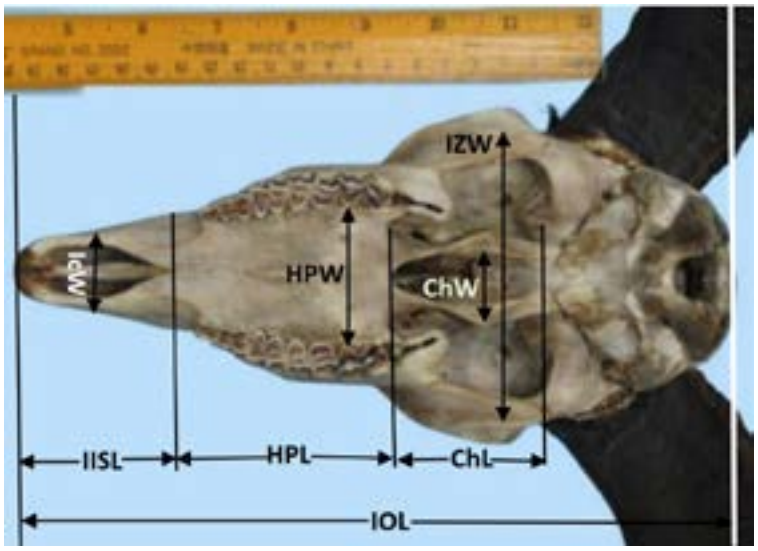

Figure 3 Skull measurements without the mandible (Ventral view) showing Incisivo-Occipital Length (IOL), Choana Length (ChL), Choana Width (ChW), Hard Palate Length (HPL), Palatine Width (HPW), Interincisive Suture Length (IISL), Incisive width (IcW) Inter-Zygomatic Width (IZW)

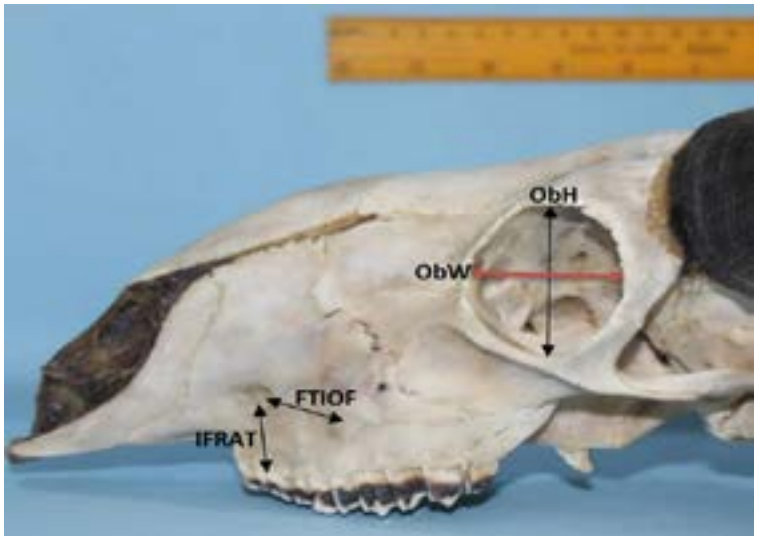

Figure 4 Skull measurements without the mandible (Lateral view) showing Orbital Height (ObH), Orbital Width (ObW), Facial Tuberosity to Infraorbital Foramen (FTIOF), Infraorbital Foramen to Root of Alveolar Tooth (IFRAT)

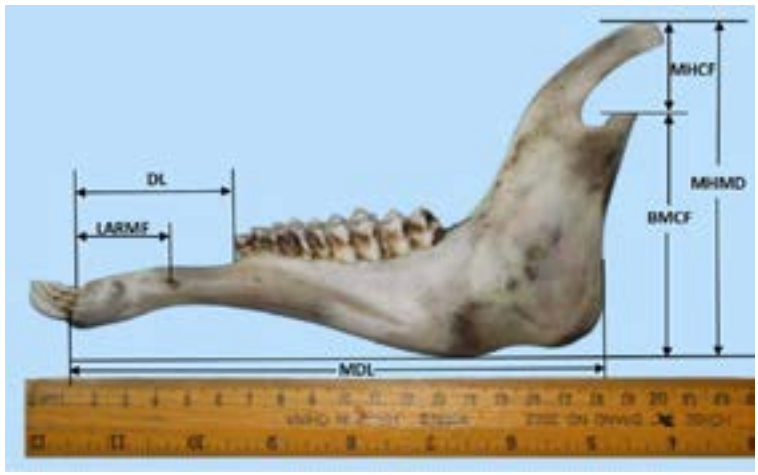

Figure 5 Mandible measurements (Lateral view) showing Mandibular Length (MDL), Maximum Height of Mandible (MHMD), Base of Mandible to Condyloid Fossa (BMCF), Maximum Height to Condyloid Fossa (MHCF), Diastemal Length (DL), Lateral Alveolar Root to Mental Foramen (LARMF)

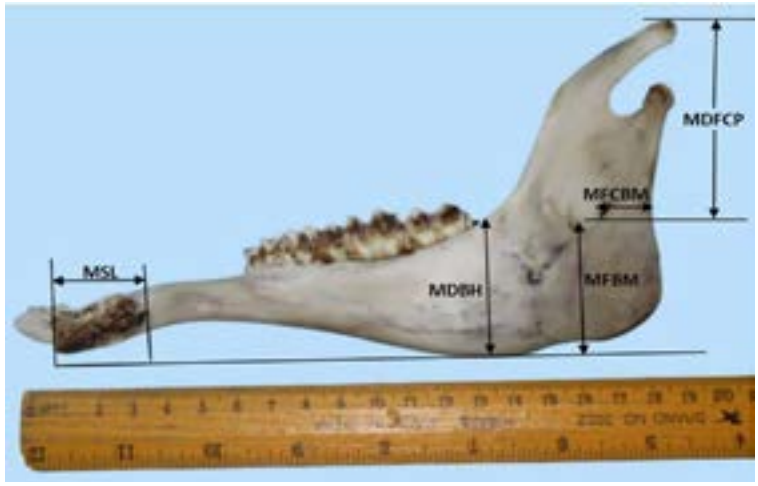

Figure 6 Mandible measurements (medial view) showing Mandibular Symphysis Length (MSL), Mandibular Foramen to Base of Mandible (MFBM), Mandibular Foramen to Caudal Border of Mandible (MFCBM), Mandibular Body Height (MDBH), Mandibular foramen to coronoid process (MDFCP)

RESULTS

Dorsal and Caudal parameters of Yankasa and Uda skulls

Fifteen morphometric parameters were recorded from the dorsal and caudal aspects of the Yankasa and Uda skulls (Table 1). The mean Incisive–Nuchal Length (INL) was 22.08 ± 2.43 cm in Yankasa and 21.08 ± 2.06 cm in Uda. The mean Viscerocranial Length (VCrL) was 9.62 ± 1.62 cm in Yankasa compared to 9.12 ± 1.39 cm in Uda, while the mean Neurocranial Length (NCrL) was 8.36 ± 0.72 cm and 8.66 ± 0.57 cm in Yankasa and Uda, respectively. The mean Neurocranial Width at the Lacrimal Bone (NWLB) was 5.60 ± 0.55 cm in Yankasa and 5.20 ± 0.84 cm in Uda, and the mean Neurocranial Width at the Horn Base (NWHB) was 8.90 ± 0.45 cm in Yankasa versus 8.48 ± 0.66 cm in Uda.

The Nasal Length (NL) averaged 8.04 ± 0.89 cm for Yankasa and 7.98 ± 1.04 cm for Uda, while Nasal Width (NW) measured 3.34 ± 0.70 cm and 3.00 ± 0.42 cm, respectively. The Inter-Supraorbital Foramen Length (ISOFL) was 4.98 ± 0.47 cm in Yankasa and 4.90 ± 0.43 cm in Uda. The Distance between the Horn Necks (DHN) recorded 5.36 ± 1.17 cm in Yankasa and 6.00 ± 0.37 cm in Uda. Mean Foramen Magnum Height (FMH) and Width (FMW) were similar between the breeds. Other parameters, including MICW, MIPCW, PCPL, and ICPF, also showed minimal variation. Overall, none of the 15 dorsal and caudal parameters exhibited statistically significant differences ($p > 0.05$) between Yankasa and Uda skulls.

Ventral and Lateral Parameters of Yankasa and Uda skulls

Twelve morphometric parameters were recorded from the ventral and lateral aspects of the Yankasa and Uda skulls (Table 2). The mean Incisivo-Occipital Length (IOL) was 21.86 ± 2.07 cm in Yankasa and 21.40 ± 2.00 cm in Uda. The Choana Length (ChL) averaged 4.70 ± 0.35 cm in Yankasa compared with 4.76 ± 0.55 cm in Uda, while the Choana Width (ChW) was 1.54 ± 0.13 cm and 1.48 ± 0.08 cm, respectively. The Hard Palate Length (HPL) was similar between the breeds, measuring 6.34 ± 0.84 cm in Yankasa and 6.40 ± 0.85 cm in Uda.

The Palatine Width (HPW) was 4.16 ± 0.29 cm in Yankasa and 3.84 ± 0.34 cm in Uda, whereas the Inter-Incisive Suture Length (IISL) was 5.36 ± 0.87 cm and 5.02 ± 0.47 cm, respectively. Incisive Width (IcW) was 3.72 ± 0.48 cm in Yankasa compared to 3.88 ± 0.97 cm in Uda. The Inter-Zygomatic Width (IZW) was 9.44 ± 0.58 cm in Yankasa and 8.76 ± 0.96 cm in Uda. Orbital Height (ObH) and Orbital Width (ObW) showed minimal variation between the breeds. The Facial Tuberosity to Infraorbital Foramen distance (FTIOF) was 2.14 ± 0.25 cm in Yankasa and 2.20 ± 0.29 cm in Uda, whereas the Infraorbital Foramen to Root of Alveolar Tooth (IFRAT) was 1.64 ± 0.29 cm and 1.52 ± 0.27 cm, respectively.

Overall, none of the twelve measured parameters showed statistically significant differences ($p > 0.05$) between the two breeds. Although several variables, including IOL, ChL, HPL, ObH, and FTIOF, demonstrated only minor variation, others such as HPW, IISL, IZW, and ObW exhibited comparatively greater differences that may indicate subtle breed-related morphological distinctions.

Mandibular Parameters of Yankasa and Uda Skulls

Twelve morphometric parameters were recorded from the lateral and medial surfaces of the mandibular bones of Yankasa and Uda skulls (Table 3). The mean Mandibular Length (MDL) was 15.72 ± 1.05 cm in Yankasa and 15.44 ± 1.68 cm in Uda, while the Maximum Mandibular Height (MMDH) was 10.24 ± 0.40 cm in Yankasa compared with 10.12 ± 1.08 cm in Uda. The Mandibular Body Height (MDBH) averaged 3.86 ± 0.26 cm in Yankasa and 3.98 ± 0.58 cm in Uda. The Base of Mandible to Condyloid Fossa (BMCF) was 7.68 ± 0.23 cm in Yankasa and 7.80 ± 0.90 cm in Uda, whereas the Maximum Height to Condyloid Fossa (MHCF) was 2.54 ± 0.15 cm and 2.28 ± 0.33 cm, respectively.

The Diastemal Length (DL) was 4.48 ± 0.40 cm in Yankasa and 4.18 ± 0.34 cm in Uda, and the Mandibular Symphyseal Length (MSL) was 2.42 ± 0.28 cm and 2.30 ± 0.21 cm, respectively. Measurements from the Mandibular Foramen to the Base of Mandible (MFBM) were 3.96 ± 0.36 cm in Yankasa and 4.00 ± 0.46 cm in Uda, while the distance from the Mandibular Foramen to the Caudal Border of the Mandible (MFCBM) was 1.42 ± 0.11 cm and 1.18 ± 0.49 cm, respectively. The Lateral Alveolar Root to Mental Foramen (LARMF) was 2.44 ± 0.34 cm in Yankasa and 2.44 ± 0.23 cm in Uda. The Inter-Mandibular Angle Width (IMDAW) averaged 5.82 ± 0.61 cm in Yankasa and 4.78 ± 0.41 cm in Uda, and the Mandibular Foramen to Coronoid Process distance (MDFCP) was 6.70 ± 0.75 cm and 6.66 ± 0.86 cm,

respectively. No statistically significant differences ($p > 0.05$) were observed for most mandibular parameters between the two breeds. However, IMDAW showed a statistically significant difference, with Yankasa exhibiting a greater mean value than Uda.

Table 1 Independent sample t-test for osteometric parameters of the dorsal and caudal surfaces of the skull in Yankasa and Uda sheep breeds

	Yankasa (n=5)			Uda (n=5)			
Parameters	**Min.**	**Max.**	**Mean ± SD**	**Min.**	**Max.**	**Mean ± SD**	**p-value**
INL	20.20	25.90	22.08±2.43	19.60	24.20	21.08±2.06	0.502 ^{ns}
VCrL	7.90	12.20	9.62±1.62	7.30	11.10	9.12±1.39	0.615 ^{ns}
NCrL	7.50	9.20	8.36±0.72	8.00	9.20	8.66±0.57	0.484 ^{ns}
NCWLB	5.0	6.0	5.60±0.55	4.00	6.00	5.20±0.84	0.397 ^{ns}
NCWHB	8.30	9.40	8.90±0.45	7.80	9.40	8.48±0.66	0.275 ^{ns}
NL	7.10	9.50	8.04±0.89	6.70	9.10	7.98±1.04	0.925 ^{ns}
NW	2.80	4.50	3.34±0.70	2.60	3.50	3.00±0.42	0.379 ^{ns}
ISOFL	4.40	5.60	4.98±0.47	4.40	5.30	4.90±0.43	0.786 ^{ns}
DHN	3.80	7.00	5.36±1.17	5.40	6.40	6.00±0.37	0.277 ^{ns}
FMH	2.00	2.40	2.22±0.15	2.00	2.50	2.24±0.21	0.865 ^{ns}
FMW	1.60	2.30	2.06±0.28	2.00	2.20	2.14±0.09	0.559 ^{ns}
MICW	4.10	6.10	5.14±0.71	4.90	5.30	5.14±0.17	1.000 ^{ns}
MIPCW	5.40	7.00	6.44±0.61	5.70	6.70	6.24±0.46	0.574 ^{ns}
PCPL	2.10	3.30	2.80±0.45	2.20	3.40	2.68±0.48	0.692 ^{ns}
ICPFM	5.00	6.00	5.62±0.39	5.50	6.00	5.80±0.23	0.402 ^{ns}

INL: Incisive-Nuchal Length; **VCrL**: Viscerocranial Length; **NCrL**: Neurocranial Length; **NCWHB**: Neurocranial Width at Horn Base; **NCWLB**: Neurocranial Width at Lacrimal Bone; **NL**: Nasal Length; **NW**: Nasal Width; **ISOFL**: Inter-Supra Orbital Foramen Length; **DHN**: Distance Between the Horn Neck; **FMH**: Foramen Magnum Height; **FMW**: Foramen Magnum Width; **MICW**: Maximum Intercondylar Width; **MIPCW**: Maximum Inter-Paracondylar Width; **PCPL**: Paracondylar Process Length; **ICPFM**: Inter-Cornual Protuberance to Foramen Magnum.
^{ns} No significant difference ($p > 0.05$).

Table 2 Independent sample t-test for osteometric parameters of the ventral and lateral surfaces of the skull in Yankasa and Uda sheep breeds

	Yankasa (n=5)			Uda (n=5)			
Parameters	**Min.**	**Max.**	**Mean ± SD**	**Min.**	**Max.**	**Mean ± SD**	**p-value**
IOL	20.00	25.00	21.86±2.07	19.10	24.20	21.40±2.00	0.730^{ns}
ChL	4.40	5.30	4.70±0.35	4.30	5.60	4.76±0.55	0.843^{ns}
ChW	1.30	1.60	1.54±0.13	1.40	1.60	1.48±0.08	0.421^{ns}
HPL	5.60	7.30	6.34±0.84	5.60	7.50	6.40±0.85	0.913^{ns}
HPW	3.80	4.60	4.16±0.29	3.40	4.30	3.84±0.34	0.145^{ns}
IISL	4.80	6.90	5.36±0.87	4.30	5.40	5.02±0.47	0.462^{ns}
IcW	3.10	4.40	3.72±0.48	3.00	5.40	3.88±0.97	0.749^{ns}
IZW	8.90	10.40	9.44±0.58	7.40	10.00	8.76±0.96	0.210^{ns}
ObH	3.30	3.80	3.58±0.22	3.30	3.90	3.62±0.24	0.789^{ns}
ObW	3.70	4.00	3.88±0.13	3.50	4.20	3.78±0.28	0.487^{ns}
FTIFOF	1.80	2.50	2.14±0.25	1.90	2.60	2.20±0.29	0.736^{ns}
IFOFAT	1.40	2.00	1.64±0.29	1.30	1.90	1.52±0.27	0.515^{ns}

IOL: Incisivo-Occipital Length; **ChL**: Choana Length; **ChW**: Choana Width; **HPL**: Hard Palate Length; **HPW**: Hard Palatine Width; **IISL**: Inter-incisive Suture Length; **IcW**: Incisive width; **IZW**: Inter-Zygomatic Width; **ObH**: Orbital Height; **ObW**: Orbital Width; **FTIFOF**: Facial Tuberosity to Infraorbital Foramen; **IFOFAT**: Infraorbital Foramen to Root of Alveolar Tooth.
^{ns} No significant difference ($p > 0.05$).

Table 3 Independent sample t-test for osteometric parameters of the mandibles in Yankasa and Uda sheep breeds

	Yankasa (n=5)			Uda (n=5)			
Parameters	**Min.**	**Max.**	**Mean ± SD**	**Min.**	**Max.**	**Mean ± SD**	**p-value**
MDL	14.50	17.10	15.72±1.05	13.70	18.00	15.44±1.68	0.760^{ns}
MMDH	9.70	10.80	10.24±0.40	9.00	11.60	10.12±1.08	0.823^{ns}
MDBH	3.50	4.20	3.86±0.26	3.40	4.70	3.98±0.58	0.684^{ns}
BMCF	7.40	8.00	7.68±0.23	6.90	8.90	7.80±0.90	0.780^{ns}
MHCF	2.30	2.70	2.54±0.15	1.90	2.70	2.28±0.33	0.152^{ns}
DL	3.90	4.90	4.48±0.40	3.70	4.60	4.18±0.34	0.240^{ns}
MSL	2.10	2.80	2.42±0.28	2.00	2.50	2.30±0.21	0.464^{ns}
MDFBM	3.70	4.40	3.96±0.36	3.60	4.50	4.00±0.46	0.882^{ns}
MDFCB	1.30	1.60	1.42±0.11	0.50	1.70	1.18±0.49	0.322^{ns}
LARMF	2.10	3.00	2.44±0.34	2.20	2.80	2.44±0.23	1.000^{ns}
IMDAW	4.90	6.60	5.82±0.61	4.10	5.10	4.78±0.41	0.14 ^{ns}
MDFCP	5.90	7.80	6.70±0.75	5.80	8.00	6.66±0.86	0.940^{ns}

MDL: Mandibular Length; **MMDH**: Maximum Mandibular Height; **MDBH**: Mandibular Body Height; **BMCF**: Base of Mandible to Condyloid Fossa; **MHCF**: Maximum Height to Condyloid Fossa; **DL**: Diastemal Length; **MSL**: Mandibular Symphysis Length; MDFBM: Mandibular Foramen to Base of Mandible; **MDFCB**: Mandibular Foramen to Caudal Border of Mandible; **LARMF**: Lateral Alveolar Root to Mental Foramen; **IMDAW**: Inter Mandibular angle width; **MDFCP**: Mandibular foramen to coronoid process

^{ns} No significant difference ($p > 0.05$).

DISCUSSION AND CONCLUSION

In this study, skull length was recorded as incisive-nuchal length (INL), which is slightly higher in Yankasa (22.08 ± 2.43 cm) compared to Uda (21.08 ± 2.06 cm), but not statistically significant. Shehu et al. (2019) reported a length of 23.90±0.14 cm, similar to the age group in this study, and a longer length of 32.50±0.99 cm in older (three years and above) Yankasa rams from Sokoto. Comparable length (22.9 ± 0.8 cm) in males and (21.7 ± 0.3 cm) in females of Hamdani sheep was reported by Dayan et al., (2022). The skull length of Yankasa and Uda sheep is shorter than many nonindigenous breeds. Yılmaz & Demircioglu (2020) reported 24.13 ± 1.40 cm in İvesi sheep of Turkey. Similarly, higher values were reported by Parés-Casanova et al., (2010), Reda et al., (2016), Dalga et al., (2018), Gündemir et al. (2020), Jashari et al., (2022), and Guzel et al. (2024) in Xisqueta sheep, Barbados Black Belly sheep in Trinidad, Hemşin sheep, Bardhoka rams of Kosovo, Sharri sheep, and Romanov sheep, respectively. Conversely, lower skull length values were equally reported in some nonindigenous breeds. Özcan et al., (2010) reported 20.45 ± 0.97 cm and 19.81 ± 0.77 cm in Morkaraman sheep and Tuj sheep, respectively. Mehraban sheep of Iran were reported to have 20.06 ± 1.71 cm (Karimi et al., 2011).

This study revealed that the Uda breed has a longer neurocranium (8.66 ± 0.57 cm) than the Yankasa (8.36 ± 0.72 cm). Conversely, Yankasa has a longer viscerocranium (9.62 ± 1.62 cm) as compared to Uda (9.12 ± 1.39 cm), though it is statistically not significant. Higher viscerocranial values were reported in Morkaraman sheep and Tuj sheep of Turkey (Ozcan et al., 2010), Akkaraman sheep and Kangal Akkaraman sheep (Hacer et al., 2023), and male Romanov sheep (Guzel et al., 2024).

Yankasa has higher nasal length, and nasal width of 8.04 ± 0.89 cm, and 3.34 ± 0.70 cm, respectively. Conversely, Uda has lower values of 7.98 ± 1.04 cm, and 3.00 ± 0.42 cm, in the respective parameters. Shehu et al. (2019) reported Nasal length value of 8.20 ± 0.42 in Yankasa in Sokoto. Dayan et al. (2022), recorded 8.36± 0.32 cm in males and 8.29 ± 0.31 cm in females of Hamdani sheep of Turkey. Dalga et al. (2018) recorded it as 8.25 ± 0.78 cm in the Hemshin sheep. While it was reported as 7.03 ± 0.67 cm in the Morkaraman sheep breed and 6.86 ± 0.31 cm in the Tuj sheep of Turkey (Ozcan et al., 2010). In Romanov sheep, the length was 7.46 ± 0.12 cm in males and 7.26 ± 0.07 cm in females (Guzel et al., 2024).

The supraorbital foramen, located on the dorsal orbital margin, was also observed to be an important cranial landmark. The mean intersupraorbital foramen length (ISOFL) was higher in Yankasa (4.98 ± 0.47 cm) compared to Uda (4.90 ± 0.43 cm). Reda et al., (2016) reported a length of 5.64 ± 0.84 cm in Barbados Black Belly sheep, and Monfared (2013) reported 9.5 ± 1.44 in the Iranian Native sheep. This foramen transmits the frontal nerve, and its clinical relevance lies in the ability to block this nerve during dehorning, trephination of the frontal sinus, and in the surgical management of horn related injuries (Gambo et al., 2015). Knowing the location across breeds indicates its reliability as a landmark for supraorbital nerve block in sheep.

Foramen magnum shape is an important dimorphic feature (Gapert et al., 2009). In this study, Foramen Magnum Height showed similar values in both breeds, 2.22 ± 0.15 cm in Yankasa and 2.24 ± 0.21 cm in Uda. Shehu et al., (2019) reported foramen magnum height of 2.1 ± 0.10, 1.9 ± 0.10 and 1.8 ± 0.00 in Balami, Uda, and Yankasa, respectively. In Sharri sheep, it was determined as 2.00 ± 0.22 cm (Jashari et al., 2022), whereas Ozcan et al. (2010) reported the same parameter as 1.94 ± 0.11 cm in Morkaraman sheep and 1.78 ± 0.15 cm in Tuj sheep. Guzel et al. (2024) reported 1.72±0.10 cm in Romanov sheep.

Similarly, Foramen Magnum Width is slightly lower in Yankasa (2.06 ± 0.28 cm) compared to Uda (2.14 ± 0.09 cm). However, it was reported as 2.00 ± 0.00 cm in Balami, 2.00 ± 0.00 cm in Uda and 1.90 ± 0.20 cm in Yankasa (Shehu et al., 2019). Dayan et al., (2022) mentioned foramen magnum width in Hamdani sheep as 2.48 ± 0.06 cm, whereas in Romanov ram it was 1.87 ± 0.07 cm (Guzel et al., 2024).

On the ventral and lateral surfaces of the skulls, the results reveal both similarities and differences between the Yankasa and Uda sheep breeds across the twelve parameters analyzed. Skull length related parameters, such as IOL, ChL, HPL, IISL and FTIFOF, show minimal differences between the breeds. However, skull width related parameters such as HPW, IcW, and IZW, exhibit variations, though not statistically significant. Wider skull width profile, such as hard palate width (HPW) and inter-zygomatic width (IZW) in Yankasa sheep, suggest distinct cranial morphology compared to Uda sheep.

In the present study, skull width was regarded as inter-zygomatic width (IZW) representing the maximum cranial width at the zygomatic arches. It was greater in Yankasa (9.44 ± 0.58 cm) compared to (8.76 ± 0.96 cm) in Uda. Comparable values have been reported in Morkaraman and Tuj sheep of Turkey, 10.30 ± 0.25 cm and 10.17 ± 0.17 cm, respectively (Özcan et al., 2010). Karimi et al., (2011) mentioned 10.44 ± 0.29 cm in Iranian Mehraban sheep, and Gündemir et al., (2020) determined it to be 10.70 ± 0.50 cm in Bardhoka sheep of Kosovo. Conversely, in İvesi sheep of Turkey it was recorded as 11.34 ± 0.89 cm in males and 11.68 ± 0.64 cm in females (Yılmaz and Demircioglu, 2020).

In the present study, Incisivo-Occipital Length (condylobasal length), Choana Width, Palatine Width and Inter-Incisive Suture Length presented a higher mean in Yankasa skulls (21.86 ± 2.07 cm, 1.54 ± 0.13 cm, 4.16 ± 0.29 cm and 5.36 ± 0.87 cm) than in Uda skulls (21.40 ± 2.00 cm, 1.48 ± 0.08 cm, 3.84 ± 0.34 cm and 5.02 ± 0.47 cm), respectively. Conversely, Uda skulls showed higher mean values in Choana Length, Hard Palate Length and Incisive Width (4.76 ± 0.55 cm, 6.40 ± 0.85 cm, 3.88 ± 0.97 cm, respectively) compared to Yankasa (4.70 ± 0.35 cm, 6.34 ± 0.84 cm, and 3.72 ± 0.48 cm, respectively).

The mean Orbital Height of Yankasa, 3.58 ± 0.22 cm, was lower compared to that of Uda, 3.62 ± 0.24 cm. Conversely, the mean Orbital Width of Yankasa was higher (3.88 ± 0.13 cm) compared to that of Uda (3.78 ± 0.28 cm). The facial tuberosity was observed to be a prominent landmark in both breeds, positioned laterally on the maxilla. Its proximity to the infraorbital foramen provides a useful guide for identifying this foramen in live animals. To locate the infraorbital foramen, it is necessary to know the distance from the infraorbital foramen to facial tuberosity. The mean Facial Tuberosity to Infraorbital Foramen (FTIOF) of Uda was 2.20 ± 0.29 cm, which is higher than that of Yankasa (2.14 ± 0.25 cm). However, Shehu et al. (2019) reported it as 3.39 ± 0.35 cm in Yankasa rams of Sokoto. Monfared, (2013) mentioned it as 1.87 ± 0.09 cm in Iranian domestic sheep. Similarly, Marzban et al., (2018) reported 1.28 ± 0.18 cm in female Zell sheep skull. It was determined by Gündemir et al., (2020) in Bardhoka sheep of Kosovo as 2.59 ± 0.17 cm in females and 2.58 ± 0.30 cm in males. Özüdoğru et al. (2023) in Konya merino sheep and Reda et al., (2016) in Barbados Black Belly sheep documented it as 3.04 ± 0.19 cm and 3.16 ± 0.70 cm, respectively. The distance between the infraorbital foramen to the alveolar teeth (IFOFAT) was found to be higher in Yankasa 1.64 ± 0.29 cm compared

to 1.52 ± 0.27 cm in Uda. This measurement provides additional guidance for avoiding alveolar injury while inserting needles for infraorbital nerve block.

Clinically, this relationship is significant for blocking the infraorbital nerve to achieve desensitization of the upper lip, nose, and maxillary incisors during dental procedures, rhinoplasty, and suturing of wounds around the muzzle (Gambo et al., 2016).

The mandible is recognized as the largest bone of the skull (Avdić et al., 2013). The mandibular parameters measured (MDL, MDH, MDBH, BMCF, MHCF, DL, MSL, BMMDF, MDFCB, LARMF, MDFCP and IMDAW) did not show any statistically significant differences between the Yankasa and Uda breeds.

Among the mandibles studied, Yankasa exhibited a higher mandibular length (15.72 ± 1.68 cm) than Uda (15.44 ± 1.68 cm). Similar values were reported in Mehraban sheep 15.76 ± 2.25 cm (Karimi et al., 2012), Gurcu goat 15.9 ± 1.04 cm (Dalga, 2021), and Roe deer 15.6 ± 1.22 cm (Avdić et al., 2013), respectively. Higher values were also reported from Sharri sheep, 18.59 ± 1.33 cm (Gündemir et al., 2020), and Barbados Black Belly sheep, 18.16 ± 1.53 cm (Reda et al., 2016). However, lower value of 14.08 ± 0.01 cm was reported in Iranian native sheep (Monfared, 2013), and 14.91 ± 0.48 cm in Norduz sheep (Dalga et al., 2022).

Distance between Base of Mandible to Condyloid Fossa (BMCF) of Yankasa was 7.68 ± 0.23 cm, which is lower compared to Uda (7.80 ± 0.90 cm). Results were comparable to those reported in the Mehraban sheep (7.75 ± 0.96 cm) (Karimi et al., 2011) and higher than those of Barbados Black Belly sheep (7.08 ± 0.73 cm) (Reda et al., 2016), Norduz sheep (6.29 ± 0.23 cm) (Dalga et al., 2022), Iranian Native sheep (6.26 ± 0.17 cm) (Monfared, 2013), Balkan chamois (6.58 ± 0.55 cm) (Duro et al., 2025), Roe deer (5.85 ± 0.21 cm) (Avdić et al., 2013), and Gurcu goat (6.23 ± 0.65 cm) (Dalga, 2021).

The results showed that the distance from mandibular foramen to the caudal border of mandible was higher in Yankasa (1.42 ± 0.11 cm) compared toUda (1.18 ± 0.49 cm). The reported values were comparable to that of Mehraban sheep (1.35 ± 0.29 cm) (Karimi et al., 2011). On the other hand, lower values were recorded in Iranian Native sheep (0.86 ± 0.03 cm) (Monfared, 2013) and Balkan chamois (1.33 ± 0.15 cm) (Duro et al., 2025). This value was higher in Barbados Black Belly sheep (2.3 ± 0.25 cm) (Reda et al., 2016).

The mean mandibular foramen to the base of the mandible was higher in Yankasa (4.00 ± 0.46 cm) than in Uda (3.96 ± 0.36 cm). This value is comparable to that reported in in Mehraban sheep (4.14 ± 0.47 cm) (Karimi et al., 2011), while in Barbados Black Belly sheep 3.75 ± 0.22 cm was reported (Reda et al., 2016). Lower values were reported in the Gurcu goat (3.22 ± 0.28 cm) (Dalga, 2021), Balkan chamois (2.49 ± 0.20 cm) (Duro et al., 2025), and Iranian Native sheep (0.86 ± 0.03 cm) (Monfared, 2013).

This study revealed that the distance between the lateral alveolar root to the mental foramen (LARMF) was nearly similar in both breeds, 2.44 ± 0.34 cm in Yankasa and 2.44 ± 0.23 cm in Uda. Higher figures were reported in the Iranian Native sheep (2.76 ± 0.05 cm) (Monfared, 2013). Value reported in Barbados Black Belly sheep was 2.25 ± 0.31 cm (Reda et al., 2016) and lower value was reported in the Mehraban sheep () (Karimi et al., 2011), Gurcu goat (1.97 ± 0.23 cm) (Dalga, 2021), and Balkan chamois (1.75 ± 0.36 cm) (Duro et al., 2025).

The Mean Inter Mandibular Angle Width of Yankasa was 5.82 ± 0.61 cm, and 4.78 ± 0.41 cm of Uda.. The findings imply that the Yankasa and Uda breeds may share genetic or environmental factors that contribute to their morphological similarities. However, it is important to note that this analysis is limited to the specific parameters measured and does not account for other potential differences, such as physiological, or production-related characteristics.

In conclusion, the comparative osteometric analysis of the skull and mandible in Yankasa and Uda sheep revealed no statistically significant differences across the parameters measured, suggesting that both breeds share a broadly similar cranial morphology. Although slight variations were observed in the dimensions of the neurocranium and viscerocranium, these differences were not statistically significant. The infraorbital foramen was consistently located near the facial tuberosity in both breeds, a clinically important landmark for regional anesthesia. Likewise, mandibular measurements including the location of the mandibular foramen, the base of the mandible to the condyloid fossa, and the distance from the alveolar root to the mental foramen were comparable and aligned with values reported for other sheep breeds. The findings provide baseline osteometric data for Uda and Yankasa sheep and contribute to improved precision in regional anesthetic techniques. Practically, these morphometric landmarks may assist veterinarians working under

field conditions where advanced imaging modalities are unavailable. However, the primary limitation of this study is the small sample size, which may reduce statistical power and limit the detection of subtle morphometric differences. Future studies incorporating larger sample sizes and wider geographic sampling are recommended to enhance statistical robustness and strengthen breed-level anatomical inference.

ACKNOWLEDGEMENTS

The authors appreciate the technical support received from the Staff of Gross Anatomy Laboratory, Department of Veterinary Anatomy, University of Maiduguri, Nigeria.

CONFLICT OF INTEREST

The authors declared that there is no conflict of interest.

CONTRIBUTIONS

BGG–Concept, Design, and Supervision; MK¬–Materials, Data collection and/or processing, Analysis and/or Interpretation of the Data, and Literature review; AMW– Analysis and/or Interpretation of the Data, Literature review, Writing and Critical review; YBM¬–Critical review; IAG– Critical review; WAK– Analysis and/or Interpretation of the Data, Literature review, and Critical review; AY– Supervision

REFERENCES

Atabo SM, Umar AA, Shehu SA, Abubakar AA. 2022. Comparative neurocranial morphology of Nigerian breeds of sheep. Arch Vet Sci, 27(1), 149-65. DOI: https://doi.org/10.5380/avs.v1i1.80871

Avdić R, Hadžiomerović N, Tandir F, Bejdić P, Ćutahija V. 2013. Analysis of morphometric parameters of the Roe deer mandible (Capreolus capreolus) and mandible of the sheep (Ovis aries). Veterinaria, 62(1-2), 1-9.

Dalga S, Aslan K, Akbulut Y. 2018. A morphometric study on the skull of the adult Hemshin sheep. Van Vet J, 29, 125-129. http://dergipark.gov.tr/vanvetj

Dalga S, Aslan K. 2021. Morphological and Osteometric Analysis of the Skull in Abaza goats (Capra aegagrus). Dicle ÜniverVet Fak Derg, 14(1), 35-38.

Dalga S, Aydın U, Çal T. 2022. Topographic, morphological and morphometric investigation of mandible in norduz sheep. Türk Doğa Fen Derg, 11(3), 129-133.

Dayan MO, Demircioğlu İ, Koçyiğit A, Guzel BC, Karaavci FA. 2022. Morphometric analysis of the skull of Hamdani sheep via three-dimensional modeling. Anatomia Histolo Embryol, 52(2), 215-222. DOI: https://doi.org/10.1111/ahe.12873

De la Barra R, Carvajal AM, Martínez ME. 2020. Variability of cranial morphometrical traits in Suffolk Down sheep. Australian Journal of Veterinary Science, 52(1), 25-31. http://dx.doi.org/10.4067/S0719-81322020000100105.

Duro S, Gündemir O, Hadžiomerović N, Kotrošan D, Szara T. 2025. Morphological and morphometric study of the head skeleton of the Balkan chamois (Rupicapra rupicapra balcanica Bolkay, 1925) in the West Balkan area. Biologia, 1-14.

Dyce KM, Sack WO, Wensing CJG. 2010. Textbook of veterinary anatomy (4th ed.). Saunders Elsevier.

Gambo BG, Yahaya A, Girgiri IA, Olopade JO. 2015. Morphometric studies of the mandibular and maxillofacial regions of the Kuri cattle and the implications in regional anaesthesia Folia Morphology. 74(2), 183-187. DOI: https://doi.org/10.5603/FM.2015.0029

Gambo BG, Yahaya A, Olopade JO. 2016. Morphological studies of the facial tuberoses and infraorbital, supraorbital and mental foramina in Kuri cattle. Global Veterinaria, 17(2), 99-104. DOI: https://doi.org/10.5603/FM.2015.0029

Gapert R, Black S, Last J. 2009. Sex determination from the foramen magnum: Discriminant function analysis in an eighteenth and nineteenth century British sample. International Journal of Legal Medicine, 123(1), 25-33. DOI: https://doi.org/10.1007/s00414-008-0256-0

Gundemir O, Duro S, Jashari T, Kahvecioğlu O, Demircioğlu İ, Mehmeti H. 2020. A study on morphology and morphometric parameters on the skull of the Bardhoka autochthonous sheep breed in Kosovo. Anatomia Histologia Embryologia, 49(3), 365-371. DOI: https://doi.org/10.1111/ahe.12538

Guzel BC, İsbilir F. 2024. Morphometric analysis of the skulls of a ram and ewe Romanov sheep with 3D modeling. Veterinary Medicine and Science, 10, e1396. DOI: https://doi.org/10.1002/vms3.1396

Hacer BE, Beşoluk K, Başpınar N. 2023. A morphometric comparison of the skulls of Akkaraman and Kangal Akkaraman sheep using computed tomography. MAE Veterinary Faculty Journal, 8(1), 37-43. DOI: 10.24880/maeuvfd.1222154

Hailu A. 2022. Review of the steps to establish a sheep and goat community-based conservation and breeding program (CBCBP) in Ethiopia. The Ethiopian Journal of Biodiversity (ethjbd), 171.

Jashari T, Duro S, Gundemir O, Szara T, Ilieski V, Mamuti D, et al. 2022. Morphology, morphometry and some aspects of clinical anatomy in the skull and mandible of Sharri sheep. Biologia, 77(2), 423-433. https://doi.org/10.1007/s11756-021-00955-y

Karimi I, Onar V, Pazvant G, Hadipour M, Mazaheri Y. 2011. The cranial morphometric and morphologic characteristics

of Mehraban sheep in Western Iran. Global Veterinaria, 6(2), 111-117.

Madikadike MK, Tyasi ThL. 2024. Growth Traits as Predictors of Body Weight in Sheep: A Review. *World Vet*. J., 14(2): 284-292. DOI: 10.54203/scil. 2024.wvj35

Marzban AB, Hajian O, Rahmati S. 2020. Investigating the Morphometric Characteristics of Male and Female Zell Sheep Skulls for Sexual Dimorphism. Anatomical Sciences. 2020; 17(1):13-20.

Monfared AL, Naji H, Sheibani MT. 2013. Applied anatomy of the head region of the iranian native goats (capra hircus). Global Veterinaria 10(1):60-64. DOI:10.5829/idosi. gv.2013.10.1.71133.

Olopade JO, Onwuka SK. 2005. Morphometric studies on the skull of West African Dwarf goats from South West Nigeria. Nigerian Veterinary Journal, 26(2), 18-21. DOI:10.4314/nvj. v26i2.3487.

Ozcan S, Aksoy G, Kurtul İ, Aslan K, Ozudogru Z. 2010. A comparative morphometric study on the skull of the Tuj and Morkaraman sheep. Kafkas Üniversitesi Veteriner Fakültesi Dergisi, 16(1), 111-114. DOI:10.9775/kvfd.2009.518.

Ozudogru Z, Ozdemir D, Teke BE, Kirbas M. 2022. Morphological and craniometrical studies on the skull of the South Karaman sheep. Acta Morphologica et Anthropologica, 29(1-2). DOI:10.7546/AMA.29.1-2.2022.17

Parés-Casanova PM, Kamal S, Jordana J. 2010. On biometrical aspects of the cephalic anatomy of Xisqueta sheep (Catalunya, Spain). International Journal of Morphology, 28(2), 347-351. DOI: 10.4067/S0717-95022010000200001.

Popoola MA, Oseni SO. 2018. Multifactorial discriminant analysis of cephalic morphology of indigenous breeds of sheep in Nigeria. Slovak Journal of Animal Science, 51(2), 45-51. DOI:10.51791/njap.vi.7315.

Ramalan SM, Adama TZ, Alemede IC, Tsado DN, Alabi JO, Alagbe JO. 2022. Growth and Reproductive Performance of Yankasa Ewes Fed Varying Levels of Dietary Premix. Journal La Lifesci, 3(1), 26-35. DOI: 10.37899/journallalifesci. v3i1.536

Reda M, Driscoll M, Mootoo N. 2016. Clinical anatomy of the skull of the Barbados Black Belly sheep in Trinidad. International Journal of Current Research in Medical Sciences, 2(8), 8-19. SOI: http://s-o-i.org/1.15/ijcrms-2016-2-8-2.

Salami SO, Ibe CS, Umosen AD, Ajayi IE, Maidawa SM. 2011. Comparative osteometric study of long bones in Yankasa sheep and Red Sokoto goats. Int J Morphol; 29(1):100–104. DOI:10.4314/nvj.v31i4.68987.

Shehu SA, Bello A, Danmaigoro A, Abdulrasheed HA, Atabo SM, Mahmud MA. 2019. Osteometrical study on age-related changes of the skull of Yankasa ram. Journal of Animal Science and Veterinary Medicine, 4(2), 71-77. https://doi.org/10.31248/JASVM2019.132.

Yilmaz B, Demircioğlu İ. 2020. Morphometric analysis of the skull in the Awassi sheep (*Ovis aries*). Fırat Üniversitesi Sağlık Bilimleri Veteriner Dergisi, 34(1), 1-6. https://veteriner.fusabil.org/pdf/pdf_FUSABIL_1388.pdf

Kraniometrijske karakteristike ovaca pasmina Uda i Yankasa (*Ovis aries*)

SAŽETAK

Cilj ove studije bio je ispitati i usporediti osteometrijske karakteristike lobanja pasmina ovaca Uda i Yankasa. Za ovu studiju korišteno je ukupno 10 lobanja autohtonih pasmina ovaca, uključujući pet ovnova Uda i pet ovnova Yankasa starosti između 12 i 18 mjeseci. Uzorci su prikupljeni u gradu Bauchi, savezna država Bauchi, Nigerija, te su transportovani u Laboratorij za topografsku anatomiju, Odsjek za veterinarsku anatomiju Univerziteta u Maiduguriju, savezna država Borno, radi obrade kostiju. Kosti su obrađene metodom maceracije u toploj vodi i tehnikama uklanjanja mekih tkiva. Identificirano je oko 39 kranijalnih i mandibularnih parametara. Komparativna analiza dorzalnih, kaudalnih, ventralnih, lateralnih i mandibularnih parametara nije pokazala statistički značajne razlike ($p > 0,05$) između pasmina Uda i Yankasa u većini mjerenja. Osteometrijski nalazi pokazali su da su parametri povezani s dužinom viscerokranijuma, kao što su INL, VCrL, NL, IOL, MDL i IISL, bili nešto veći kod pasmine Yankasa nego kod pasmine Uda. Međutim, parametri povezani s dužinom neurokranijuma, kao što su NCrL, ChL i HPL, bili su nešto veći kod pasmine Uda nego kod pasmine Yankasa. Yankasa je također pokazala širi profil lobanje, što se odražava u vrijednostima IZW, HPW, ChW, IMDAW, NW i NCWLB, iako razlike nisu bile statistički značajne. Ova studija pruža vrijedne osteometrijske podatke o pasminama ovaca Uda i Yankasa, koji mogu biti korisni za taksonomsku klasifikaciju, evolucijska istraživanja, kao i za veterinarsku kliničku primjenu, uključujući regionalnu anesteziju i hirurške zahvate na području glave.

Ključne riječi: Kraniometrija, osteometrija, ovce, Uda, Yankasa

RESEARCH ARTICLE

Renal alterations after single application of dinuclear ruthenium(II) Schiff-base complex in Swiss albino mice

Samra Čustović[1¶*], Višnja Muzika[1¶], Dina Kapić[1], Esad Ćosović[1], Maida Šahinović[1], Adnan Zahirović[2], Emira Kahrović[3]

[¶] Equally contributed to this paper
[1]Department of Histology and Embryology, University of Sarajevo – Faculty of Medicine, Sarajevo, Bosnia and Herzegovina
[2]Department of Chemistry, University of Sarajevo - Faculty of Science, Sarajevo, Bosnia and Herzegovina
[3]Academy of Sciences and Arts of Bosnia and Herzegovina, Sarajevo, Bosnia and Herzegovina

[*]**Corresponding author:**
Asst. Prof. dr. Samra Čustović

Address: Čekaluša 90 Sarajevo 71 000 Bosnia and Herzegovina
Phone: +38761381655
ORCID: 0000-0001-8996-0507
E-mail: samra.custovic@mf.unsa.ba

Original Submission:
5 January 2026
Revised Submission:
3 March 2026
Accepted:
12 March 2026

How to cite this article: Čustović S, Muzika V, Kapić D, Ćosović E, Šahinović M, Zahirović A, Kahrović E 2026. Renal alterations after single application of dinuclear ruthenium(ii) Schiff-base complex in Swiss albino mice. Veterinaria, 75(1), 63-72.

ABSTRACT

Ruthenium complexes represent a relatively new generation of metal-based substances that are increasingly investigated as potential chemotherapeutic agents. The aim of this study was to evaluate and quantify the extent of injury of a single dose of a dinuclear ruthenium(II) Schiff-base complex on mouse kidneys using stereological and morphometric approaches. Adult (8–10 weeks old) Swiss albino mice of both sexes were used. Two experimental groups received intraperitoneal injections of the dinuclear ruthenium(II) Schiff-base complex at doses of 25 mg/kg and 175 mg/kg, respectively, while the control group received vehicle (DMSO) only. After a 14-day observation period, animals were sacrificed, and both kidneys were excised for gross measurements (mass and volume) and histological processing. Quantitative and qualitative light microscopy analyses were performed, and the results were statistically evaluated. Low-dose treatment resulted in increased kidney volume, enlargement of renal corpuscles and Bowman's spaces, and tubular dilation compared to controls. In contrast, high-dose treatment induced decreased kidney mass, reduced corpuscular and tubular parameters, and increased tubular cellularity relative to both the low-dose and control groups. Also, high-dose exposure was associated with a higher incidence of atypical tubules. Treatment with a low dose of the ruthenium complex induced mild, potentially reversible alterations in renal corpuscles and proximal tubules, whereas high-dose exposure caused atrophic and possibly irreversible changes, suggesting dose-dependent nephrotoxicity.

Keywords: Histology, kidney, mouse, ruthenium, toxicology

INTRODUCTION

Ruthenium complexes represent a relatively new generation of metal-based substances that are increasingly being investigated as potential chemotherapeutic agents. They show both impressive anticancer and antimicrobial activity combined with reduced toxicity, making them a desirable alternative to platinum-based drugs (Wang et al., 2015), whose major concern is nephrotoxicity (Malyszko et al., 2017).

The kidneys are particularly susceptible to the toxic effects of drugs, and the occurrence of reversible or irreversible renal injury is frequent—even after a single administration (Perazella, 2009). Therefore, in assessing the safety profile of a new therapeutic agent, it is critical to evaluate its potential for nephrotoxicity.

Although numerous ruthenium-based complexes proved their biological activity *in vitro, in vivo* studies are still rarely conducted. Only four of these complexes such as NAMI-A, KP1019, NKP1339 and TLD1443 were approved for human clinical trials (Florea and Büsselberg, 2011; Spreckelmeyer et al., 2014; Lin et al., 2018).

Ruthenium complexes are generally considered to exhibit low toxicity. Only mild adverse effects were observed on the kidneys, bone marrow and reproductive system (Wang et al., 2015; Ciftci et al., 2017).

The aim of this study was to identify the renal structures most affected and quantify the extent of injury using morphometric and stereological methods in order to better understand the effects of this intriguing complex.

MATERIAL AND METHODS

Animals

The study was performed on adult (8-10 weeks old) Swiss albino mice (*Mus musculus*) of both sexes (18 males and 18 females). The mice were kept in controlled conditions (12-hour light-dark cycle, temperature 23±2°C) and were provided with standard food and water *ad libitum*.

All procedures were carried out according to the internationally accepted principles for the care and use of laboratory animals (The Council for International Organizations of Medical Sciences – CIOMS and The International Council for Laboratory Animal Science – ICLAS, 2012.) and were approved by Ethics Committee of Medical Faculty, University of Sarajevo (No. 02-3-4-4943/18).

Experimental protocol

Mice were randomly allocated into three equal-sized groups, with gender balanced across groups (6 males and 6 females in each group). At the beginning of the experiment, a single dose of the tested substance (dinuclear(II) Schiff-base ruthenium complex) was applied intraperitoneally (i.p.). Two experimental groups received the dinuclear(II) Schiff-base ruthenium complex at different dosages (25 mg/kg and 175mg/kg), and the control group was treated with equal volume of vehicle - dimethyl sulfoxide (DMSO). This was followed by a 14-day period of observation and consequent sacrifice of all animals using ketamine. Every effort was made to minimize the suffering of animals.

The dinuclear ruthenium(II) Schiff base complex [Ru2L2Cl2(Et2NH)(H2O)], where L is N-(2-pyridyl)-5-chlorosalicylideneimine, was prepared according to previously reported procedure (Kahrović et al., 2016). The purity of the compound was confirmed by IR spectroscopy and elemental analysis. DMSO was obtained from a commercial supplier.

Biochemical analysis

Blood samples were obtained prior to sacrifice, according to a previously described method in anesthetized mice (Parasuraman et al., 2010). Urea and creatinine serum levels were measured as indicators of renal function.

Macroscopic observations and measurements

At sacrifice, both kidneys were excised, carefully inspected and weighed. Length, width and thickness of each kidney were measured after formalin fixation using an electronic digital caliper (accuracy: ±0.02 mm). Kidney volume was then estimated using the ellipsoid formula, as proposed by Breau et al. (2013).

Histological analysis

Both kidneys were immersed in 10% neutral buffered formalin for 14 days. Left kidneys were then cut longitudinally and processed using routine histotechnology. Five-micrometer-thick sections were cut using a microtome (Microm HM 340E, Thermo Scientific, USA) and stained with hematoxylin-eosin (HE) and periodic acid Schiff (PAS). Using the obtained slides, qualitative and quantitative histological analyses were performed using light microscopy.

Modular software for interactive image processing and analysis (Ellipse, Version 2, 0, 8, 1) was used for

the quantitative analysis. Measurements were done on central PAS stained kidney slides that included the hilum, under 400x magnification, applying systematic field sampling. Prior to each morphometric measurement, distance calibration was performed. Quantitative analysis included both morphometry and sterology. For the renal corpuscles, the following morphometric parameters were measured: area (µm2), average diameter (µm), perimeter (µm), roundness (arbitrary unit, where 1.00 corresponds to a perfect circle) and number of nuclei (per 1000 µm2).

For proximal and distal tubules, similar morphometric parameters were measured (outer and inner diameter, area and nuclei per 1000 µm2, cell height). Additionaly, only for the proximal tubules, the brush border height was determined. At least 80 corpuscles, 100 proximal and 90 distal tubules were measured in each group.

Volumetric density (Vv%) was determined for following compartments/phases: corpuscles, normal tubules, atypical tubules, interstitium, Bowman's space and glomerular open capillary loops. At least 50 fields in each experimental group were inspected. Volume density was expressed as number of points/hits of the selected compartment/phase divided by the total number of points (N=157) overlaying the microscopic field. Atypical tubules were defined according to criteria proposed by Lanzoni et al. (2007).

Statistical analysis

Statistical analysis was performed using IBM SPSS Statistics for Windows, version 27.0 (IBM Corp., Armonk, N.Y., USA) and Microsoft Excel 2024. The normality of data distribution was evaluated using QQ plots. For skewed data, logarithmic transformation was applied prior to statistical testing. Results are presented as mean and standard deviation (mean±SD). Comparisons of groups were made using one-way ANOVA, with effect size reported as eta squared.

RESULTS

Serum urea levels were not significantly affected by the application of the investigated complex according to the ANOVA testing results, whereas a larger effect was observed for creatinine levels (eta squared = 0.15) as reported in Table 1.

Table 1 Urea and creatinine levels in the experimental and control animal groups

	Urea (mmol/L)	**Creatinine (µmol/L)**
Control	7.8 ± 2.35	39.49 ± 10.65
Low-dose	7.65 ± 1.07	41.73 ± 11.22
High-dose	7.12 ± 1.08	41.64 ± 9.12
ANOVA		
F	0.594	0.179
df1, df2	2, 33	2, 33
p	0.558	0.837
Eta squared	0.035	0.011

The results are expressed as mean ± SD.

Body mass and both absolute and relative kidney mass were not significantly affected by ruthenium complex application, indicating no dose effect (Table 2). Interestingly, a larger effect was observed for kidney volume and thickness. The highest mean values were recorded in the low-dose group (Table 2), which also corresponded to the macroscopic appearance of the kidneys (Figure 1).

Table 2 Body mass and gross kidney measurements in control and experimental groups

	Control (N=12)	**Low-dose (N=12)**	**High-dose (N=12)**	**ANOVA** **F** **df1, df2** **p** **Eta squared**
Body mass (g)	27.69 ± 1.53	29.10 ± 1.19	28.85 ± 2.84	1.726 2, 33 0.194 0.095
Kidney				
Mass (g)	0.16 ±0.03	0.16 ± 0.02	0.16 ± 0.03	0.121 2, 33 0.886 0.007
Relative mass	0.58 ± 0.09	0.54 ± 0.07	0.54 ± 0.06	1.310 2, 33 0.284 0.074
Length (mm)	9.65± 0.68	10.08 ± 0.46	9.62 ± 0.76	1.874 2, 33 0.169 0.102
Width (mm)	5.99 ± 0.73	6.29 ± 0.41	6.07 ± 0.61	0.808 2, 33 0.455 0.047
Thickness (mm)	4.30 ± 0.34	4.79 ± 0.21	3.98 ± 0.20	29.602 2, 33 <0.001 0.642
Volume (mm3)	132.44 ± 31.82	159.67 ± 22.26	122.01 ± 21.50	6.910 2, 33 0.003 0.295
Volume/Mass	0.82 ± 0.10	1.04 ± 0.06	0.79 ± 0.08	31.945 2, 33 <0.001 0.659

The results are expressed as mean ± SD; relative mass=kidney mass/body mass.

Figure 1 Representative kidneys in control and experimental groups (A – Regular appearance of kidneys in the control group; B - Swollen and pale kidneys in the low-dose group; C - Dark and small kidneys in the high-dose group)

In the high-dose group, the renal corpuscles were notably irregular in shape, with a prominent reduction of Bowman's space and glomerular open capillary loops. The glomerular cellularity appeared increased. Atypical tubules were frequently observed, showing tubular enlargment and epithelial alteration with large, eosinophilic cuboidal to columnar cells, which were occasionally multilayered.

In contrast, in the low-dose group the renal corpuscles appeared round, enlarged and more numerous with a dilated Bowman's space. Both proximal and distal tubules were increased in size with brush border loss or alteration (Figure 2.).

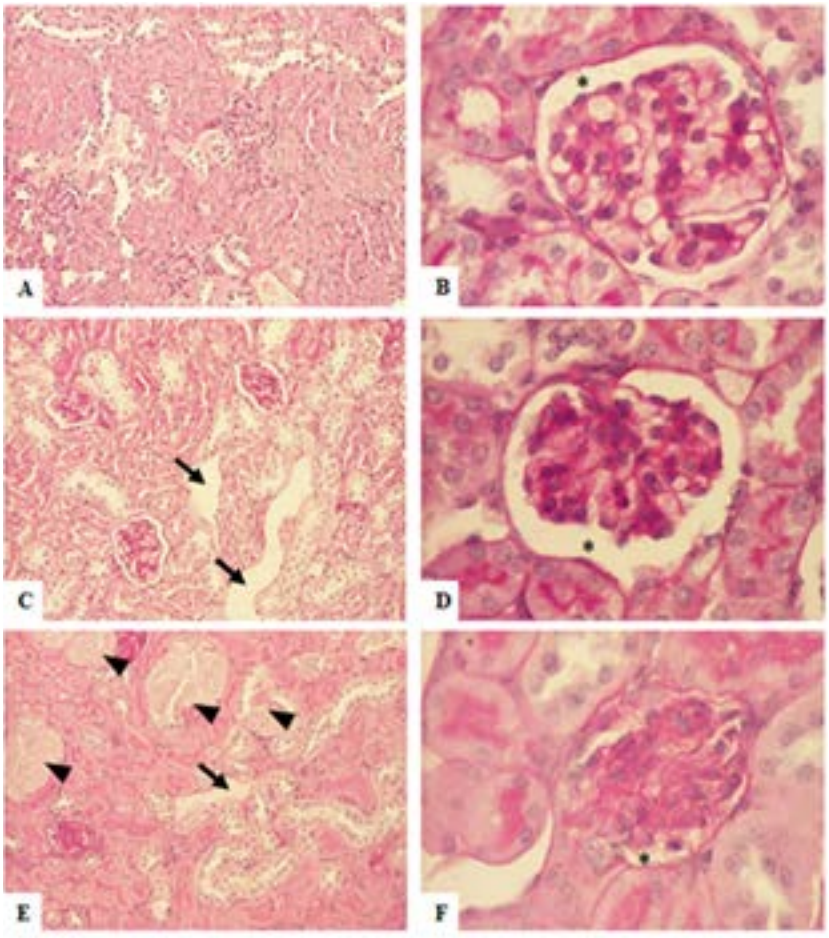

Figure 2 Photomicrographs of mouse kidneys (PAS sections). Normal appearance of cortical structures in the control group (A, B). In the low-dose group interstitium (arrows) and tubules are slightly widened (C) while the Bowman's space (asterix) is markedly dilated (D). Numerous atypical tubules (arrowheads) (E) and altered renal corpuscle (F) found in the high-dose group. Magnification: A,C,E – 100x; B,D,F – 400x

Findings from the qualitative analysis were generally confirmed by the stereological and morphometric measurements. Corpuscular measurements are presented in Table 3.

One-way ANOVA revealed highest eta squared values for area, roundness and Bowman's space, indicating the largest effect of the investigated complex in the low-dose group. The most affected tubular parameters by the tested ruthenium complex were inner diameter and brush border in the proximal tubules, as indicated by the highest eta squared values (Table 4.). The highest mean values for inner diameter and smallest for the brush border were both detected in the low-dose group. For the distal tubules, according to the eta squared values, only a medium effect of the ruthenium complex was observed in the low-dose group for inner diameter and nuclei number.

Table 3 Morphometry and volumetric density (Vv%) of the renal corpuscles

	Average diameter (µm)	Area (µm²)	Perimeter (µm)	Roundness	Bowman's space Vv (%)	Open capillary loops Vv (%)
Control	69.88 ± 7.45	3595.26 ± 756.25	238.56 ± 25.18	0.79 ± 0.08	11.37 ± 8.27	13.18 ± 6.91
Low-dose	78.09 ± 6.97	4722.64 ± 812.55	264.65 ± 22.45	0.84 ± 0.05	21.43 ± 7.23	8.71 ± 3.31
High-dose	70.73 ± 8.55	3643.99 ± 879.52	249.32 ± 31.17	0.75 ± 0.09	7.87 ± 7.10	10.40 ± 6.13
ANOVA						
F	*31.23*	*51.05*	*20.72*	*30.27*	*75.08*	*13.36*
df1, df2	*2, 269*	*2, 269*	*2, 269*	*2, 269*	*2, 269*	*2, 269*
p	*<0.001*	*<0.001*	*<0.001*	*<0.001*	*<0.001*	*<0.001*
Eta squared	*0.188*	*0.275*	*0.134*	*0.184*	*0.358*	*0.090*

The results are expressed as mean ± SD.

Table 4 Morphometry parameters of proximal and distal renal tubules

		Outer diameter (µm)	Inner diameter (µm)	Cell height (µm)	Brush border (µm)	Area (µm²)	Nuclei/ 1000µm²
Control	PT	35.59 ± 5.61	8.22 ± 4.59	13.68 ± 2.94	3.09 ± 1.58	1164.72 ± 746.87	4.54 ± 1.62
	DT	32.56 ± 6,50	15.32 ± 5.27	8.62 ± 2.39	/	786.93 ± 226.29	7.18 ± 1.64
Low-dose	PT	35.84 ± 5.62	11.23 ± 4.78	12.3 ± 2.66	1.51 ± 0.59	1338.83 ± 1476.38	4.30 ± 1.47
	DT	38.06 ± 6.05	20.41 ± 5.29	8.83 ± 1.63	/	888.84 ± 230.07	6.17 ± 1.63
High-dose	PT	30.83 ± 5.04	5.12 ± 2.98	12.85 ± 2.26	3.09 ± 1.24	836.32 ± 237.21	4.30 ± 1.47
	DT	30.72 ± 6.83	11.79 ± 4.30	9.46 ± 2.69	/	808.43 ± 277.83	7.91 ± 2.25
ANOVA							
F	PT	*27.16*	*53.22*	*7.09*	*32.19*	*7.00*	*13.94*
df1, df2		*2, 301*	*2, 301*	*2, 301*	*2, 301*	*2, 301*	*2, 301*
p		*<0.001*	*<0.001*	*0.001*	*<0.001*	*0.001*	*<0.001*
Eta squared		*0.153*	*0.261*	*0.45*	*0.176*	*0.44*	*0.085*
	DT	*2.76*	*17.50*	*2.92*	/	*14.77*	*22.11*
		2, 288	*2, 288*	*2, 288*		*2, 288*	*2, 288*
		0.065	*<0.001*	*0.056*		*<0.001*	*<0.001*
		0.019	*0.108*	*0.020*		*0.093*	*0.133*

PT=proximal tubule; DT=distal tubule. The results are expressed as mean ± SD.

No significant dosing effect was detected regarding the volume density of either the interstitium or corpuscles. One-way ANOVA revealed the highest eta square values for the volumetric density of all tubules in the renal cortex (Table 5).

Animals in the high-dose group had the highest Vv of the atypical tubules. This change was significantly more pronounced in male mice than in females, while sex-related differences were not detected for any other investigated parameter.

Table 5 Volumetric density (Vv) of the renal cortical structures

	Vv corpuscles (%)	Vv interstitium (%)	Vv atypical tubules (%)	Vv tubules (%)
Control	3.53 ± 2.54	4.51 ± 3.25	3.99 ± 3.14	87.94 ± 5.56
Low-dose	4.33 ± 2.55	5.19 ± 3.69	6.01 ± 4.80	84.47 ± 7.93
High-dose	4.16 ± 2.42	6.17 ± 4.28	9.24 ± 6.61	80.43 ± 6.91
ANOVA				
F	*1.42*	*2.49*	*13.96*	*15.29*
df1, df2	*2, 149*	*2, 149*	*2, 149*	*2, 149*
p	*0.245*	*0.086*	*<0.001*	*<0.001*
Eta squared	*0.019*	*0.032*	*0.158*	*0.170*

The results are expressed as mean ± SD.

DISCUSSION AND CONCLUSION

This study focused on the detailed assessment of renal effects induced by a single dose of a dinuclear ruthenium (II) Schiff-base complex in mice. As this complex has previously shown promising anticancer and antimicrobial properties, it was selected for *in vivo* evaluation of its potential toxicity (Kahrović et al., 2016; Muzika et al., 2019). Given earlier indications of nephrotoxic effects (Muzika et al., 2019), particular attention was paid to identifying the renal structures most affected and quantifying the extent of injury using morphometric and stereological methods. These quantitative analytical tools form an integral part of the tiered morphological approach applied in contemporary toxicologic pathology, refining morphological evaluation and improving detection of subtle changes (Boyce et al., 2010).

Urea and serum creatinine levels remained unchanged in the ruthenium treated groups compared to control mice. A study conducted on cisplatin-induced kidney injury supports our findings and has shown that early morphological changes precede changes in urea and creatinine levels (Jana et al., 2023).

Additionally, a study on ochratoxin-induced kidney injury has demonstrated that these standard measures of nephrotoxicity often fail to detect early injury, becoming apparent only after significant loss of renal function (Rached et al., 2008).

The absolute and relative kidney mass were not significantly changed in experimental groups in comparison to control animals. On gross examination, kidneys in the low-dose group appeared swollen and pale, consistent with the markedly increased renal volume. In contrast, the kidneys in the high-dose group were small and dark with a reduction in all gross parameters. To our knowledge, changes in kidney volume and mass may reflect alterations in renal hemodynamics, although such findings are rarely reported in nephrotoxic studies. A reduction in kidney mass was also observed by Alves de Souza et al. (2017), which investigated the toxicity of cisplatin and ruthenium complexes, supporting our findings in the high-dose group.

In the low-dose treated animals, renal corpuscles were enlarged, as evidenced by increases in their diameter, area, and perimeter. Additionally, the proximal tubular lumen was dilated, with alterations of the brush border and reduced cellularity. Similar changes were described by other authors as reversible tubular injury (Tobar et al., 2013; Kapic et al., 2022; Larson et al., 1984). These findings may result from accumulation of the ruthenium complex in the renal cortical structures

(Guichard et al., 2006; Vadori et al., 2013) or from glomerular hyperfiltration as an adaptive response, with insufficient adaptation to elevated pressure being transmitted distally (Kapic et al., 2022). The increased cellularity observed in the corpuscles of the low-dose group may reflect mesangial expansion, leading to capillary loop collapse and a subsequent increase in glomerular volume, as reported by Pourghasem et al. (2015).

Although most corpuscular measurements in the high-dose treated animals were comparable to those of the control group, exceptions were observed in corpuscular shape and Bowman's space. The observed corpuscles appeared oval with barely visible Bowman's spaces, accounting for the lowest roundness and volumetric density values compared to both the control and low-dose groups. Similar changes were reported by Medeiros et al. (2021) and were attributed to renal atrophy. Other authors (Alves at al., 2021) correlated reduction of the subcapsular space with progressive kidney disease, as it can interfere with glomerular filtration. In addition, significantly lower values of most tubular parameters in morphometric and stereological analyses relative to the other groups may reflect tubular atrophy, as described by Medeiros et al. (2021). The observed increased tubular cellularity may indicate high proliferative activity, which is also associated with tubular atrophy (Nadasdy et al., 1994).

In the present study, the interstitium of all animals treated with the dinuclear ruthenium complex was widened, containing dilated interstitial blood vessels without evidence of congestion, although quantitative analysis indicated only a minor dose-dependent effect. In contrast, other authors reported congestion as a prominent finding following cisplatin treatment and mild hyperemia after ruthenium administration; however, these studies lacked quantification and rigorous statistical analysis (Mello-Andrade et al., 2018; Alhoshani et al., 2017).

Atypical tubular hyperplasia was observed in all examined animals, with the highest incidence among high-dose treated groups, particularly in males. This gender difference might be the result of hormonal or differences in renal metabolism of the tested substance. Although renal atypical tubular hyperplasia is generally considered a sporadic finding (Lanzoni et al., 2007), its increased frequency in treated animals may suggest that the ruthenium complex exerts a promoting or predisposing effect, similar to that described for ochratoxin A and 1,2,3-trichloropropane (Huff, 1991; National Toxicology Program, 1993). However, the short duration of exposure and the predominance of tubular acidophilia – rather than the basophilia typically associated with chemically induced renal preneoplastic lesions (Hard et al., 2011) – suggest that these changes more likely represent adaptive or regenerative responses than true toxicologically driven neoplastic alterations.

As this study was designed as a short-term experiment, we were unable to demonstrate the hypothesized reversibility of the kidney alterations induced by the tested ruthenium complex. Future subacute or chronic studies should focus on this aspect.

Treatment with a low dose of the dinuclear ruthenium(II) Schiff-base complex in mice exhibited damage to renal corpuscles and proximal tubules, likely reflect in mild and potentially reversible signs of toxicity. In contrast, alterations observed in the high-dose treated animals suggest a more severe and possibly progressive injury. Further studies are warranted to provide a more detailed understanding of the nature of these changes and to elucidate the underlying mechanisms.

CONTRIBUTION

Conception: SČ, VM, AZ, EK; Design: SČ, VM, AZ, EK; Supervision: SČ, VM; Fundings: SČ, VM; Materials: SČ, VM, AZ, EK; Data Collection and/or Processing: SČ, VM; Analysis and/or Interpretation of the Data: SČ, VM, DK, EČ, MŠ, AZ, EK; Literature Review: SČ, VM, DK, EČ, MŠ; Writing: SČ, VM, DK, EČ, MŠ; Critical Review: SČ, VM, DK, EČ, MŠ, AZ, EK.

CONFLICT OF INTEREST

The authors declared that there is no conflict of interest.

REFERENCES

Alhoshani AR, Hafez MM, Husain S, Al-Sheikh AM, Alotaibi MR, Al Rejaie SS, et al. 2017. Protective effect of rutin supplementation against cisplatin-induced nephrotoxicity in rats. BMC Nephrol, 18(1):194. doi: 10.1186/s12882-017-0601-y.

Alves de Souza CE, Alves de Souza HM, Stipp MC, Corso CR, Galindo CM, Cardoso CR, et al. 2017. Ruthenium complex exerts antineoplastic effects that are mediated by oxidative stress without inducing toxicity in Walker-256 tumor-bearing rats. Free Radic Biol Med, 110: 228-39. doi: 10.1016/j.freeradbiomed.2017.06.011.

Alves RDC, Ferreira CGM, Ferreira de Melo IM, Baptista MGP, Lima de Albuquerque YM, do Nascimento BJ, et al. 2021. Renal and hepatic changes in the offspring of rats that received biological insecticides during pregnancy and lactation. Acta Histochem, 123(8): 151799. doi: 10.1016/j.acthis.2021.151799.

Boyce RW, Dorph-Petersen KA, Lyck L, Gundersen HJ. 2010. Design-based stereology: introduction to basic concepts and practical approaches for estimation of cell number. Toxicol Pathol, 38(7):1011-25. doi: 10.1177/0192623310385140.

Breau RH, Clark E, Bruner B, Cervini P, Atwell T, Knoll G, et al. 2013. A simple method to estimate renal volume from computed tomography. Can Urol Assoc J, 7(5-6):189-92. doi: 10.5489/cuaj.1338.

Ciftci O, Beytur A, Vardi N, Ozdemir I. 2012. Evaluation of reproductive toxicity in male rats treated with novel synthesized ruthenium(II) and gold (I)-NHC complexes. Drug Dev Ind Pharm, 38(1):40-6. doi: 10.3109/03639045.2011.589853.

Florea AM, Büsselberg D. 2011. Cisplatin as an Anti-Tumor Drug: Cellular Mechanisms of Activity, Drug Resistance and Induced Side Effects. Cancers (Basel), 3(1): 1351-71. doi: 10.3390/cancers3011351

Guichard SM, Else R, Reid E, Zeitlin B, Aird R, Muir M, et al. Jodrell DI. 2006. Anti-tumour activity in non-small cell lung cancer models and toxicity profi les for novel ruthenium(II) based organo-metallic compounds. Biochem Pharmacol, 71(4): 408-15. doi: 10.1016/j.bcp.2005.10.053.

Hard GC, Bruner RH, Cohen SM, Pletcher JM, Regan KS. 2011. Renal histopathology in toxicity and carcinogenicity studies with tert-butyl alcohol administered in drinking water to F344 rats: a pathology working group review and re-evaluation. Regul Toxicol Pharmacol, 59(3): 430-6. doi: 10.1016/j.yrtph.2011.01.007.

Huff JE. 1991. Carcinogenicity of ochratoxin A in experimental animals. IARC Sci Publ, (115):229-44.

Jana S, Mitra P, Dutta A, Khatun A, Kumar Das T, Pradhan S, et al. 2023. Early diagnostic biomarkers for acute kidney injury using cisplatin-induced nephrotoxicity in rat model. Curr Res Toxicol, 5:100135. doi: 10.1016/j.crtox.2023.100135

Kahrović E, Zahirović A, Turkušić E, Bektaš S. 2016. A dinuclear ruthenium(II) Schiff base complex with dissimilar coordination: synthesis, characterization, and biological activity. Z Anorg Allg Chem, 642:480-5. doi: 10.1002/zaac.201600008.

Kapic D, Sahinovic M, Cosovic E, Alicelebic S, Custovic S. Musanovic J. 2022. Morphometric Analysis of the Ameliorative Potential of Melatonin on Gentamicin-Induced Renal Corpuscle Changes in Rats. HealthMed, 16(1)3-8.

Lanzoni A, Piaia A, Everitt J, Faustinelli I, Defazio R, Cavaliere et al. 2007. Early onset of spontaneous renal preneoplastic and neoplastic lesions in young conventional rats in toxicity studies. Toxicol Pathol, 35(4):589-93. doi: 10.1080/01926230701383202.

Larson M, Sjöquist M, Wolgast M. 1984. Renal interstitial volume of the rat kidney. Acta Physiol Scand, 120(2):297-304. doi: 10.1111/j.1748-1716.1984.tb00137.x.

Lin K, Zhao Z-Z, Bo H-B, Hao X-J, Wang J-Q. 2018. Applications of Ruthenium Complex in Tumor Diagnosis and Therapy. Front Pharmacol, 9:1323. doi: 10.3389/fphar.2018.01323.

Malyszko J, Kozlowska K, Kozlowski L, Malyszko J. 2017. Nephrotoxicity of anticancer treatment. Nephrol Dial Transplant, 32(6):924-36. doi: 10.1093/ndt/gfw338.

Medeiros KA, Siqueira BS, Urrutia MAD, Porto EM, Grassiolli S, Amorim JPA. 2021. Vagotomy associated with splenectomy reduces lipid accumulation and causes kidneys histological changes in rats with hypothalamic obesity. Acta Cir Bras, 22; 36(2):e360205. doi: 10.1590/ACB360205.

Mello-Andrade F, Cardoso CG, Silva CRE, Chen-Chen L, Melo-Reis PR, Lima AP, et al. 2018. Acute toxic effects of ruthenium (II)/amino acid/diphosphine complexes on Swiss mice and zebrafish embryos. Biomed Pharmacother, 107: 1082-92. doi: 10.1016/j.biopha.2018.08.051.

Muzika V, Custovic S, Alicelebic S, Cosovic E, Zahirovic A, Kahrovic E. 2019. Dinuclear ruthenium(II) Schiff base complex: a first in vivo study in Swiss albino mice. Bratisl Med J, 120(1):26-34. doi: 10.4149/BLL_2019_004.

Nadasdy T, Laszik Z, Blick KE, Johnson DL, Silva FG. 1994. Tubular atrophy in the end-stage kidney: a lectin and immunohistochemical study. Hum Pathol, 25(1):22-8. doi: 10.1016/0046-8177(94)90166-x.

National Toxicology Program. 1993. NTP Toxicology and Carcinogenesis of 1,2,3-Trichloropropane (CAS No. 96-18-4) in F344/N Rats and B6C3F1 Mice (Gavage Studies). Natl Toxicol Program Tech Rep Ser, 384:1-384.

Parasuraman S, Raveendran R, Kesavan R. 2010. Blood sample collection in small laboratory animals. J Pharmacol Pharmacother, 1(2):87-93. doi: 10.4103/0976-500X.215702.

Perazella MA. 2009. Renal Vulnerability to Drug Toxicity. CJASN.; 4(7):1275-83. doi: 10.2215/CJN.02050309.

Pourghasem M, Shafi H, Babazadeh Z. 2015. Histological changes of kidney in diabetic nephropathy. Caspian J Intern Med, 6 (3):120-7.

Rached E, Hoffmann D, Blumbach K, Weber K, Dekant W, Mally A. 2008. Evaluation of putative biomarkers of nephrotoxicity after exposure to ochratoxin a in vivo and in vitro. Toxicol Sci, 103(2):371-81. doi: 10.1093/toxsci/kfn040.

Spreckelmeyer S, Orvig C, Casini A. 2014. Cellular transport mechanisms of cytotoxic metallodrugs: an overview beyond cisplatin. Molecules, 19(10):15584-610. doi: 10.3390/molecules191015584.

Tobar A, Ori Y, Benchetrit S, Milo G, Herman-Edelstein M, Zingerman B, et al. 2013. Proximal tubular hypertrophy and enlarged glomerular and proximal tubular urinary space in obese subjects with proteinuria. PLoS One, 25; 8(9):e75547. doi: 10.1371/journal.pone.0075547.

Vadori M, Pacor S, Vita F, Zorzet S, Cocchietto M, Sava G. 2013. Features and full reversibility of the renal toxicity of the ruthenium-based drug NAMI-A in mice. J Inorg Biochem, 118:21-7. doi: 10.1016/j.jinorgbio.2012.09.018.

Wang JQ, Zhang PY, Ji LN, Chao H. 2015. A ruthenium(II) complex inhibits tumor growth in vivo with fewer side-effects compared with cisplatin. J Inorg Biochem, 146:89-96. doi: 10.1016/j.jinorgbio.2015.02.003.

Bubrežne promjene nakon jednokratne primjene dinuklearnog rutenijum(II) Schiff-baznog kompleksa kod švicarskih albino miševa

SAŽETAK

Kompleksi rutenijuma predstavljaju relativno novu generaciju supstanci na bazi metala koje se sve više istražuju kao potencijalni kemoterapijski agensi. Cilj ovog istraživanja bio je procijeniti i kvantificirati stepen oštećenja bubrega miševa nakon jednokratne primjene dinuklearnog rutenijum(II) Schiff-baznog kompleksa, koristeći stereološke i morfometrijske pristupe. U istraživanju su korišteni odrasli (8–10 sedmica stari) švicarski albino miševi oba spola. Dvije eksperimentalne grupe primile su intraperitonealne injekcije dinuklearnog rutenijum(II) Schiff-baznog kompleksa u dozama od 25 mg/kg i 175 mg/kg, dok je kontrolna grupa primila samo rastvarač (DMSO). Nakon perioda praćenja od 14 dana, životinje su žrtvovane, a oba bubrega su izdvojena radi makroskopskih mjerenja (masa i volumen) i histološke obrade. Provedene su kvantitativne i kvalitativne analize svjetlosnom mikroskopijom, a rezultati su statistički obrađeni. Tretman niskom dozom doveo je do povećanja volumena bubrega, uvećanja bubrežnih tjelašaca i Bowmanovih prostora, kao i dilatacije tubula u poređenju s kontrolom. Nasuprot tome, tretman visokom dozom izazvao je smanjenje mase bubrega, redukciju parametara tjelašaca i tubula, te povećanu celularnost tubula u odnosu na grupu s niskom dozom i kontrolnu grupu. Također, izloženost visokoj dozi bila je povezana s većom učestalošću atipičnih tubula. Tretman niskom dozom rutenijumskog kompleksa izazvao je blage, potencijalno reverzibilne promjene u bubrežnim tjelašcima i proksimalnim tubulima, dok je izloženost visokoj dozi uzrokovala atrofične i vjerovatno ireverzibilne promjene, što ukazuje na nefrotoksičnost zavisnu od doze.

Ključne riječi: Bubreg, histologija miš, rutenijum, toksikologija

CASE REPORT

Intra-articular platelet-rich plasma for advanced carpometacarpal osteoarthritis in an Arabian horse: Long-term clinical outcome

Nermina Spahija[1], Bora Jovanović[2], Muamer Obhođaš[1], Aida Glavinić[1*], Soraja Kučlar Muftić[1], Alan Maksimović[1]

[1]Department of Clinical Sciences in Veterinary Medicine, University of Sarajevo – Veterinary faculty, Zmaja od Bosne 90, 71000 Sarajevo, Bosnia and Herzegovina
[2]Self-employed veterinarian, Independent researcher, Belgrade, Serbia

***Corresponding author**:
Aida Glavinić, DVM
Address: Zmaja od Bosne 90, 71000 Sarajevo, Bosnia and Herzegovina
Phone: +387 33 729 100
ORCID: 0000-0001-8661-7180
E-mail: aida.glavinic@vfs.unsa.ba

Original Submission: 01 March 2026
Revised Submission: 28 March 2026
Accepted: 31 March 2026

How to cite this article: Spahija N, Jovanović B, Obhođaš M, Glavinić A, Kučlar Muftić S, Maksimović A. Intra-Articular Platelet-Rich Plasma for Advanced Carpometacarpal Osteoarthritis in an Arabian Horse: Long-Term Clinical Outcome. Veterinaria, 75(1), 73-78.

ABSTRACT

Osteoarthritis (OA) is a common degenerative joint disease in horses, characterized by cartilage degradation, synovial inflammation, and progressive lameness. Intra-articular platelet-rich plasma (IA-PRP) therapy has emerged as a promising regenerative treatment, aimed at promoting cartilage repair and reducing inflammation through growth factor release. A 10-year-old Arabian stallion presented with acute carpal lameness, graded 3/5 on the AAEP scale. Initial treatment with phenylbutazone and intra-articular corticosteroid (IA-GCs) injection resulted in temporary improvement, however lameness progressed to grade 5/5. Due to failure of conventional therapy and the inability to pursue further referral, IA-PRP therapy was initiated. The treatment protocol consisted of four IA-PRP injections administered at two-week intervals, followed by a prophylactic booster (fifth IA-PRP injection) six months after the fourth treatment. PRP was prepared using a double-spin centrifugation protocol. Early improvement was observed after PRP initiation, allowing NSAID discontinuation. Lameness progressively improved to near-normal function, with no recurrence of pain or gait abnormalities at the 18-month follow-up. This case highlights the potential of IA-PRP therapy as a steroid-sparing treatment option in the management of equine osteoarthritis.

Keywords: Equine osteoarthritis, intra-articular therapy, lameness management, platelet-rich plasma (PRP), regenerative medicine

INTRODUCTION

Osteoarthritis (OA) in horses is a complex disorder characterized by articular cartilage degradation, subchondral bone sclerosis, synovial inflammation, and osteophyte formation (McIlwraith et al., 2012). The disease may originate in any joint structures or result from combined pathological changes affecting multiple structures (McIlwraith, 2005). OA develops due to mechanical stress, joint instability, or age-related degeneration (McIlwraith et al., 2012; Ribitsch et al., 2021) and has a multifactorial etiology (Nedergaard et al., 2024). It causes pain, reduced mobility, and impaired performance. Breed predisposition has been reported, e.g., Arabian horses appear at increased risk of severe carpometacarpal osteoarthritis, possibly related to anatomical variations in the metacarpal region (Malone et al., 2003). Diagnosis of OA is based on clinical signs and imaging, with radiography used to assess bone changes and ultrasonography to evaluate soft tissues (Baccarin et al., 2022). Advanced diagnostic techniques may be limited to specialized centers, making their use challenging in regions with restricted diagnostic resources, such as Bosnia and Herzegovina (BiH). As no single therapy can halt OA progression or restore joint homeostasis, combined treatments are commonly used to improve outcomes and support return to athletic performance (Baccarin et al., 2022). In recent years, regenerative therapy has emerged as a promising alternative and is becoming increasingly prevalent in the treatment of equine OA (Baccarin et al., 2022). Among these, platelet-rich plasma (PRP) therapy has received increasing interest because several *in vitro* and *in vivo* studies have demonstrated that platelets can modulate inflammation and promote healing (Garbin and Olver, 2020). PRP exerts its therapeutic effects through bioactive molecules released from platelets, including growth factors and cytokines, which modulate the intra-articular inflammatory environment. These factors promote cartilage repair, synovial regeneration, and reduce pro-inflammatory signaling, contributing to pain reduction and improved joint function (Garbin et al., 2021; Fraile et al., 2023; Carmona and López, 2025). Autologous PRP is prepared by centrifuging patient's peripheral whole blood. Different centrifugation protocols have been described (Cavallo et al., 2014; Garbin and Olver, 2020; Hessel et al., 2015; Textor et al., 2011). This case report describes an effective use of IA-PRP (intra-articular platelet-rich plasma) therapy for treatment of carpometacarpal joint lameness in a 10-year-old Arabian stallion, showcasing this IA-PRP centrifugation protocol's potential to resolve lameness and restore joint function.

CASE PRESENTATION

Informed Consent

Written informed consent was obtained from the owner prior to all diagnostic procedures and therapeutic interventions described in this case report, including consent for publication.

A 10-year-old Arabian stallion was referred to the University of Sarajevo-Veterinary Faculty for acute carpal lameness. The horse was purchased a year earlier with a cold non-painful swelling over the left carpal joint that gradually became firmer but remained painless. No history of trauma was reported, and the owner observed no signs of discomfort during rest or movement. Consequently, the horse had not undergone any veterinary examinations or diagnostic imaging. At presentation, the horse had a lameness grade 3/5 according to the American Association of Equine Practitioners (AAEP) scale. Conservative treatment was initiated with stall rest and phenylbutazone (Eqipalazolone, Dechra, Denmark) at a dose of 2.2 mg/kg q12h per os. Radiographic examination included lateral, dorsopalmar, flexed lateromedial, dorsolateral- palmaromedial oblique (DLPMO), and palmarolateral- dorsomedial (PLDMO) oblique. The lateral projection is presented in the main manuscript (Figure 1), while additional projections are provided in the Supplementary Material.

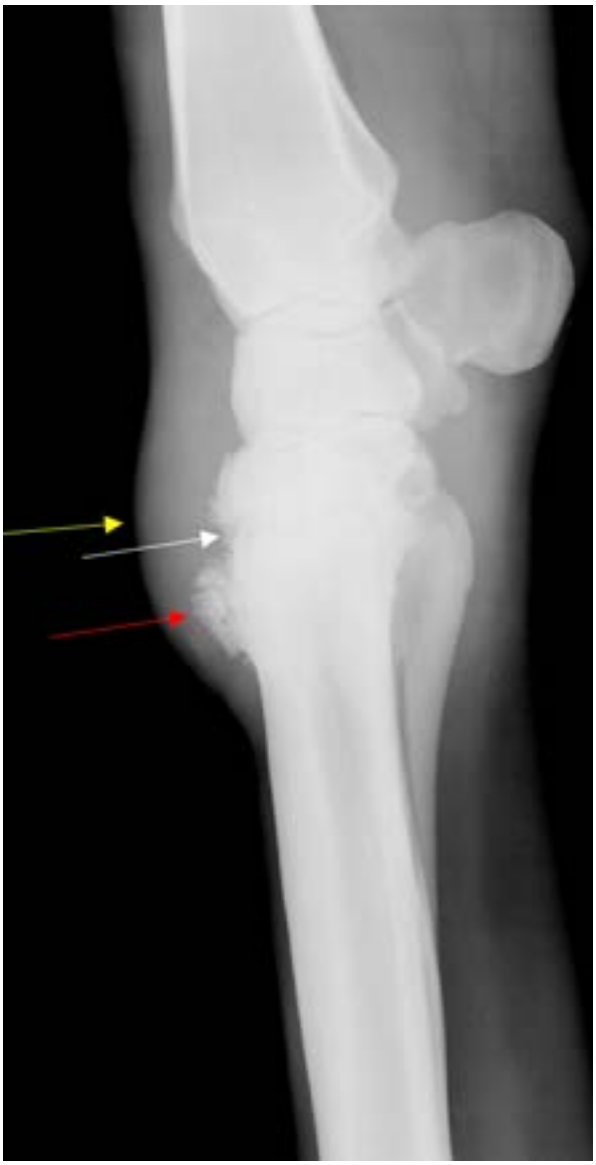

Figure 1 Lateral view of the carpal joint, demonstrating findings consistent with carpal osteoarthritis, including irregular bony proliferation (red arrow), narrowing of the joint space (white arrow), and soft tissue swelling (yellow arrow)

Radiographs revealed severe degenerative changes consistent with advanced carpometacarpal osteoarthritis, including extensive periarticular osteophyte formation, marked irregular remodeling of the proximal metacarpus and adjacent carpal bones, and narrowing or loss of the carpometacarpal joint space. A follow-up examination, conducted seven days later, showed moderate improvement with lameness reduced to 2/5 on the AAEP scale. One time IA administration of triamcinolone (Kenalog, Krka, Slovenia; 12 mg) and amikacin (Amikacin, Zentiva, Czech Republic; 250 mg) was performed. Clinical improvement persisted for one month, after which lameness worsened to grade 5/5 on the AAEP scale. Due to the insufficient response to previous therapy and the inability for further referral of the horse due to financial constraints, PRP therapy was initiated. Blood was aseptically collected from the jugular vein using an 18G needle into five 10 ml sodium citrate tubes (BD Vacutaner®), 50 ml whole blood in total. After resting for two hours at room temperature, as previously suggested to potentially improve platelet yield (Miranda et al., 2019), samples were centrifuged at 252 g for 10 minutes. The plasma was transferred into 10ml conical tubes and centrifuged again at 447 g for 10 minutes (Kwirant et al., 2019). Following the second centrifugation, 1 mL of plasma from the bottom of each tube was preserved and deemed as PRP, while the supernatant was considered platelet poor plasma (PPP). Both centrifugations were performed at room temperature and PRP was administered one hour after preparation. For each IA treatments, the horse was sedated with an intravenous bolus of 0.5 mg/kg xylazine (Xylazine Bio 2%, Bioveta, Czech Republic) and 0.02 mg/kg butorphanol (Torphadine, Le Vet B.V., Netherlands). The joint was clipped and prepared aseptically using chlorhexidine soap and solution. A total of 4 ml of PRP was administered intra-articularly into the middle carpal joint using a sterile 18G needle to target the communicating carpometacarpal joint. Using a dorsal approach, the middle carpal joint was identified by palpating the distal edge of the radial carpal bone and the medial aspect of the proximal third carpal bone before needle insertion (Garvican and Clegg, 2007). Afterward, a protective bandage was applied. The same protocol was consistently followed for every subsequent application of PRP. The treatment included four PRP injections into the left CMC joint at two-week intervals. Five days after the first injection, the horse began to bear weight while standing and shifted weight more comfortably, moving from static weight-

bearing to deliberate movements. Phenylbutazone was discontinued due to indicators of reduced pain. At day 14 (2nd PRP injection), lameness was assessed at grade 3/5, with improved gait fluidity and voluntary movement. At day 42 (4th PRP injection), lameness reduced to grade 2/5, showing mild stride inconsistencies during trot. At day 60, the horse showed no behavioral and facial signs of pain and returned to near-normal function, with slight gait changes on hard surfaces graded 1/5. Six months after the 4th PRP injection, an additional 5th IA PRP treatment was administered as a prophylactic booster to support long-term joint stability. Follow-up radiographs performed at that time suggested minimal progression of the previously described changes, without significant clinical relevance. At the 18-month follow up after the booster injection, no gait abnormalities or signs of pain were observed.

DISCUSSION AND CONCLUSION

A retrospective study of carpometacarpal osteoarthritis (CMC-OA) in Arabian horses reported severe form of this condition affecting primarily older Arabian horses (Malone et al., 2003). Malone et al. (2003) suggest that absence of the MC2-MC3 articulation in this breed, a variation that compromises joint stability, may predispose them to severe OA. Consequently, CMC-OA in this breed is often associated with guarded prognosis (Malone et al., 2003; Panizzi et al., 2009). Long-term follow up after regenerative IA therapies, such as PRP, is rarely reported (Carmona and López, 2025; Mayet et al., 2023). Documenting an 18-month soundness outcome offers practical value for clinicians working under field conditions where corticosteroid treatments frequently provide only transient improvement. This case provides a valuable, real- world example of PRP as a steroid-sparing therapeutic option for advanced CMC-OA. The horse in our case had a gradual onset of joint changes, which were left untreated for an extended period of time, resulting in the development of severe lameness. The absence of objective gait analysis represents a limitation; however, subjective lameness grading remains widely used in equine clinical practice and continues to serve as a standard method for evaluating treatment response (Nedergaard et al., 2024). Additional limitations include the lack of standardized PRP characterization and the absence of advanced imaging, which would have strengthened diagnostic certainty and helped exclude concurrent pathology. In this case, quantitative characterization of the PRP product, including platelet concentration, leukocyte content, and classification, was not performed due to limited laboratory resources. However, the double-spin protocol used has been previously described to yield platelet-enriched plasma with reduced leukocyte content, suitable for intra-articular use (Segabinazzi et al., 2021). Despite this, the observed clinical improvement supports the biological effectiveness of the preparation. Nevertheless, the marked clinical improvement following intra-articular PRP supports the presumptive diagnosis, as therapeutic response may provide indirect diagnostic confirmation when comprehensive diagnostics are not feasible. Automated PRP preparation methods are standardized and minimize operator variability, but their high cost may limit accessibility in smaller practices. Manual techniques are more cost-effective and do not require specialized equipment. These protocols include one or two centrifugation steps to concentrate platelets into a small plasma volume (2–5 mL) suitable for tendon or IA applications. The double-spin PRP preparation protocol, as used in this case, has been shown to maximize platelet concentration while minimizing leukocyte content, making it suitable for joint injections (Segabinazzi et al., 2021). Before centrifugation, the blood sample was rested for two hours at room temperature, as it has been suggested that this may be beneficial for obtaining a higher platelet count (Miranda et al., 2019). The inclusion of a resting period prior to centrifugation, although not universally applied, reflects the variability and lack of standardization in PRP preparation protocols (Carmona and López, 2025). The four-injection protocol administered at two-week intervals appeared to support gradual tissue regeneration. Mirza et al. (2016) demonstrated that repeated PRP injections over several weeks lead to cumulative improvements in lameness scores and joint homeostasis, which is consistent with the progressive clinical recovery observed in our case. PRP does not provide immediate analgesia, and clinical improvement develops only once its biological effects manifest. Previous studies similarly report a delayed therapeutic response, with improvement occurring from the second week onward (Bertone et al., 2014; Mirza et al., 2016). Improvement was maintained at the six-month follow-up, when 5th, booster PRP injection was administered. The observed clinical effects are likely mediated by PRP-derived growth factors and cytokines that modulate inflammation and support tissue repair within the joint (Carmona and López, 2025). These findings align with Textor et al. (2013), who reported sustained pain relief for up to six months post-PRP

therapy. A prophylactic booster PRP injection was administered to support long-term joint homeostasis, since the biological activity of PRP is known to be time-limited, with growth factor release and anti-inflammatory effects diminishing over time (Moraes et al., 2015; Textor et al., 2013). Clinical improvements following intra-articular PRP administration have also been reported in recent studies (Park et al., 2022; Peng et al., 2024).

This case report demonstrates that IA-PRP therapy can reduce lameness and improve joint function in an Arabian horse with advanced carpometacarpal osteoarthritis. The treatment resulted in sustained clinical improvement over an 18-month follow-up period, suggesting that PRP may represent a viable steroid-sparing option for managing advanced CMC-OA in field conditions. Further standardized studies are required to clarify its long-term efficacy and role in equine osteoarthritis management.

CONTRIBUTION

Conception: NS, BJ, AG; Design: NS, AG; Supervision: NS, AG, AM; Materials: NS, BJ, MO, AG, SKM; Data Collection and/or Processing: SKM, AM; Literature Review: NS, BJ, MO, AG, SKM, AM; Writing: NS, BJ, MO, AG, SKM, AM; Critical Review: NS, BJ, MO, AG, SKM, AM.

CONFLICT OF INTEREST

The authors declared that there is no conflict of interest.

REFERENCES

Baccarin RYA, Seidel SRT, Michelacci YM, Tokawa PKA, Oliveira TM. 2022. Osteoarthritis: A common disease that should be avoided in the athletic horse's life. Anim Front, 12, 25–36. https://doi.org/10.1093/af/vfac026

Bertone AL, Ishihara A, Zekas LJ, Wellman ML, Lewis KB, Schwarze RA, et al. 2014. Evaluation of a single intra-articular injection of autologous protein solution for treatment of osteoarthritis in horses. Am J Vet Res, 75, 141-51. https://doi.org/10.2460/ajvr.75.2.141

Carmona JU, López C. 2025. Platelet-rich plasma in equine osteoarthritis: A systematic review of clinical and experimental evidence. Animals, 15(18), 2647. https://doi.org/10.3390/ani15182647

Cavallo C, Filardo G, Mariani E, Kon E, Marcacci M, Pereira Ruiz MT, et al. 2014. Comparison of platelet-rich plasma formulations for cartilage healing: An in vitro study. J Bone Joint Surg, 96, 423-29. https://doi.org/10.2106/JBJS.M.00726

Fraile AP, González-Cubero E, Martínez-Flórez S, Olivera ER, Villar-Suárez V. 2023. Regenerative medicine applied to musculoskeletal diseases in equines: A systematic review. Vet Sci, 10, 666. https://doi.org/10.3390/vetsci10060666

Garbin LC, Lopez C, Carmona JU. 2021. A critical overview of the use of platelet-rich plasma in equine medicine over the last decade. Front Vet Sci, 8, 641818. https://doi.org/10.3389/fvets.2021.641818

Garbin LC, Olver CS. 2020. Platelet-rich products and their application to osteoarthritis. J Equine Vet Sci, 86, 102820. https://doi.org/10.1016/j.jevs.2019.102820

Garvican E, Clegg P. 2007. Clinical aspects of the equine carpal joints. Companion Anim, 12, 5-12. https://doi.org/10.1111/j.2044-3862.2007.tb00109.x

Hessel LN, Bosch G, van Weeren PR, Ionita JC. 2015. Equine autologous platelet concentrates: A comparative study between different available systems. Equine Vet J, 47, 319-25. https://doi.org/10.1111/evj.12288

Kwirant LA, De La Corte FD, Cantarelli C, Cargnelutti JF, Martins M, Cabral MW, et al. 2019. Cooling and cryopreservation of equine platelet-rich plasma with dimethyl sulfoxide and trehalose. J Equine Vet Sc, 72, 112-6. https://doi.org/10.1016/j.jevs.2018.10.009

Malone ED, Les CM, Turner TA. 2003. Severe carpometacarpal osteoarthritis in older Arabian horses. Vet Sur, 32, 191-5. https://doi.org/10.1053/jvet.2003.50026

Mayet A, Zablotski Y, Roth SP, Brehm W, Troillet A. 2023. Systematic review and meta-analysis of positive long-term effects after intra-articular administration of orthobiologic therapeutics in horses with naturally occurring osteoarthritis. Front Vet Sci, https://doi.org/10.3389/fvets.2023.1125695

McIlwraith CW. 2005. Frank Milne Lecture: From arthroscopy to gene therapy: 30 years of looking in joints. Proc Am Assoc Equine Prac, 51, 65–113.

McIlwraith CW, Frisbie DD, Kawcak CE. 2012. The horse as a model of naturally occurring osteoarthritis. Bone Joint Rev, 1, 297-309. https://doi.org/10.1302/2046-3758.111.2000132

Mirza MH, Bommala P, Richbourg HA, Rademacher N, Kearney MT, Lopez MJ. 2016. Gait changes vary among horses with naturally occurring osteoarthritis following intra-articular administration of autologous platelet-rich plasma. Front Vet Sci, 3, 1-9. https://doi.org/10.3389/fvets.2016.00029

Moraes APL, Moreira JJ, Brossi PM, Machado TSL, Michelacci YM, Baccarin RYA. 2015. Short- and long-term effects of platelet-rich plasma upon healthy equine joints: Clinical and laboratory aspects. Can Vet J, 56, 831-8.

Nedergaard A, Carlsson LE, Lindegaard C. 2024. Evidence of the clinical effect of commonly used intra-articular treatments of equine osteoarthritis. Equine Vet Edu, 36, 646-58. https://doi.org/10.1111/eve.13984

Panizzi L, Barber SM, Lang HM, Carmalt JL. 2009. Carpometacarpal osteoarthritis in thirty-three horses. Vet Sur, 38, 998–1005. https://doi.org/10.1111/j.1532-950X.2009.00589.x

Park CS, Jo YJ, Eo KY, Park TM, Cho GJ. 2022. Therapeutic effect of equine musculoskeletal disease using autogenous platelet-rich plasma. Int J Vet Sci, 11, 520-5. https://doi.org/10.47278/journal.ijvs/2022.150

Peng C, Yang L, Labens R, Gao Y, Zhu Y, Li J. 2024. A systematic review and meta-analysis of the efficacy of platelet-rich plasma products for treatment of equine joint disease. Equine Vet, 56, 858-69. https://doi.org/10.1111/evj.14042

Ribitsch I, Oreff GL, Jenner F. 2021. Regenerative medicine for equine musculoskeletal diseases. Animals, 11, 1-30. https://doi.org/10.3390/ani11010234

Segabinazzi LGTM, Podico G, Rosser MF, Nanjappa SG, Alvarenga MA, Canisso IF. 2021. Three manual noncommercial methods to prepare equine platelet-rich plasma. Animals, 11, 1-16. https://doi.org/10.3390/ani11061478

Textor JA, Norris JW, Tablin F. 2011. Effects of preparation method, shear force, and exposure to collagen on release of growth factors from equine platelets. Am J Vet Res, 72, 271–8.

Textor JA, Willits NH, Tablin F. 2013. Synovial fluid growth factor and cytokine concentrations after intra-articular injection of a platelet-rich product in horses. Vet J, 198, 217–23. https://doi.org/10.1016/j.tvjl.2013.07.020

Intraartikularna primjena plazme bogate trombocitima kod uznapredovalog karpometakarpalnog osteoartritisa kod arapskog konja: Dugoročni klinički ishod

SAŽETAK

Osteoartritis (OA) je česta degenerativna bolest zglobova kod konja, karakterisana degradacijom hrskavice, sinovijalnom inflamacijom i progresivnom hromošću. Intraartikularna terapija plazmom bogatom trombocitima (IA-PRP) pojavila se kao perspektivna regenerativna metoda, usmjerena na poticanje reparacije hrskavice i smanjenje upale putem oslobađanja faktora rasta. Desetogodišnji arapski pastuh prikazan je sa akutnom hromošću karpalnog zgloba, ocijenjenom kao 3/5 po AAEP skali. Početno liječenje fenilbutazonom i intraartikularnom injekcijom kortikosteroida (IA-GC) rezultiralo je privremenim poboljšanjem, međutim hromost je napredovala do ocjene 5/5. Zbog neuspjeha konvencionalne terapije i nemogućnosti daljeg upućivanja na specijalistički tretman, započeta je IA-PRP terapija. Protokol liječenja se sastojao od četiri IA-PRP injekcije primijenjene u razmaku od dvije sedmice, praćene profilaktičkim pojačavajućim tretmanom (peta IA-PRP injekcija) šest mjeseci nakon četvrte aplikacije. PRP je pripremljen korištenjem dvostrukog centrifugiranja. Rano poboljšanje je primijećeno nakon početka PRP terapije, što je omogućilo prekid upotrebe NSAIL-a. Hromost se postepeno poboljšala do skoro normalne funkcije, bez ponovne pojave bola ili abnormalnosti hoda u 18-mjesečnom praćenju. Ovaj slučaj ističe potencijal IA-PRP terapije kao alternativne metode koja smanjuje potrebu za kortikosteroidima u liječenju osteoartritisa kod konja.

Ključne riječi: Intraartikularna terapija, osteoartritis kod konja, plazma bogata trombocitima (PRP), regenerativna medicina, upravljanje hromošću

UNIVERZITET U SARAJEVU • VETERINARSKI FAKULTET

VETERINARSKI INSTITUT

Akreditirane laboratorije

Akreditirane laboratorije Veterinarskog instituta, kao nacionalne referentne laboratorije u sklopu svojih mnogobrojnih aktivnosti vrše i dijagnostiku afričke kuge svinja.

Uzorci moraju poticati od nađene uginule jedinke divlje svinje ili odstrijeljene divlje svinje koja je pokazivala znakove bolesti („Službeni glasnik BiH“ broj 22/20) te propisno upakovani i dostavljeni na pomenutu adresu.

Uzorci za ispitivanje koji se dostavljaju u laboratorije Veterinarskog instituta su:

- puna krv (ako nije moguće dostaviti punu krv može se dostaviti i transudat odnosno tečni sadržaj trbušne ili plućne duplje),
- tkiva tonzila,
- limfni čvorovi (gastrohepatalni, bubrežni, submandibularni i retrofaringealni),
- slezena,
- bubreg i
- pluća.

Ukoliko je moguće, potrebno je dostaviti i krpelje koji se zateknu na tijelu leša divlje svinje.

Uzorci se dostavljaju na adresu Veterinarskog instituta:

Ismeta Alajbegovića Šerbe br. 7, Stup 71000 Sarajevo

u terminu **od 7:30 do 16:00** sati svakim radnim danom.

Kontakt:

E-mail: lejla.velic@vfs.unsa.ba

Tel.: +387 62 211 791

E-mail: toni.eterovic@vfs.unsa.ba

Tel.: +387 61 242 069

UNIVERZITET U SARAJEVU
VETERINARSKI FAKULTET

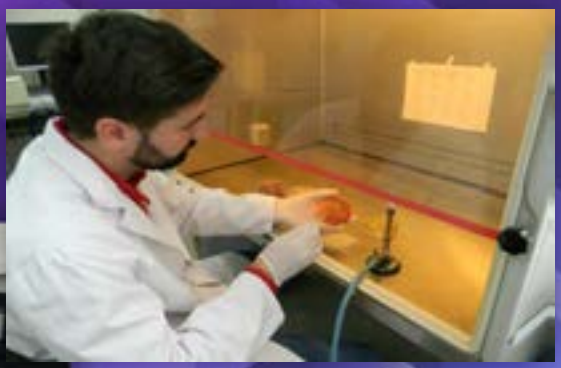

ISPITNE LABORATORIJE VETERINARSKOG FAKULTETA ispunjavaju zahtjeve standarda BAS EN ISO/IEC 17025:2006

u pogledu osposobljenosti za izvođenje:

- mikrobioloških i fizičko-hemijskih ispitivanja hrane i hrane za životinje,
- detekcije rezidua veterinarskih medicinskih proizvoda,
- toksikoloških ispitivanja rezidua i kontaminanata u hrani,
- mikrobiološke, molekularne i serološke dijagnostike infektivnih oboljenja životinja,
- dijagnostike spongiformne encefalopatije (BSE),
- detekcije specifične aktivnosti radionuklida u tlu, živežnim namirnicama i stočnoj hrani.

Veterinarski fakultet, Zmaja od Bosne 90
71000 Sarajevo, Bosna i Hercegovina

www.vfs.unsa.ba **info@vfs.unsa.ba**
tel: (+387) 033 729 100 **fax: (+387) 033 617 850**

Author Guidelines

Instructions to authors

Veterinaria is an international open access journal of veterinary research that publishes original papers and reviews on a wide range of veterinary topics.

Manuscripts

Manuscripts should describe original research in form of Research Article or Short Communication. Given that a case report makes a significant contribution to veterinary knowledge, it will be considered for publication as Short Communication. In general, Review Articles should be written in support of original research.
Research articles, Review Articles and Short Communications are subject to peer review. Letters to the Editor are also welcome and reflect the opinions of other researchers on articles in previously published issues of the same journal.
Other items (professional papers, book reviews, student papers, news, reports…) should be written in the Bosnian or English language and they are published at the discretion of the Editor (non peer reviewed articles).

Submission of manuscripts

Submission of manuscripts to Veterinaria is online via our site at: http://www.vfs.unsa.ba/veterinaria
Papers are accepted for evaluation on the understanding that:

- they have not been published,
- they are not being considered for publication simultaneously elsewhere,
- they are not going to be submitted for publication elsewhere.

Authors should certify that neither the manuscript nor its main contents have already been published or submitted for publication in another journal. The copyright release form, which can be found at http://www.vfs.unsa.ba/veterinaria must be signed by the corresponding author on behalf of all authors and must accompany all papers submitted. Please see the form for additional copyright details.
Authors will be step-by-step guided through the uploading file process and options to select the manuscript category (Research Article, Review Article, Short Communication, …) will be offered to the author.
Also, in the section Comments for the Editor the authors may suggest list of reviewers (name and e-mail contact) for their manuscript. Queries concerning the submission process or journal procedures should be sent by E-mail to veterinaria@vfs.unsa.ba
Submission of a manuscript implies its originality: i.e. it is not published or submitted for publication elsewhere. It is expected that all authors should have a significant intellectual contribution to the work. In addition, submission of a manuscript also implies that all of the authors have approved its publication and have agreed upon its content. All contributions are subject to editorial revision. The Editor's decision will be final.
Manuscripts should be written in the English language (American English). For spelling of lay terms, refer to the latest American edition of the Merriam-Webster Dictionary. Authors whose first language is not English are strongly advised to consult a native English speaker familiar with the concerned research field prior to submission.
Precise titles of Tables and Figures should be embedded in the manuscript at the appropriate place. For example: „Table 1. Results of....".
Manuscripts should be submitted in MS Word A4 format, written in Times New Roman 12 pt font, with double-spacing. All margins should be set at 2,5 cm. Authors submitting papers that are suitable for consideration but do not comply fully with this Guide will be asked to amend the text and re-submit.

Manuscript Preparation

Research Article should be arranged as follows:
Title page: title, author(s), affiliation(s), full address for correspondence, including telephone and and e-mail address. Except where all authors come from the same department, each author should be identified using a superscript (a,b,c etc.), and the Corresponding Author designated by an asterisk. Research articles should be no longer than 30 pages, should have an abstract of 300 words at most, should contain a limit of 60 references, and should have no more than 10 figures and tables combined.
Title page should not be run within text, it should be uploaded as separate Word document.
Main text sub-divided into:

1. Title of paper (without authors names),
2. Abstract of not more than 250 words (with no sub-headings),
3. Up to five keywords should be supplied below the abstract (avoid the same words from the title), in selecting key word the author should strictly refer to the *Medical Subject Headings (MeSH) list of the Index Medicus*,
4. Introduction,
5. Materials and Methods,
6. Results,
7. Discussion and Conclusion,
8. Acknowledgements,
9. References.

Short Communications and short clinical case reports for publication as short communications should follow the same format as Research Article, but the text must not exceed 1,500 words with no more than twenty references.
Review Articles may be commissioned or proposed. Authors wishing to submit a review article are advised to contact the Editor. In general, reviews are written in support of original research. They may cover any relevant aspect of veterinary science or comparative medicine. The first author of the review article should have at least three published papers from that field. Reviews should follow the layout for Research Article, but with the main text sub-divided as appropriate to the subject matter. Review articles should be no longer than 50 pages, should have an abstract of 300 words at most, should contain a limit of 120 references.
Letter to Editor reflect the opinions of other researchers on articles in previously published issues of the same journal. Typically, letters address the contents of an original journal article for one or more of the following reasons: to identify errors and make a correction, provide an alternate theory, provide additional information, offer additional evidence, or provide a counterpoint. The letter should be brief and concise. Letters to the editor should not exceed 800 words and 10 references. Letters are always written to the editor; they are never addressed to the authors of the article in question. While writing a letter, one should avoid assuming a personal and biased attitude or the use of aggressive language. All suggestions should be supported by scientific data.
Authors should provide running title for all types of the manuscript. The running title is an abbreviated form of the main title, usually cited at the top of right published page.

Citations and References

All publications cited in the text should be presented in a list of references at the end of the manuscript. The manuscript should be carefully checked to ensure that the spelling of author's names and dates are exactly the same in the text as in the reference list. In the text refer to the author's name (without initial) and year of publication. When multiple references are cited in the same sentence, the citations must appear in chronological order from oldest to newest.
If citation is referred to a single-author publication it should be indicated as (Osmanoglu, 2019). In the sentence, example: According to Osmanoglu (2019)...
However, if cited paper has been written by two authors, both names should be indicated followed by year of publication (Casu and Prodi, 2014).
If reference is made in the text to a publication written by more than two authors the name of the first author should be used followed by „et al."
„Since Elitok et al. (2020) has shown that..."
„This is in agreement with results obtained later (Bregoli et al., 2006)."
References by the same author(s) in the same year: (Michalek et al., 2004a, 2004b)
Multiple references cited in the same sentence: (Knott, 1987; Güneş et al., 2002; Jones et al., 2004)
Journal articles:
Journal names in the reference list should be written in accordance with the Journal Title Abbreviations list available at:
https://images.webofknowledge.com/images/help/WOS/A_abrvjt.html
Harvey N, Kingsley M, Terek F. 2019. Anatomical aspect of the red fox lung. Veterinaria, 64(3), 20-5.
Include the doi number if one exists
When more than a six authors:
Catanese G, Grau A, Valencia JM, Garcia-March JR, Vázquez-Luis M, Alvarez E, et al. 2018. Haplosporidium pinnae sp. nov., a haplosporidian parasite associated with mass mortalities of the fan mussel, Pinna nobilis in the Western Mediterranean Sea. J Invertebr Pathol, 157, 9-24.
Books:
Brown C, Laland K, Krause J. 2011. Fish Cognition and Behavior. 2nd ed. Oxford, UK: Wiley-Blackwell.
Chapters in books:
King AS. 1993. Apparatus urogenitalis. In Baumel JJ, King AS, Breazile JE, et al (Eds), Handbook

of Avian Anatomy: Nomina Anatomica Avium (2nd ed., pp. 329-90). Cambridge, USA: Nuttall Ornithological Club.

Conference proceedings:

Bregoli M, Dediasi K, Pasolli C. 2006. Antibiotic resistant E. Coli in free-ranging alpine wild ruminants, in: VII Conference of the European Section of the Wildlife Diseases Association. p. 78.

Web Adresses:

Papazoglou LG, Basdani E. 2015. Exploratory laparotomy in the dog and cat. https://www.cliniciansbrief.com/article/exploratory-laparotomy-dog-cat (accessed 4.18.17).

Theses:

Donker SA. 2010. Arctic ground squirrels in the Southwest Yukon Territory: evidence for habitat specific demography and source-sink dynamics. MSc, University of British Columbia, Vancouver, Canada.

Watts AJR. 2012. Nutritional status and trophic dynamics of the Norway lobster Nephrops norvegicus (L.). PhD, University of Glasgow, Glasgow, UK.

Tables and Figures

Tables - Submission of excessive tabular data is not favored, and tables should be limited to those containing data important to understanding and interpreting results of the study. Authors will be asked to delete tables containing data that could be reported more succinctly in the text. Tables that focus solely on findings in individual animals rather than summary data from groups of animals are to be avoided. Tables should be created in MS Word® and embedded in the text of the article as well as a separate excell document Each table should be numbered (1, 2, etc.) and supplied with the title placed above each table. Table titles should contain sufficient information to allow the table to be understood without reference to the text. Footnotes to tables should be superscripted by a, b etc. and explained in the legend at the bottom of the table. Tabulated results should not be duplicated in figures and vice versa.

Figures – Figures should be limited to those that reduce or clarify the text. Text and symbols should be large enough that they will still be visible when the figure is reduced to the size of 8,5 cm across. Text labels should start with a capital letter (eg, Posterior vena cava). For figures that include multiple panels, each panel should be sequentially labeled with a capital letter in the same corner of each panel. If a figure contains 2 or more rows of panels, the letter labels should be applied sequentially from left to right in the first row, then from left to right in the second row and so on. Digital images should be sent as TIFF or JPEG files, at a minimum resolution of 300 dpi at an image size of 8.5 cm across.

Figure and figure legends should be embedded in the text of the article as well as a separate TIFF or JPEG files (for figures).

Abbreviations defined in the text do not need to be expanded; however, newly introduced abbreviations in figures should be defined in the figure legend, in alphabetical order. When applicable, stains used for histologic sections should be indicated in the legend as well as the scale of the marker bar (eg, H&E stain; bar = 100 µm).

Abbreviations, Terms and Units of Measurement

If possible, use standard abbreviations. In general, use of abbreviations other than standard abbreviations and units of measures should be kept to a minimum. In the Abstract, a term should be abbreviated only if it is used at least 3 times in the structured abstract. The term must be expanded at first mention, with the abbreviation given in parentheses after the expanded term.

Similarly, in the text, figures, and tables, a term should be abbreviated only if it is used at least 3 times. All abbreviations except for standard abbreviations and units of measure should be listed in alphabetical order at the beginning of the manuscript text, along with their definitions. These abbreviations should then be used without expansion in the text, except when used to start a sentence.

Abbreviations that appear only in the figures or tables should be defined in the table or figure legend. Except for the abbreviations ELISA, PCR, ACTH, EDTA, DNA, and RNA, abbreviations should not be used in titles.

For anatomic terms, use anglicized versions of official terms listed in the Nomina Anatomica Veterinaria. Refer to Bergey's Manual of Determinative Microbiology for spelling and correct taxonomic classifications of microorganisms. Refer to the latest editions of the International Drug Names for proper spelling of chemical and drug names and to the latest edition of Dorland's Illustrated Medical Dictionary for proper spelling and use of medical terms.

Measurements should be reported in metric units in accordance with SI standards. Doses and dosages must be given on a mg/kg basis. All dosages must include route of administration and interval (eg, 10 mg/kg, IV, q 12 h).

Products, equipment, drugs, and other materials

Materials used in the research or referred to in the text should be identified by chemical or generic names or descriptions. A trade name may be included in parentheses if that specific product, equipment, or drug was essential for the outcome. Trademark and similar proprietary symbols are not needed.

Offprints

The corresponding author will, at no cost, be provided with a PDF file of the article via e-mail and one copy of the journal via post.

Veterinaria has no submission and page charge.

Submission Preparation Checklist

As part of the submission process, authors are required to check off their submission's compliance with all of the following items, and submissions may be returned to authors that do not adhere to these guidelines.

Double-spaced typing in A4 size white paper with 12-point font, and margins of 2,5 cm. Title page should be uploaded as separate Word document.

Manuscript should be arranged as follows:

- ✓ Title
- ✓ Abstract
- ✓ Keywords
- ✓ Introduction
- ✓ Materials and Methods,
- ✓ Results
- ✓ Discussion and conclusion;
- ✓ Acknowledgements;
- ✓ References

Tables should be created in MS Word® and embedded in the text of the article as well as a separate excell document.

Figures and images with proper resolution and size are embedded in the text of the article as well as a separate TIFF or JPEG file.

Ensure that graphics are high-resolution. Be sure all necessary files have been uploaded/attached. All figure captions are available. All tables are present (including title, description, footnotes).

Where available, URLs for the references have been provided.

All references mentioned in the Reference list must be cited in the text, and vice versa.

Copies of any permission to reproduce published material, pictures, illustrations, diagrams should be included in the work. Verify that permission has been obtained for use of copyrighted material from other sources (including the Web).

If the work includes experiments conducted on animals and humans, it must be indicated that the authors have respected the International Statute on Experiments Conducted on Humans and Animals, but also that all experiments on humans have been carried out in conformity with the Helsinki Declaration from 1975 and its changed version from 1983.

Copyright Notice

Privacy Statement

The names and email addresses entered in this journal site will be used exclusively for the stated purposes of this journal and will not be made available for any other purpose or to any other party.

UNIVERZITET U SARAJEVU • VETERINARSKI FAKULTET

Join us